THE UNIVERSITY OF CHICAGO

THE ROLE OF AUTOPHAGY IN TUMOR PROGRESSION AND METASTASIS

A DISSERTATION SUBMITTED TO

THE FACULTY OF THE DIVISION OF THE BIOLOGICAL SCIENCES

AND THE PRITZKER SCHOOL OF MEDICINE

IN CANDIDACY FOR THE DEGREE OF

DOCTOR OF PHILOSOPHY

INTERDISCIPLINARY SCIENTIST TRAINING PROGRAM: CANCER BIOLOGY

BY

ERIN ELIZABETH MOWERS

CHICAGO, ILLINOIS

JUNE 2016

TABLE OF CONTENTS

LIST OF FIGURES

LIST OF TABLES

ABBREVIATIONS

AMPK	AMP-activated protein kinase
Atg	Autophagy-related
Atg14L	Atg14-like protein
BafA1	Bafilomycin A1
CLEAR	Coordinated lysosomal expression and regulation
CSC	Cancer stem cell
DCIS	Ductal carcinoma *in situ*
ECM	Extracellular matrix
EMT	Epithelial-mesenchymal transition
FAK	Focal adhesion kinase
FEZ1	Fasciculation and elongation protein zeta 1
GABARAP	GABA(A) receptor-associated protein
GABARAPL1	GABA(A) receptor-associated protein-like 1
GABARAPL2	GABA(A) receptor-associated protein-like 2
GABARAPL3	GABA(A) receptor-associated protein-like 3
GAP	GTPase activating protein
GATE16	General protein transport factor p16
GEF	Guanine exchange factor
GEMM	Genetically-engineered mouse model
HCC	Hepatocellular carcinoma

HCQ	Hydroxychloroquine
HIF-1	Hypoxia-inducible factor-1
iBMK	Immortal, non-tumorigenic baby mouse kidney epithelial [cells]
IHC	Immunohistochemistry
LC3A	Microtubule-associated protein 1 light chain 3A
LC3Av1	Microtubule-associated protein 1 light chain 3A variant 1
LC3Av2	Microtubule-associated protein 1 light chain 3A variant 2
LC3B	Microtubule-associated protein 1 light chain 3B
LC3C	Microtubule-associated protein 1 light chain 3C
LIR	LC3-interacting region
LIR	LC3-interacting region
MEF	Mouse embryonic fibroblast
MET	Mesenchymal-epithelial transition
MLCK	Myosin light-chain kinase
mTOR	Mammalian target of rapamycin
mTORC1	mTOR complex-1
Nbr1	Neighbor of BRCA1 gene 1
NSCLC	Non-small cell lung carcinoma
PAS	Phagophore assembly site
PDAC	Pancreatic ductal adenocarcinoma
PE	Phosphatidylethanolamine
PI	Phosphatidylinositol
PI3KC3	Class III phosphatidylinositol 3-kinase complex

PI3P	Phosphatidylinositol-3-phosphate
ROCK1	Rho-associated kinase 1
ROS	Reactive oxygen species
SCOC	Short coiled-coil protein
SQSTM1	Sequestosome 1
ULK	Unc-51-like kinase
UPR	Unfolded protein response
UVRAG	UV irradiation resistance-associated gene

ACKNOWLEDGEMENTS

I am incredibly grateful for the wealth of support and encouragement that I have received throughout my time as a PhD student at the University of Chicago. I always found myself surrounded by a group of people willing to offer help and support during the difficult periods and to cheer me on when things were going well. I would like to first thank my PhD advisor and mentor, Dr. Kay Macleod. Her breadth of knowledge, scientific enthusiasm, and commitment to me as her student were invaluable. She gave me both the freedom to explore and pursue interesting questions as well as the gentle guidance needed to ensure that I continued to make forward progress. During the inevitable dark days that plague every project at some point, Kay's unwavering optimism and scientific pep-talks were essential to motivating me to keep going and to understanding the ebb and flow inherent in scientific data-gathering. She has pushed me to be a better scientist, and I will always be grateful for the skills I have gained in her laboratory.

I am also greatly thankful to my thesis committee, Drs. Mark Lingen, Seungmin Hwang, and Ezra Cohen. My meetings with them were always productive, encouraging, and insightful, and I had the lucky experience of never dreading a meeting with them. Mark was an invaluable and patient teacher and graciously sat with me for all of the histopathological diagnoses. He asked tough questions during my meetings but always in the kindest way. Seungmin's broad knowledge in the field of autophagy was incredibly helpful during the troubleshooting phases of my projects and in making connections to the broader field. Despite his incredibly busy schedule and moving to a different institution in the middle of my training, Ezra continued to be an active member of my committee and helped to remind me to think of the clinical implications of the

work. I am so grateful to all of them for helping me weather the unanticipated challenges of my proposed projects and supporting me as my project evolved.

My personal happiness during graduate school was hugely affected by the wonderful group of people with whom I had the pleasure of working every day. The senior graduate students in my lab, Michelle Boland, Aparajita Chourasia, Lauren Drake, and Marina Sharifi, welcomed me with open arms, and together with the members of the lab who came after me, Maya Springer, Logan Poole, and Chanelle Robinzine, made the lab a happy place. They were wonderful sources to help troubleshoot protocols, learn new techniques, bemoan experimental failures, and celebrate successes. Marina in particular deserves thanks for sharing with me her experience in the lab when I was deciding to join as well as for all of her initial work on the paxillin project and allowing me to take it in a new direction after she left. I am also thankful for my peers in the Medical Scientist Training Program for their support during our long years of training and helping me to look forward to the next step.

Finally, I would like to thank my family, who support me through everything unconditionally. My mother, in particular, was full of constant encouragement and believed I would succeed even when I doubted, and my grandfather sent me clippings of interesting science articles that always arrived at the right time to give my spirits a boost. Most importantly, I would like to thank Elliott, for being an incredible partner in this journey and all of our future journeys together. The wealth of love, support, patience, and laughter he brings to my life makes everything else possible.

ABSTRACT

Autophagy is a conserved catabolic process critical for the degradation of damaged organelles and protein aggregates as well as the intracellular recycling of proteins and lipids. Autophagy occurs at a basal rate in all cells and may be upregulated under conditions of stress; in particular, some tumor cells utilize autophagy to survive nutrient stress, hypoxic conditions, and cytotoxic therapies. Research into the role of autophagy in primary tumor growth suggests that autophagy may be tumor suppressive through its promotion of genome stability, limitation of necrosis and inflammation, and induction of growth arrest. However, other studies indicate a tumor-promoting role for autophagy, highlighting the fact that the role of autophagy is highly context-dependent, varying with oncogenic status, state of progression, and environment. With respect to metastasis, autophagy can facilitate the survival of tumor cells during detachment from the extracellular matrix, withdrawal of growth factors, and glucose deprivation. Additionally, autophagy is upregulated under conditions that promote metastasis, including hypoxia and TGFβ exposure. Finally, clinical studies have correlated increased autophagic flux with tumor metastases.

Previous work in our lab has demonstrated that autophagy is not required for primary tumor growth in the 4T1 orthotopic murine model of breast cancer but is critical to the formation of metastases. *In vitro*, autophagy-deficient tumor cells exhibit a rounded morphology and impaired motility; this phenotype is due to the impaired disassembly of focal adhesions. Therefore, I sought to determine the mechanism by which autophagy inhibition prevents focal adhesion disassembly and inhibits metastasis. I demonstrate that the levels of the focal adhesion

protein paxillin are dependent on autophagy but that the p62/Sqstm1 and Nbr1 cargo adaptors are dispensable for paxillin. Furthermore, I demonstrate that paxillin can bind LC3B directly and that the conserved LC3-interacting region motif in paxillin is required for binding and subsequent cell motility. Finally, oncogenic Src can stimulate the binding of paxillin with LC3B, and the ability of Src to promote cell motility requires intact autophagy. These results establish a novel function for autophagy in tumor motility and metastasis by promoting paxillin degradation.

CHAPTER 1

INTRODUCTION

Autophagy is a highly conserved catabolic pathway

Macroautophagy, hereafter referred to as autophagy, is a highly conserved catabolic process of cellular recycling. Extracellular materials and plasma membrane proteins are delivered to the lysosome, the key organelle for intracellular degradation[1,2], via the endocytic pathway, and cytoplasmic materials rely on autophagy for lysosomal delivery and subsequent bulk degradation. These cytoplasmic materials, which may include proteins, lipids, glycogen, organelles, and intracellular pathogens, are subsequently broken down to produce sugars, nucleosides/nucleotides, amino acids, and fatty acids, which may then be used for synthetic pathways and energy production[3,4]. Autophagy occurs at a constant basal level under normal growing conditions, with an estimated 1%-1.5% of cellular proteins being turned over by autophagy per hour, but can be induced by more than 10-fold in states of cellular stress[3–5]. Thus, autophagy is generally thought to act as an intracellular quality control system as well as an adaptive response to stress[6,7]. During the process of autophagy, a double-membrane structure called an isolation membrane (or phagophore) engulfs and sequesters a small portion of cytoplasm and cytoplasmic material, resulting in the formation of a double-membraned autophagosome[3,5,8]. This autophagosome fuses with endosomes and, ultimately, a lysosome to form an autophagolysosome that degrades the intracellular cargo via the catalytic activity of lysosomal hydrolases[1,5]. The autophagosomal and lysosomal systems are tightly intertwined, both with respect to their transcriptional regulation[9] and their discovery.

Characteristic double-membraned autophagosomal structures containing cytoplasm or organelles were first observed by electron microscopy in the late 1950s and early 1960s[10–13]. Shortly thereafter, in 1963, the term "autophagy" was coined at the CIBA Foundation Symposium on Lysosomes by Christian de Duve, a pioneer in the field of lysosomal biology and winner of the 1974 Nobel Prize in Physiology or Medicine[13,14]. Much of the work in the following decades focused on the morphological description of autophagy, including the identification of the phagophore[14]. However, the understanding of the genetic and molecular mechanisms underlying the autophagic process remained elusive until the 1990s and the development of yeast as a model organism for the study of autophagy[15]. In yeast, the autophagic machinery localizes to the phagophore assembly site (PAS), which greatly facilitated the identification of autophagy-related (*ATG*) genes and their roles[14,16,17]. Yeast genetic studies identified 35 *ATG* genes, beginning with the *ATG1* in 1997[18], and a subset of these genes (*ATG1-10, 12-14, 16-18, 29,* and *31*) are essential for canonical autophagy[3,19]. The first mammalian *ATG* homologs were identified the following year[20]. Broadly speaking, the Atg proteins can be subdivided into five subgroups: the Atg1/Unc-51-like kinase (ULK)-1 complex, which functions at the most upstream steam step of autophagy; the autophagy-specific phosphatidylinositol 3-kinase complex, which promotes autophagosome formation; the Atg12 conjugation system, which is essential for the elongation of the phagophore; the Atg8 conjugation system, which functions in the elongation and closure of the phagophore; and a subgroup of other Atg proteins that do not fall into one of the above categories[3,19]. Together, the Atg proteins function to promote a process of cellular "self-eating" whose dysregulation has been linked to numerous pathologies (Figure 1.1)[5,6].

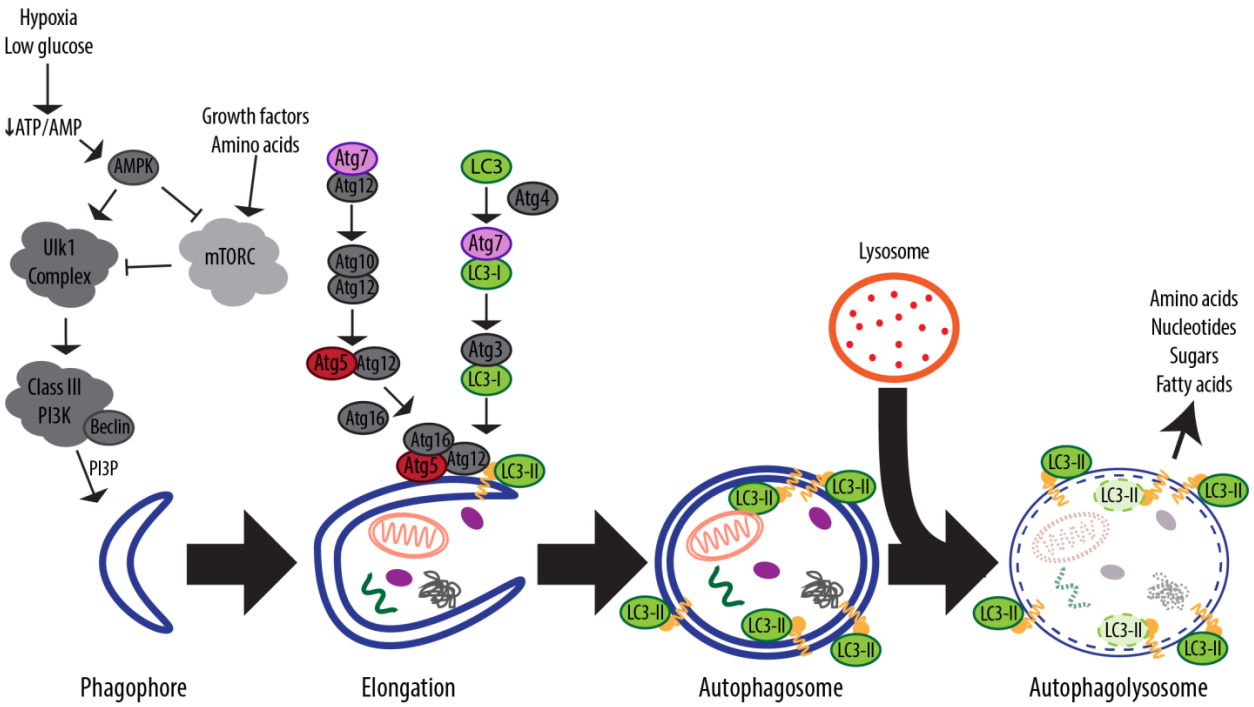

Figure 1.1 The autophagy machinery. Under nutrient-replete conditions, autophagy is inhibited by mTORC. Autophagy induction can occur upon growth factor or amino acid withdrawal or upon mTORC inhibition by AMPK downstream of hypoxia or low glucose. Activation of the Ulk1 complex leads to activation of the Beclin1-containing Class III PI3K complex, which produces PI3P and stimulates phagophore formation. Elongation is controlled by two conjugation reactions. The first results in the formation of the Atg12-Atg5~Atg16 complex, which participates in the second conjugation reaction to link LC3-I to phosphatidylethanolamine to form membrane-bound LC3-II. LC3-II is required for the closure of the autophagosome, which can engulf bulk cytoplasm or specific substrates. Autophagosomes fuse with lysosomes, and the engulfed substrates are degraded by hydrolytic enzymes.

The role of the Atg proteins in autophagosome formation

The most upstream component of the autophagy pathway is the Atg1/ULK complex, which includes ULK1, Atg13, FIP200, and Atg101 in mammals; each of these components are required for canonical autophagy[3,21]. Of the five human orthologs to yeast atg1, ULK1is the best studied and functions as a serine/threonine kinase, the only protein kinase among the Atg-related proteins[3,21]. The ULK complex is present within the cytosol under nutrient-rich conditions in association with the mammalian target of rapamycin (mTOR) complex-1 (mTORC1), which phosphorylates ULK1 and Atg13 to inhibit autophagy[22,23]. Release of inhibition by mTORC1 can occur either under nutrient withdrawal[22,23] or downstream of the AMP-activated protein kinase (AMPK)[24–28] and leads to relocation of the ULK1 complex to autophagic membranes, the origin of which is the endoplasmic reticulum (ER), trans-Golgi network, or outer mitochondrial membrane[29]. Active ULK1 autophosphorylates and phosphorylates FIP200 and Atg13[30]. The activity of the ULK1 complex is thought to be responsible for the regulation of the autophagy pathway at several different levels, including feedback inhibition of mTORC1[31,32], negative regulation of AMPK[33], and membrane targeting of ULK1 and other Atg proteins[21]. In *Drosophila*, dAtg1 can phosphorylate the focal adhesion protein paxillin, which is believed to play a positive role in autophagosome formation[34]. Most immediately, however, the ULK1 complex is believed to direct the activation of the next Atg complex in the autophagy pathway, the Beclin1-class III phosphatidylinositol 3-kinase complex (PI3KC3)[35]. Although the exact mechanism of activation remains opaque, it may involve the phosphorylation and activation of the Beclin1 interactor Ambra[36]. Alternatively, the mechanism may involve the short coiled-coil protein (SCOC)-fasciculation and elongation protein zeta 1 (FEZ1), which promotes ULK1

activation by removing inhibitory FEZ1/ULK1 binding and also interacts with UV irradiation resistance-associated gene (UVRAG), a binding partner of the Beclin1 complex[37].

The core structure of the Beclin1 complex is formed by Vps34, p150, and Beclin1[38]. Vps34 is a class III lipid kinase responsible for the conversion of phosphatidylinositol (PI) to phosphatidylinositol-3-phosphate (PI3P), which may act either to change the composition of the forming autophagosomal membrane on the ER or in the recruitment of effector proteins[3,21]. PI3P formation is critical for autophagosome formation, and the PI3K inhibitors wortmannin and 3-methyladenine have been demonstrated to inhibit autophagy[39–42]. In mammals, two mutually exclusive Beclin1-PI3KC3 complexes exist, one of which includes Atg14-like protein (Atg14L), and the other of which includes UVRAG[39]. The former may function in autophagosomal membrane nucleation and expansion through stabilization of PI3P-enriched, curved membrane regions[43], whereas the latter may modulate the expansion and curvature of membranes[21,39–42]. The Beclin1 complex functions as a central regulatory node controlling autophagy in response to multiple growth/proliferation pathways[44]. One method of regulation is binding of the anti-apoptotic proteins Bcl-2, Bcl-X_L, and Mcl-1 to the BH3 domain of Beclin-1, thereby preventing association of Beclin1 with Vps34 and autophagy initiation[45,46]. The pro-apoptotic protein Bim also binds Beclin1 through its BH3 domain and sequesters it with the Dynein motor complex[47].

Downstream of the Beclin1 complex lie two ubiquitin-like conjugation systems, the Atg12 conjugation system and the Atg8/LC3 conjugation system. Together with the transmembrane Atg9 protein, these conjugation systems drive the elongation and closure of the phagophore[3]. Atg12 is activated by the E1-like Atg7 through its C-terminal glycine, transferred to the E2-like Atg10, and ultimately conjugated to Atg5[48]. Subsequently, the Atg12-Atg5 complex interacts non-covalently with Atg16L to form a multimeric complex via

homodimerization of Atg16L through its C-terminal coiled-coil motif[49,50]. This complex is formed constitutively under both nutrient-replete and nutrient-deficient conditions and localizes to the outer surface of the phagophore, dissociating from the membrane immediately before or after the completion of autophagosome formation[3,51].

The second conjugation system, Atg8/LC3, culminates in the conjugation of Atg8 to phosphatidylethanolamine (PE) on both the inner and outer surface of the autophagosomal membrane[52,53]. The Atg12-Atg5~Atg16L complex is necessary for this formation, potentially through facilitating the transfer of Atg8 to PE[54] or by determining the site of Atg8 lipidation[55]. There are 8 mammalian homologs of Atg8: microtubule-associated protein light chain 3 (LC3)-A variant 1 (LC3Av1), LC3A variant 2 (LC3Av2), LC3B, LC3C, GABA(A) receptor-associated protein (GABARAP), GABARAP-like 1 (GABARAPL1), General protein transport factor p16 (GATE-16)/GABARAP-like 2 (GABARAPL2), and GABARAP-like 3 (GABARAPL3), although LC3B is the best-studied[56–58]. The first step in Atg8/LC3 conjugation is cleavage of its carboxyl terminus through the action of Atg4 to form LC3-I[52,59,60]. The C-terminal glycine-exposed form is subsequently activated by Atg7, which also participates in the Atg12-Atg5~Atg16L conjugation system, transferred to Atg3, and covalently linked to PE to form LC3-II[61]. Atg8/LC3-II may be deconjugated through the action of Atg4 to regulate the level of free Atg8/LC3[59,62]. Experimentally, detection of the LC3-I/LC3-II ratio is a critical means of measuring autophagic flux upon inhibition of downstream lysosomal proteases[63]. Formation of Atg8/LC3-PE is critical to proper elongation and closure of the phagophore[60]; in mammals, the LC3 subfamily is suggested to be involved earlier in the process during elongation, whereas the GABARAP/GATE-16 subfamily is suggested to promote maturation[56].

Once autophagosome closure is complete, autophagosomes are transported along microtubules to the endosome or lysosome, with which they subsequently fuse under the control of the vesicle fusion machinery, including ESCRT complexes, SNAREs, Rab7, and the class C Vps complex[64]. Members of the Atg family also participate in this process, including the promotion of the maturation of early endosomes and autophagosomes by UVRAG through recruitment of Rab7, which regulates late endosome transport and fusion with lysosomes[65,66]. Atg5 has also been implicated in the biogenesis of late endosome and lysosomes through recruitment of v-ATPase D to acidic organelles[67]. Inhibition of lysosomal acidification by bafilomycinA1 (BafA1) and hydroxychloroquine (HCQ) can prevent fusion of autophagosomes with late endosomes and lysosomes and is used experimentally to inhibit autophagy and promote a relative increase in the LC3-I/LC3-II ratio that is used to measured autophagic flux[68–71,63].

Selective autophagy and substrate specificity

Autophagosomes can direct degradation non-selectively, as in the case of nutrient deprivation-stimulated degradation of cytosolic contents, or selectively through the association of adaptor proteins or targets directly with Atg8 family members through a conserved LC3-interating region (LIR) motif[72]. One of the classic autophagy adaptor proteins is p62/sequestosome 1 (SQSTM1). First identified as an interacting partner of Lck-tyrosine kinase and atypical protein kinases C, p62/Sqstm1 is a multidomain protein adaptor able to direct a complex host of responses dependent on its binding partners[73,74]. Through its C-terminal ubiquitin-associated domain, p62/Sqstm1 is able to interact with ubiquitinated cargo, including ubiquitinated protein aggregates, and direct its cargo to the autophagosome for degradation by binding to LC3[75–78]. Inhibition of autophagy results in p62/Sqstm1 accumulation and the

formation of p62/Sqstm1- and ubiquitin-positive aggregates[76]. P62/Sqstm11 can also stabilize the Nrf2 transcription factor through binding to Keap1, promoting the transcription of genes encoding antioxidant proteins and detoxification enzymes[79]. Other downstream functions of p62/Sqstm1 include NF-κB activation and cell survival as well as caspase-8 aggregation and apoptosis[73,74,80–82]. Another autophagy receptor, neighbor of BRCA1 gene 1 (Nbr1), also functions like p62/Sqstm1 in directing ubiquitinated cargo to the autophagosome[83,84], although it may do so through predominantly through interaction with GABARAPL1[85].

Autophagosomal degradation of mitochondria, or mitophagy, is also thought to be regulated by adaptor proteins. Interactions between LC3 and the LIR domain of BNIP3, an outer mitochondrial membrane-anchored protein, promote mitophagy in response to various stresses, including hypoxia and starvation[86]. Similarly, the mitochondrial outer membrane protein FUNDC1 promotes hypoxia-induced mitophagy in a phosphorylation-dependent manner[87]. PINK1, a mitochondrial kinase, is activated at depolarized mitochondria and recruits the E3 ligase Parkin, which ubiquitinates mitochondrial proteins that are bound by cargo adaptors such as p62/Sqstm1 to promote mitophagic turnover of damaged mitochondria[88]. Intracellular pathogens may also be targets of autophagy (or xenophagy) through ubiquitination- or diacylglycerol-mediated targeting or through interactions of adaptor proteins[89]. For example, both optineurin[90,91] and NDP52[92,93] have been show to bind in ubiquitin-dependent and ubiquitin-independent manners to restrict the proliferation of intracellular bacteria. Still other adaptors have been identified in the autophagic degradation of ferritin (NCOA4)[94] and glycogen (Stbd1)[95]. Finally, individual proteins may be targeted for autophagy directly through LIR motifs, including targeting of the cellular tyrosine kinase Src for degradation by the E3 ubiquitin ligase C-Cbl[96]. The number of recognized adaptor proteins, as well as their targets, is growing.

Thus, autophagy, by controlling the levels of adaptor proteins, can have numerous downstream consequences.

Autophagy as a cellular response to stress

Autophagy can be induced as a response to various stress stimuli, including but not limited to nutrient and energy stress, ER stress, hypoxia, redox stress, and mitochondrial damage[7,8]. Of these, nutrient deprivation is the most potent physiological inducer. Sirtuins, a family of NAD-dependent deacetylases that sense environmental stress[97], are required for the induction of starvation-induced autophagy[98–100], and the acetylation of numerous members of the core autophagy machinery can regulation autophagic flux[7]. Sirt1 can promote AMPK activation[101], which can also sense energy status directly through the AMP:ATP ratio. As mentioned earlier, AMPK promotes autophagy by inhibiting mTORC1. mTORC1 serves as a key regulation hub in autophagy and can be regulated downstream of growth factors through Akt and ERK1/2[7,8].

Given the potential importance of the ER as a source of the autophagic isolation membrane as well as its role in the unfolded protein response (UPR), it is perhaps unsurprising that ER stress is a potent stimulator of autophagy[102,103]. During UPR, the ER membrane-associated proteins PERK, ATF6, and IRE1 repress global translation and activate transcription factors that target ER stress response genes. Two of these transcription factors, ATF4 and CHOP, can promote the transcription of *MAP1LC3B* and *ATG5* downstream of PERK[104]. Through autophagic degradation of the ER ("ER-phagy"), autophagy may serve to ameliorate cytotoxicity resulting from the accumulation of aberrant or misfolded proteins[105,106].

Hypoxia (O_2<1%), whether physiological or pathological, can also promote autophagy. The primary transcription factor of hypoxia-related genes, Hypoxia-inducible factor-1 (HIF-1), actives *BNIP3* transcription to promote mitophagy[107]. Hypoxia, particularly severe hypoxia or anoxia, can also stimulate autophagy independent of HIF-1 through AMPK activity[108].

At the transcriptional level, autophagy is regulated by the MiTF/TFE subfamily of basic/helix-loop-helix/leucine zipper transcription factors, which includes MITF, TFEB, TFE3, and TFEC[109]. Although MITF and TFEC exhibit cell type-specific expression, TFE3 and TFEB are expressed more ubiquitiously[109]. Lysosomal biogenesis is controlled by recognition of Coordinated Lysosomal Expression and Regulation (CLEAR) elements in the promoter region of different lysosomal genes by members of this transcription family[110], and overexpression of TFEB can promote the transcription of many lysosomal genes, including subunits of the v-ATPase, lysosomal transmembrane proteins, and lysosomal hydrolases[110,111]. TFEB is also the key transcriptional regulator of autophagy and can direct the transcription of *UVRAG*, *MAP1LC3B*, *SQSTM1*, and *ATG9B*, among others[9]. TFEB is itself regulated by mTORC1; under nutrient-replete conditions, mTORC1 phosphorylates TFEB to promote the occlusion of the TFEB nuclear import signal by binding to the cytosolic chaperone 14-3-3[112,113]. Conversely, under conditions of mTORC1 inhibition, starvation, or lysosomal disruption, TFEB is free to translocate to the nucleus and direct autophagy- and lysosome-specific transcriptional responses[9,114].

Autophagy can also be modulated by the master regulator p53, which controls the cellular response to such diverse stimuli as redox stress, hypoxia, nutrient deprivation, DNA damage, and oncogene activation[115]. Nuclear p53 acts as a transcription factor to drive the expression of genes that repress mTORC1 as well as the transcription of *DRAM1*[116], whereas cytoplasmic p53

inhibits autophagy, possibly through FIP200 interaction[117,118]. Interestingly, the core autophagy protein Atg7 has been shown to bind p53 to regulate cell cycle and cell death pathways[119]. The interplay between p53 and autophagy has also been reported in human pathologies, as will be discussed in the next two sections.

Tumor-suppressive functions of autophagy

The year 1999 marked the first report linking autophagy with tumorigenesis with the finding that monoallelic deletions of *BECN1* were observed in a large fraction of breast and ovarian cancers[120]. This report sparked a surge of research into the role of autophagy in tumorigenesis and tumor malignancy, with significant excitement over the possibility of targeting autophagy for therapeutic purposes. Altered levels of Beclin1 have been observed in brain, gastric, and colorectal neoplasias[121], *AMBRA1* is mutated in select endometrial, colorectal, and urinary tract neoplasms[122], and *UVRAG* is monoallelically mutated in gastric and colon tumors[123,124]. Furthermore, Atg5 is downregulated in melanomas[122], and Atg7 is silenced in a subset of head and neck cancers[125]. Activation of autophagy inhibitors are also observed in human cancers, including frequent activation of the PI3K/Akt pathway and subsequent stimulation of mTORC1[126]. Active epidermal growth factor receptor (EGFR), which is upregulated or mutated in a variety of epithelial cancers, can bind to and inhibit Beclin1 to inhibit activation of downstream Vps34[127]. Furthermore, expression of a Beclin1 tyrosine phosphomimetic can enhance growth and chemoresistance in non-small cell lung carcinomas (NSCLCs)[127].

Since the 1999 observation linking autophagy deficiency with tumor progression and the subsequent increased research in the area, investigators have begun to appreciate the highly

context-dependent role of autophagy, which can serve to either promote or suppress tumor progression at different stages (Figure 1.2). Determining the precise conditions, both cell-autonomous and cell-non-autonomous, that dictate the tumor-suppressive or tumor-promoting effects of autophagy remains an ongoing challenge. However, at present, the generally held opinion is that autophagy serves to inhibit malignant transformation and early tumorigenesis but promotes subsequent survival and progression of transformed cells and established tumors (Figure 1.2)[128–130] .

Murine models of whole-body or tissue-specific autophagy deficiency have emerged as key tools in our understanding of the interplay of autophagy and cancer. For example, mice heterozygous for deletion of *BECN1* develop spontaneous lymphomas as well as lung and liver carcinomas[120,131,132]. Similarly, heterozygous deletion of the gene encoding the Beclin1-interacting protein AMBRA1 promotes higher rates of spontaneous tumorigenesis[122]. Mosaic deletion of *Atg5* or liver-specific deletion of *Atg7* results in the acquisition of benign hepatic neoplasms[133]. Other mouse studies have combined knockout of *Atg* genes with other genetic alterations or stresses to accelerate tumor formation. The combination of *Atg4c* loss and carcinogen exposure promotes accelerated fibrosarcoma formation[134], whereas $BRAF^{V600E}$ mutation and *Atg7* deletion promote the development of lung carcinomas[135]. $KRAS^{G12D}$ has been combined with *Atg5* and *Atg7* loss in both lung and pancreas to accelerate carcinoma formation[136–138].

Precisely how loss of autophagy promotes tumor progression is a matter of considerable debate; in all likelihood, the answer lies in a combination of factors[130]. Autophagy may serve to limit levels of reactive oxygen species and reduce oxidative stress; dysfunctional mitochondria, like those targeted for mitophagy, are known to produce genotoxic ROS[139,140]. The potential

tumorigenic consequences of dysregulated mitophagy are particularly attractive to some groups whose have reported observations of aberrant activity of the glycolytic, pentose phosphate, and fatty acid oxidation pathways[135,137,141]. The autophagy target p6/Sqstm12 has also been associated with oxidative stress, NF-κB activation, and increased DNA damage, and its position as a hub of protein and signaling interactions suggests that p62/Sqstm1 accumulation may alter the course of tumorigenesis[73,74,142,143]. Indeed, elimination of p62/Sqstm1 by autophagy has been reported to suppress tumorigenesis in *Atg5*-null cells and *FIP200*-null tumors[142,144]. Elevated ROS in the absence of intact autophagy may also promote tumorigenesis through the promotion of an inflammatory microenvironment[145].

In addition to these more general effects on tumorigenesis, autophagy has been suggested to contribute to oncogene-induced cell death or oncogene-induced senescence[130]. This hypothesis may explain why loss of autophagy potentiates the effects of $KRAS^{G12D}$- and $BRAF^{V600E}$-driven mouse models of tumorigenesis[135–138]. *In vitro*, depletion of Atg5, Atg7, and Beclin1 can inhibit the death or senescence of $HRAS^{G12V}$- or $BRAF^{V600E}$-expresing cells [146–148]. Furthermore, overexpression of ULK3, an ULK1 homolog, promoted autophagy and limited the proliferative potential of these cells[147]. In the context of dominant negative *TP53* mutation, pharmacologic or genetic inhibition of autophagy genes prevented spontaneous senescence[149]. Whether the effects of autophagy on tumorigenesis in the context of oncogene activity are mediated directly through autophagic degradation of these proteins, as has been suggested by some groups in the cases of mutant p53, p62/Sqstm1, PML-RARA, and BCR-ABL1[130], or whether these effects reflect changes in the metabolic requirements or oxidative stress levels in these cells[128] remains unclear.

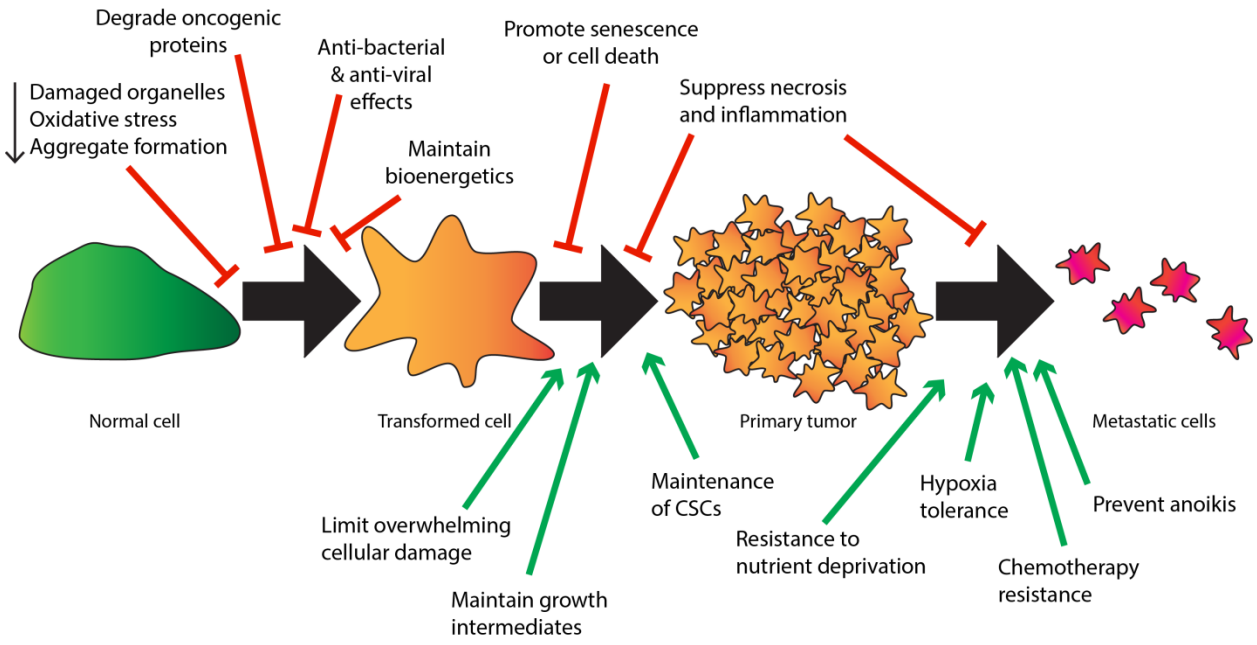

Figure 1.2 Autophagy can be tumor-suppressive or tumor-promoting. Early during tumor progression, the tumor-suppressive functions of autophagy predominate. Autophagy allows normal, healthy cells to cope with nutrient and genotoxic stress to prevent the accumulation of potentially pro-tumorigenic damage. However, after malignant transformation, the tumor-promoting functions of autophagy take over, and autophagy allows tumors to continue to grow and survive under environmentally unfavorable conditions and allows malignant cells to metastasize.

Tumor-promoting functions of autophagy

Although autophagy is tumor suppressive in some cancers during malignant transformation, autophagy may be upregulated as a tumor-promoting mechanism in other contexts (Figure 1.2). Indeed, in human tumors, expression of punctate LC3B, a marker of autophagosomes and ongoing autophagic flux, is commonly observed and is associated with proliferation, invasion, metastasis, high nuclear grade, and poor patient outcomes[150]. *In vitro*, autophagy has been shown to be required for $KRas^{V12}$-induced malignant cell transformation; Atg5 and Atg7 are upregulated in $KRas^{V12}$-expressing cells, and shRNA-mediated knockdown of these two autophagy genes inhibited *in vitro* growth and *in vivo* tumor formation in nude mice[151]. Similarly, in immortal, non-tumorigenic baby mouse kidney epithelial (iBMK) cells transformed by expression of $HRas^{V12}$ or $KRas^{V12}$, autophagic flux was increased relative to non-transformed cells[141]. When autophagy was inhibited in these transformed cells by knockout of *Atg5* or *Atg7*, *in vitro* growth under nutrient-depleted conditions as well as tumor growth in nude mice were suppressed, although the cells did not exhibit any growth defect under nutrient-replete conditions[152]. In contrast, inhibition of autophagy in $HRas^{V12}$-transformed MEFs and MDA-MB-231 cells was sufficient to decrease cell proliferation under nutrient-replete conditions, possibly through increased glycolysis[153]. Inhibition of autophagy in pancreatic ductal carcinoma (PDAC) cell lines, which frequently harbor *KRas* mutations, reduced xenograft growth in association with increased ROS, decreased oxidative phosphorylation, and decreased cellular ATP, although these changes were independent of mitochondrial damage or defective mitophagy, suggesting a role for the autophagic production of biosynthetic intermediates[154].

Autophagy has also been shown to inhibit tumor progression in systems not relying on strong oncogene drivers. In a $Tsc2^{-/-};p53^{-/-}$ MEF xenograft model of renal cancer, inhibition of

autophagy through Atg5 down-regulation caused extensive necrosis in tumors[155]. Furthermore, monoallelic *BECN1* loss caused a significant reduction in spontaneously arising renal tumors in *Tsc2*$^{+/-}$ mice, which is contrary to most reports of Beclin1 as a tumor suppressor[155]. Thus, there is an abundance of evidence suggesting that inhibition of autophagy can promote the progression of a wide variety of tumor types, albeit with the caveat that the majority of the studies have focused on autophagy in the context of strong oncogene drivers.

More recently, focus has shifted to the development of genetically engineered mouse models (GEMMs) to study the tumor-specific effects of autophagy. In genetic mouse models, autophagy has been shown to inhibit the latency of early tumors, as was discussed in the previous section. However, GEMMs also provide evidence that autophagy may be required for a more malignant phenotype. For example, although systemic mosaic deletion of *Atg5* and liver-specific deletion of *Atg7* does result in spontaneous hepatic neoplasms, these lesions are largely benign and do not progress[133]. Work in two models of NSCLC in the laboratory of Dr. Eileen White has suggested that autophagy loss promotes the development of oncocytomas, which are rare, largely benign tumors[135,141]. In an NSCLC model driven by *KRas*^{V12}, autophagy was induced during the transition of adenomas to invasive adenocarcinomas[141]. However, although deletion of *Atg7-flox* in the lung through intranasal delivery of adenovirus *Cre* did not alter tumor onset, the tumors did not progress to adenocarcinomas but to low-grade oncocytomas, which were comparatively smaller in size. These oncocytomas were characterized by dysfunctional mitochondria, leading the authors to suggest a causative link between mitochondrial dysfunction and blockade to adenocarcinoma progression[141]. When the group extended this model to include *p53* deletion, *Atg7*deficiency continued to reduce overall tumor burden and inhibit progression to oncocytomas, in conjunction with significant lipid

accumulation, suggesting that autophagy may be important in adaption to metabolic changes downstream of *p53* loss[141]. In the group's second NSCLC model, the authors focused on the effect of *Atg7*ablation in a *Braf*^{V600E} model[135]. In this model, unlike the first, autophagy deficiency caused accelerated tumor burden; however, these tumors exhibited blunted growth and were histologically diagnosed as oncocytomas, and the mice ultimately survived longer than their autophagy-competent counterparts. In this model, as before, the authors attributed the effects of autophagy inhibition to impaired mitochondrial metabolism and a particular requirement for glutamine[135]. However, the link between dysfunctional mitochondria and tumor progression remains correlative in these models, and the phenotype has not been reported by others.

Interestingly, when an independent group generated a second autophagy-deficient *KRas*^{G12D}-driven model of NSCLC, this time through tissue-specific inactivation of *Atg5*, they did not observe oncocytomas, although they did report impaired mitochondrial energy homeostasis[136]. In this model, autophagy deficiency resulted in enhanced early tumors but ultimately prevented their progression relative to autophagy-competent tumors, and tissue-specific deletion of *p53* was sufficient to restore the ability of autophagy-deficient tumors to progress[136]. The critical role of p53 was again shown in a model of *KRas*-driven pancreatic cancer[137]. In this model, deficiency of *Atg7* or *Atg5* accelerated PDAC onset but inhibited progression to intraepithelial neoplasias, although the analysis was impaired by the significant morbidity of *Atg7*$^{-/-}$ mice due to pancreatic destruction. Intriguingly, a change in *p53* status reversed the effects of autophagy on tumor growth; *KRas*^{V12D}*;p53*$^{-/-}$ mice deficient for autophagy exhibited accelerated tumor growth, possibly as a result of altered metabolism[137]. Thus, p53 status may represent a critical determinant of the role of autophagy in certain cancers.

Three additional autophagy GEMMs have extended the exploration of autophagy into melanoma, prostate cancer, and mammary cancer. Human melanomas are frequently characterized by $Braf^{V600E}$ mutation and *Pten* loss; in mice harboring alterations in these genes, *Atg7* deficiency inhibited melanoma development as well as melanoma growth, with *Pten* heterozygosity versus homozygosity determining the extent of these effects[156]. The effect of autophagy deficiency in the context of *Pten* deletion was also explored in a prostate cancer GEMM, in which *Atg7* deletion delayed tumor progression and promoted ER stress[157]. Finally, *FIP200* deletion was shown to suppress tumor progression in polyoma middle T antigen-driven mammary carcinogenesis in associated with increased immune surveillance, similar to suggestions that regulatory T cells play a role in the increased oncogenesis in autophagy-deficient $KRas^{G12D}$-driven NSCLC[158]. Thus, there is ample evidence for a tumor-promoting role for autophagy, particularly in the setting of established tumors. The ability of autophagy to mitigate the effects of stress under physiologic conditions are likely to be co-opted by tumors to allows them to overcome the challenges inherent in tumor growth and malignancy, including hypoxia, nutrient deprivation, metabolic alterations, and ROS, among others[128–130].

Autophagy in tumorigenesis: A tightrope act

Although *BECN1* monoallelic loss was the first suggestion that autophagy might act as a tumor suppressor[120], the finding has been challenged by observations that *BECN1* is often co-deleted with the oncosuppressor *BRCA1,* leading some to suggest that the correlation between *BECN1* and cancer is merely a red herring[159,160]. However, this position has been countered by analyses of breast cancer patient cohorts that have linked the mRNA levels of Beclin1 with decreased patient survival and adverse prognostic markers independent of BRCA1 mRNA

levels[161]. The confusion over the role of Beclin1 is emblematic of the difficulty in interpreting both human and mouse autophagy data.

Given the many stimuli to which autophagy can respond and the numerous downstream outcomes, it is perhaps unsurprising that past research focusing on autophagy in cancer as a single, unified phenomenon has produced results that are sometimes contradictory. It is critical to understand that autophagy may have different effects at different points in tumor progression (Figure 1.2) as well as different effects within a tumor depending on the cells' metabolic demands, oncogene status, immune surveillance, ROS levels, and microenvironment (Figure 1.3). These properties can vary widely from tumor to tumor as well as among cells within a single tumor; thus, autophagy inhibition may be affecting different cell populations in unique ways. This point is highlighted by the fact that deletion of the core autophagy genes in many of the GEMMs studied thus far is known to be mosaic[133,137,162]; whether the effects observed in these animals are inherent to the heterogeneity of autophagy deficiency as opposed to uniform inhibition remains to be determined.

Furthermore, much of the *in vivo* research has focused on relatively few members of the core autophagy machinery, notably *Atg7*, and generally limited to the context of *Ras* activation. However, more recent studies have expanded both the cancer models and genetic contexts in which autophagy is studied. This is particularly important in light of the growing appreciation that some forms of macroautophagy do not require the frequently studied Atg5 and Atg7 proteins[163] as well as the growing list of non-autophagic roles of autophagy proteins[164]. Thus, future research, particularly future GEMMs, will need to carefully consider both these autophagic and non-autophagic roles when attempting to interpret studies relying on complete knockout of individual components of the autophagy machinery. In support of this, a recent

study made use of a murine knock-in of a FIP200 mutant unable to interact Atg13 that was therefore unable to undergo autophagy *in vivo*[165]. The authors found that the mutant was able to support embryogenesis through inhibition of TNFα-induced apoptosis but that the inhibition of the autophagy-specific functions of FIP200 lead to neonatal mortality and inhibited the growth of tumor xenografts[165].

In conclusion, investigations into the role of autophagy in cancer must carefully consider (1) the point during tumor progression at which autophagy is inhibited or promoted (Figure 1.2), (2) the unique properties of the tumor cells with respect to their intracellular state and microenvironment (Figure 1.3), and (3) the potential non-autophagic effects of autophagy-related proteins. These requirements highlight the importance of using well-defined and manipulable systems and studying the role of autophagy in specific contexts. One area of increasing importance, particularly given the historical focus on autophagy in primary tumor growth, is the field of cancer metastasis.

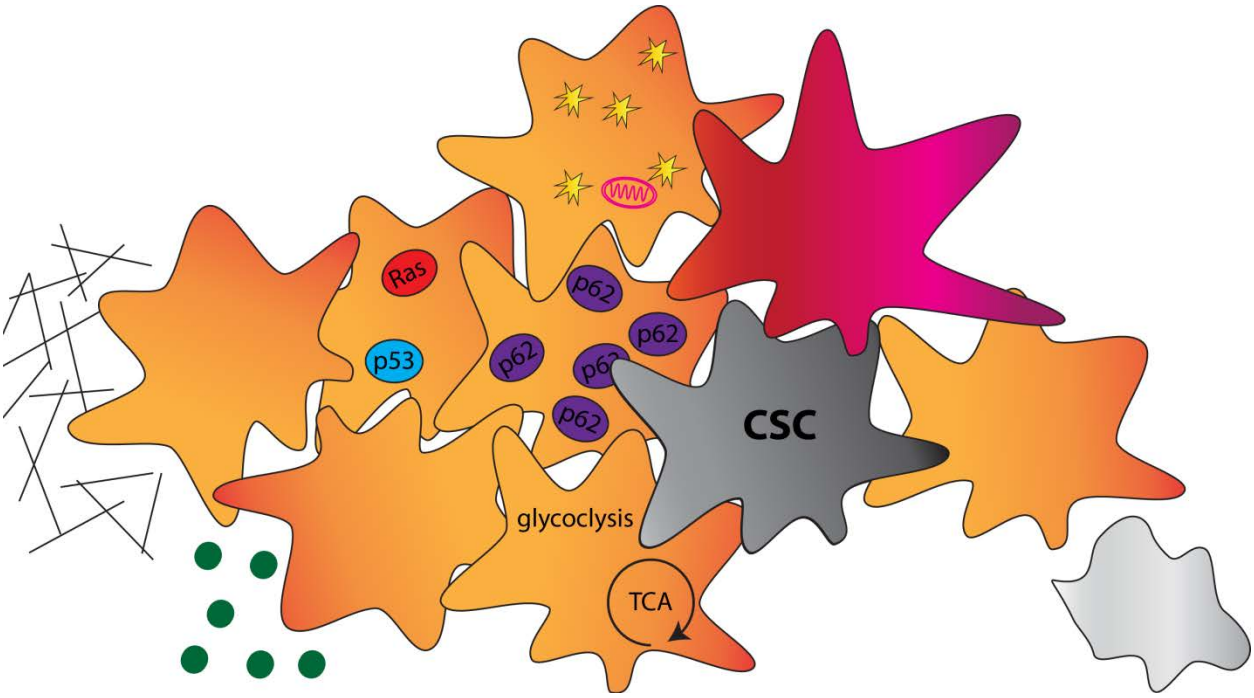

Figure 1.3 The tumor-specific role of autophagy depends on the cellular context. In addition to the stage of tumor progression, individual differences among tumor cells can determine whether autophagy may be tumor-promoting or tumor-suppressive. These cell-specific effects can include the following (clockwise from top): levels of ROS and damaged organelles, tumor motility, interactions with immune cells, cancer stem-like cell phenotypes, metabolic requirements, cell secretion, interactions with the extracellular matrix, the expression of oncogenes and tumor suppressors, and the levels of autophagy-associated signaling molecules like p62.

The metastatic cascade

Although cancer research and therapeutic developments have historically been most focused on primary tumor growth, metastasis represents the greater clinical challenge. Metastatic disease is responsible for more than 90% of cancer-related deaths, which is due both to its systemic nature and to the resistance of disseminated tumor cells to currently available therapeutic agents or delivery/targeting methods[166–168]. Even in patients who do not present with disseminated disease, metastases will be detected at a later time[169]. However, it is clear that oncogenic transformation alone is not sufficient for the acquisition of a metastatic phenotype, a finding that is supported by observations that oncogene-based GEMMs are not all metastatic[170,171]. Rather, the acquisition of a metastatic phenotype requires molecular changes in either a stochastic or coordination fashion that render cells capable of leaving the primary tumor, surviving transit, and establishing new tumors at secondary sites[168]. The numerous challenges that tumor cells must face during this process is perhaps underlined by the estimation that less than 0.01% of tumor cells entering the systemic circulation will successfully develop macroscopic metastases[169].

The metastatic cascade can be divided into a series of stages: local invasion, intravasation, survival in the circulation, and extravasation, which all are involved in the physical translocation of a cancer cell to its new environment, and colonization (Figure 1.4). During local invasion, epithelial cancer cells must breach the basement membrane and acquire a motile phenotype. This aspect of the metastatic cascade is dependent on epithelial-mesenchymal transition (EMT) and reflects a co-opting of the epithelial-mesenchymal plasticity observed in development and wound healing[172,173]. The acquisition of EMT involves the expression and activation of transcription factors (e.g., Snail, Slug, ZEB1, and Twist, among others), the

expression of specific surface proteins, altered cytoskeletal organization, and the production of extracellular matrix (ECM)-degrading enzymes[172]. Next, the now-motile cancer cells must cross pericyte and endothelial cell barriers to enter the circulation; this process may utilize some of the same matrix-degrading enzymes as were acquired during EMT and may be facilitated by the inherently leaky and disordered organization of the tumor vasculature[174]. Once within the circulation, tumor cells must overcome cell death signals typically triggered in the absence of anchorage to the ECM (i.e., anoikis)[175] and survive the mechanical injury inherent in transit. At the target organ, the tumor cells must either extravasate, the reverse process of intravasation, or may grow intraluminally until the new lesion ruptures the walls of the containing vessel[168]. Upon arrest at the target site, many cancer cells undergo a process of reverse EMT termed mesenchymal-epithelial transition (MET) in order to revert to their original epithelial state to proliferate and drive the formation of macrometastases. The factors determining the target organ at which the tumor cell arrests and potentially grows has been the subject of historical debate between the "seed and soil" theory, wherein certain tumors (the "seed") exhibit tropism for select secondary sites above others (the "soil")[176], and the theory that circulatory patterns are sufficient to dictate sites of tumor cell arrest[177]; however, it is likely that both factors play a role to different degrees in different cancers[178].

The last stage of metastasis, colonization, can itself be divided into dormancy, micrometastasis, and macrometastasis phases[168]. Colonization represents the greatest challenge to metastasis formation, as was demonstrated in a series of experiments involving B16F1 melanoma cells. These cells were injected intraportally to target the mouse liver and were monitored using *in vivo* videomicroscopy and cell counting assays. The series of experiments demonstrated that greater than 80% of the injected cells successfully extravasated, but less than

3% of the injected cells formed micrometastases; furthermore, less than 0.02% of the injected cells generated macroscopic metastases[179]. Once in a new location, tumor cells must adapt to new interactions with stromal components; whether and how quickly tumor cells form micrometastases may be related to the similarities or differences between the origin and terminus of metastasis[168].

The metastatic cascade represents a series of challenges that tumor cells must overcome to survive at sites distant to the primary tumor. Given the relatively small proportion of tumor cells ultimately successful in colonization, it is possible that the most effective therapeutic targets involve the latter steps of metastasis. However, our understanding of the metastatic process is most comprehensive for the earlier stages, particularly with respect to the acquisition of cell motility.

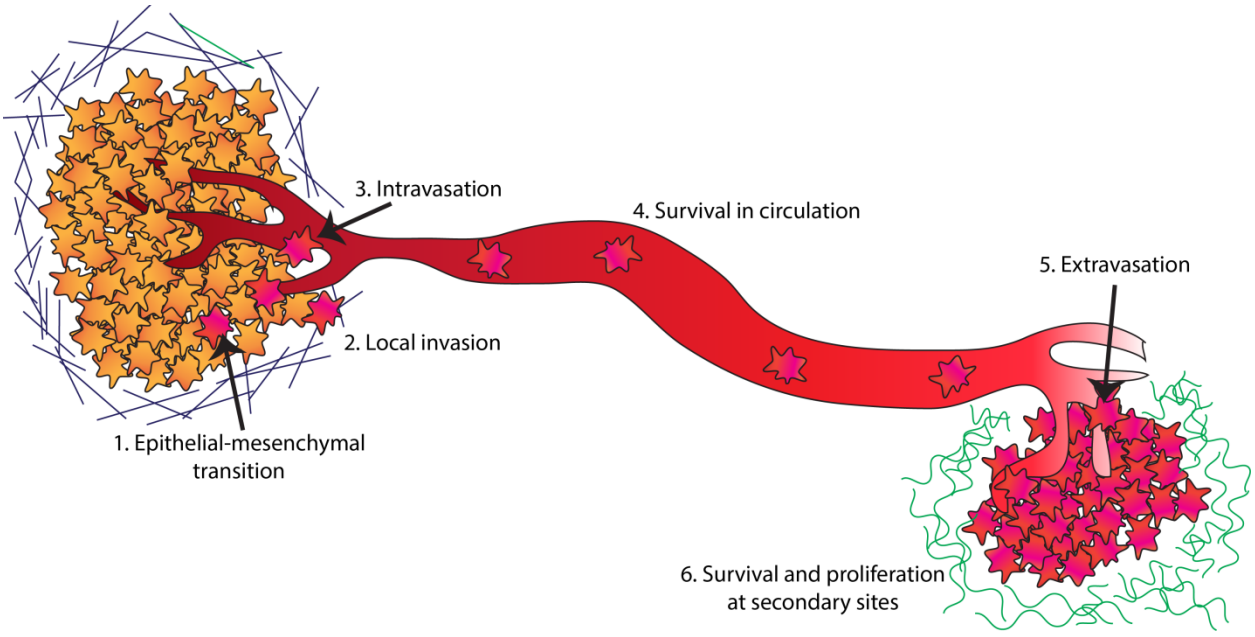

Figure 1.4 The metastatic cascade. For a primary tumor cell to successful metastasize and form overt metastases at a distant site, it must overcome a series of challenges. (1) The tumor cell must acquire a motile phenotype so that it may migrate and invade, which may be accompanied by epithelial-mesenchymal transition. (2) The tumor cell must invade through the basement membrane and surrounding extracellular matrix. (3) The cell must intravasate into a blood or lymph vessel to obtain access to the circulation and systemic transport. (4) It must survive transit within the circulation, which includes avoiding anoikis (detachment-induced cell death) and surviving the mechanical stress of the circulation. (5) The tumor cell must leave the blood vessel and invade new tissues. (6) Finally, the metastasized cell must survive and adapt within a new microenvironment and eventually successfully proliferate into a macroscopic tumor.

Focal adhesion regulation underlies cell motility

The cellular motility program is highly complex and requires the complex coordination of proteins involved in mechanical adherence, contraction, scaffolding, and signaling pathways. In sum, the cyclic process of cell motility involves the polarization and protrusion of one edge of a cell, the formation of adhesions linking the cytoskeleton to the extracellular matrix, movement over these adhesions through contractility, and disassembly of the adhesions to release the rear of the cell (Figure 1.5)[180]. The direction of cellular migration can be signaled by a variety of cues, including mechanical forces, ECM proteins, chemokines and growth factors[181]. The protrusions at the leading edge of a cell take the form of broad, large lamellipodia useful for directional migration or spike-like filopodia used as sensors and local exploration[180]. In the former, actin is organized into a branching network, whereas in the later, actin is organized into long, parallel bundles. The branching pattern of actin in the cell front is mediated by the Arp2/3 and WASP/WAVE family members. Towards the center and rear of the cell, actin is organized into thick bundles called stress fibers[182]. These stress fibers undergo contraction through the act of myosin II to generate the force to move the cell.

Cellular migration also relies critically on the Rho family of small GTP-binding proteins, notably Rac, Cdc42, and RhoA. These proteins are active when bound to GTP and inactive when bound to GDP, and their activity is regulated by a host of guanine exchange factors (GEFs) and GTPase activating proteins (GAPs). In their active, GTP-bound state, these proteins are able to interact with their numerous downstream targets, which include protein kinases, lipid-modifying enzymes, and activators of the Arp2/3 complex[180]. Broadly speaking, Rac and Cdc42 are present and control activities at the leading edge of the cell[183], whereas RhoA is predominantly active at the cell rear, although it may also play a role in early protrusion[183,184].

While Rac and Cdc42 seem to be responsible for activating WASP and WAVE, thereby leading to Arp2/3 activation and actin branching, the role of RhoA seems to be more related to the regulation of adhesions and myosin II-mediated contractility[181]

The formation of adhesions connecting the cellular cytoskeleton with the extracellular matrix is key to providing points of traction for cell motility; adhesions also serve as important signaling hubs to convey environmental information to the cell interior. The collection of proteins involve in the mechanical and signaling role of adhesions is referred to as the "adhesome"; a 2010 study estimated that there are 180 protein-protein interactions in the network, with the number likely to grow with new research[185]. Integrins, a family of transmembrane heterodimeric receptors, bind to extracellular substrates, like collagen and fibronectin, thereby inducing a confirmational change that promotes their intracellular interaction with the actin cytoskeleton[186]. Because the cytoplasmic domains of integrins possess no intrinsic enzymatic activity, the recruitment of a host of additional proteins to these adhesions is necessary for the transmission of force and signaling necessary for migration[187]. The integrin adhesions can be classified according to their size, stability, and location within the cell. In general, the term nascent adhesion is used to refer to the small, short-lived adhesions in the lamellipodium; focal complex is used to refer to the slightly larger, more persistent adhesions that reside immediately behind the lamellipodium; and focal adhesion is used to refer to larger adhesions that connect with actin stress fibers and form the traction points for movement. These focal adhesions move towards the rear of the cell as the cell moves forward and are eventually disassembled to release the cell rear.

Signaling proteins recruited to focal adhesions help regulate the connection between cell-matrix adhesions and the actin cytoskeleton. One of the earliest proteins to be recruited to

focal adhesions is paxillin, a multi-domain scaffold protein[188]. Paxillin was among the earliest identified members of adhesome[189]; originally thought to act as a passive structural component, its role as a signaling molecule was suggested upon the observation that paxillin became tyrosine phosphorylated upon cellular adhesion to the ECM[190]. Structurally, the 68-kDa paxillin protein is organized into a C-terminal half that contains four LIM domains and an N-terminal half responsible for the majority of its signaling activity. The LIM domains, which are double-zinc-finger motifs, mediate protein-protein interactions and are critical to targeting of paxillin to the focal adhesion, although the direct binding partner of paxillin responsible for this localization is unknown[187,191]. The N-terminal region of paxillin contains five leucine- and aspartate-rich LD motifs and several tyrosine phosphorylation sites; through this region, paxillin can bring together and facilitate the activation of multiple members of the adhesome.

Two such key players and paxillin-binders include focal adhesion kinase (FAK) and Src. Adhesions induce the autophosphorylation of FAK, which recruits and binds Src; Src in turn phosphorylates FAK on additional sites to create an active signaling complex[192]. The FAK-Src complex and its phosphorylation of paxillin on tyrosine 31 and 118 can activate Rac1 and inhibit RhoA, thereby promoting actin and adhesion dynamics and organization[187,193,194]. In addition to this role in early focal adhesion assembly and signaling, FAK and Src play roles in focal adhesion disassembly; fibroblasts lacking *Src* or *FAK* exhibit abnormally enlarged focal adhesions and impaired migration[195–197]. However, the precise mechanism by which either Src or FAK regulates focal adhesion disassembly is unclear, although Src tyrosine kinase activity is required[198,199].

The normal cellular motility program can be co-opted by cancer cells during the process of invasion and metastasis. Indeed, dysregulation of the motility program and components of the

adhesome is observed in some cancers; for example, activation or overexpression of Src family kinases is frequently observed in solid tumors[192,200,201]. Thus, they have emerged as attractive targets for therapeutic intervention[201]. However, it is likely that future therapies targeting the cellular motility program will require combination with agents targeting other aspects of tumor biology. The emerging role of autophagy in cancer metastasis suggests that autophagy therapies may be an attractive target.

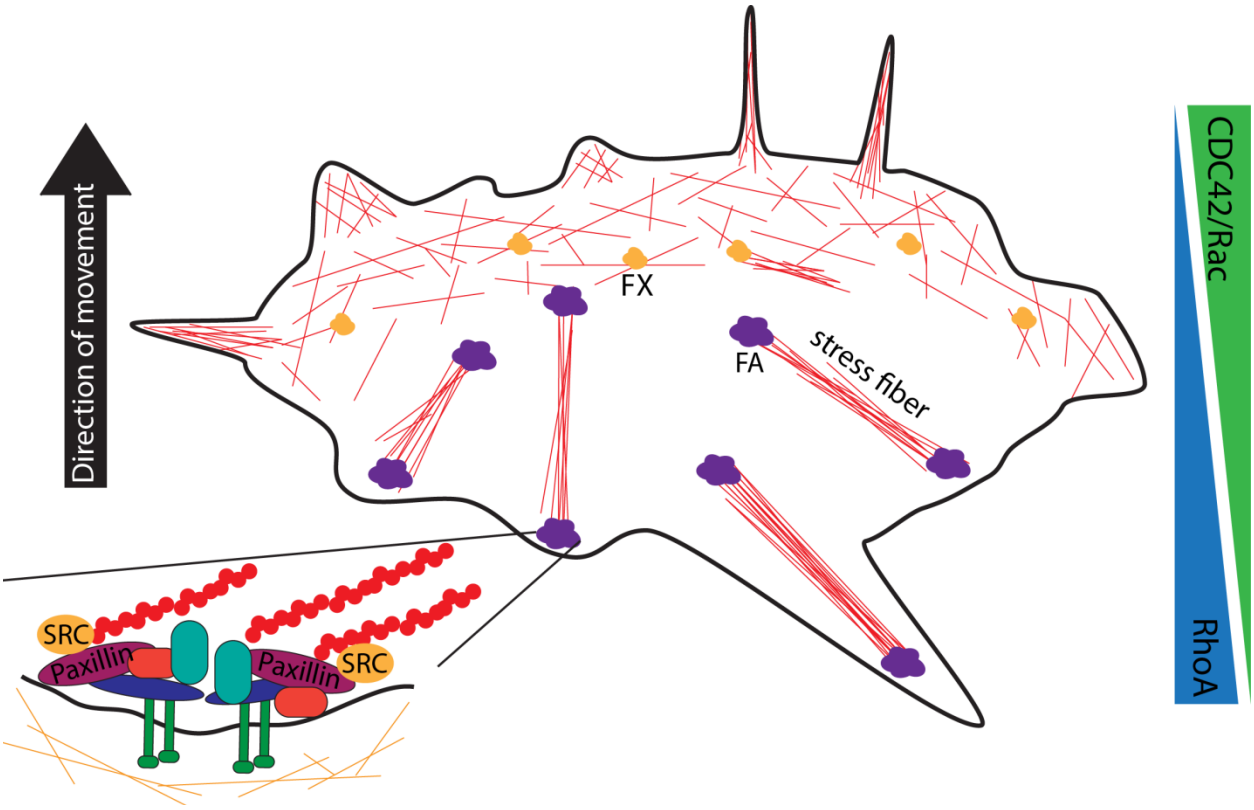

Figure 1.5 The cell motility program requires careful coordination. Cellular motility requires a cell to polarize and extend protrusions in the direction of movement. Polymerization of actin subunits is used to drive membrane protrusion. Toward the leading edge of the cell, actin is organized into a branching network; in the middle to rear of the cell, actin filaments are bundled into thick stress fibers. Actin polymerization and organization is controlled in part by the Rho family of small GTPases. Cdc42 and Rac activity predominates towards the leading edge, whereas RhoA activity is required in the rear. The cell must also lay down adhesion complexes that link the actin cytoskeleton to the membrane-spanning integrins, which make contact with the extracellular matrix. Early adhesions formed in the filopodia of the leading edge are called focal complexes (FX), which mature into the larger and more stable focal adhesions (FA). Focal adhesions are made up of a large complex of proteins, including paxillin, which serves both a signaling and scaffolding function. Continued forward movement requires the disassembly of focal adhesions as the rear of the cell, which is controlled in part by Src activity.

The role of autophagy in cell motility and tumor cell metastasis

Explorations of the role of autophagy in tumor cell metastasis have gained increasing interest in recent years. Lazova and Han reported that autophagy, as measured through punctate LC3B staining, was associated with node positivity, increased nuclear grade, and reduced survival in breast cancer[150]. Furthermore, metastatic melanoma, particularly metastatic melanoma associated with abnormal vascularity, and distant melanoma metastases exhibited increased LC3B staining[150,202,203]. LC3 expression is also correlated with metastasis in hepatocellular carcinoma (HCC), with higher LC3 staining in metastases relative to primary tumors and in early metastatic colonies relative to late metastatic colonies[204]. Given the numerous challenges that metastatic tumor cells must overcome to successfully establish distant colonies (e.g., invasion, anoikis resistance, and colonization) and the critical role of autophagy as a cellular stress response, numerous roles for autophagy in the metastatic cascade have been postulated[205]. As with the role of autophagy in primary tumor growth, it is highly likely that the role of autophagy in metastasis is dependent on tissue type, oncogene status, and stage within the metastatic cascade.

EMT is characteristically acquired early in the metastatic process to promote local tissue invasion. Interestingly, potential inducers of EMT, including hypoxia and TGFβ, are also inducers of autophagy[107,108,206–208]. EMT has also been linked to the acquisition of stem cell markers and a stem-cell phenotype[209]. Populations of cancer stem cells (CSCs) have been postulated to be responsible for metastasis due to both their more motile and plastic phenotype and their ability to give rise to populations of new cells[168]. Indeed, there have been several reports of a clinical correlation between CSCs or CSC markers and increased invasiveness and metastasis[210–212]. Intriguingly, autophagy has been linked to stem cell maintenance and control of

differentiation[213–216], and hematopoietic stem cells appear to be dependent on autophagy for survival[217]. In human breast ductal carcinoma *in situ* (DCIS), subpopulations of cells exhibit increased tumor-initiating capacity and migration/invasion capabilities, which was correlated with increased upregulation of cellular autophagy. Furthermore, these cells were dependent on autophagic flux for their continued survival[218]. Autophagy has also been shown to be required by the $CD44^{+}CD24^{-/low}$ breast cancer stem cell population; knockdown of autophagy genes decreased this subpopulation *in vitro*. Furthermore, autophagy was required for the acquisition of an EMT phenotype in response to TGFβ[219]. An independent group confirmed this requirement for autophagy in $CD44^{+}/CD24^{-/low}$ breast cancer cells by identifying Atg4 as a regulator of this cell population and the ability to form mammospheres *in vitro* and form tumors *in vivo*[220].

Irrespective of whether the connection between autophagy and a stem cell-like phenotype reflects a context-specific relationship or a general property of CSCs, autophagy has been linked to EMT and early invasion. In HCC cell lines, under nutrient-deficient conditions, autophagy promotes invasion through EMT by downregulating the expression of E-cadherin and CK18 while upregulating fibronectin and MMP-9. Furthermore, autophagy induces the expression of TGFβ and activates TGFβ signaling, and the treatment of autophagy-deficient cells with exogenous TGFβ was sufficient to rescue cellular invasion[221]. Conversely, in glioblastoma cells, autophagy has been reported to impair invasion by decreasing the expression of the EMT regulators Snail and Slug[222]. However, another group reported that autophagy promoted invasion in glioma[223]. Ubiquitinated Twist1, another EMT transcription factor, can be stabilized by p62/Sqstm1. In autophagy-deficient cells, up-regulation of p62/Sqstm1 prevented Twist1 degradation by both autophagosomes and the proteosome and promoted downstream loss of E-cadherin, *in vitro* cell migration, and *in vivo* metastasis[224]. Autophagy may also promote local

invasion through the secretion of pro-migratory factors; in *Ras*-transformed cells, treatment with conditioned media from autophagy-competent cells can rescue the decreased migration and invasion of autophagy-deficient cells[225].

When epithelial cells become detached from the extracellular matrix, as occurs during intravasation of tumor cells into blood vessels, they commonly undergo a form of apoptotic cell death or anoikis[226]. Thus, tumor cells must overcome anoikis in order to survive transit in the vasculature. Autophagy may be induced by cells undergoing ECM detachment downstream of the ER stress response kinase PERK and subsequent mTORC1 inhibition[227]. Furthermore, induction of autophagy during ECM detachment can promote cell survival and facilitate subsequent clonogenic recovery[228]. *In vivo,* inhibition of autophagy in HCC cells attenuates anoikis-resistance and inhibits lung colonization[229]. Thus, autophagy may promote tumor cell survival in the circulation.

Once at a secondary site, autophagy may promote adaptation to the foreign microenvironment by prolonging cell survival. For example, growth factor withdrawal can prevent cells from properly taking up extracellular nutrients[230], but autophagy can compensate for growth factor withdrawal by maintaining ATP production and preventing energetic catastrophe[231]. Alternatively, autophagy proteins may facilitate tumor cell survival at secondary sites by promoting quiescence; for example, Atg7 is required for p53-mediated growth arrest through expression of $p21^{CDKN1A}$ in an autophagy-independent fashion[119]. Thus, autophagy may be a means of promoting the survival of metastatic tumor cells while they adapt to their new microenvironment. Following adaptation, autophagy may facilitate the outgrowth of metastases in a program analogous to the role of autophagy in primary tumor growth.

The above discussion of the role of autophagy in tumor cell metastasis largely focuses on cell-intrinsic effects. It is important to note that the immune system has been demonstrated to play a critical role in metastasis and tumor surveillance, potentially acting to either facilitate or inhibit tumor cell dissemination. Furthermore, stromal cells can secrete factors that promote or inhibit local invasion or create a metastatic niche more or less conducive to outgrowth. As autophagy is known to function in both secretion and immune cell function[145,232,233], it is likely that autophagic flux within the stroma may alter the metastatic phenotype of tumor cells independent of their own levels of autophagy. Furthermore, communication between the stroma and tumor may carefully orchestrate the appropriate levels of extracellular signals and intracellular nutrients needed for tumor growth and metastasis.

A wealth of studies both *in vitro* and *in vivo* has demonstrated that autophagy proteins and autophagic flux can alter the fate of cancer cells and tumors. However, the existence of conflicting reports on the pro- versus anti-tumorigenic effects of autophagy clearly demonstrates that autophagy is not a uniform phenomenon but is highly context-dependent. As the field has become to expand its focus from the effects of autophagy on primary tumor growth to its effects on metastasis, it is critical that we keep in mind this lesson. The work in this thesis explores the role of autophagy in cellular motility and metastasis in highly metastatic tumor cells. Specifically, this work focuses on the role of autophagy in the regulation of cell migration through the degradation of the focal adhesion protein paxillin (Chapter 3). Furthermore, I demonstrate that paxillin interacts directly with the focal adhesion protein LC3B (Chapter 4) and that this interaction is regulated by oncogenic Src (Chapter 5). These findings shed light on a new mechanism by which autophagy can promote tumor cell metastasis.

CHAPTER 2

MATERIALS AND METHODS

Chemicals

BafilomcyinA1 was purchased from Enzo and was used at a final concentration of 100 µM. Puromycin was purchased from Fisher and was used at a final concentration of 4 µg/mL. Rat tail collagen 1 was obtained from BD and was used at 0.02 mg/mL in PBS.

Cell culture

4T1 cells[234] were obtained from Fred Miller at Wayne State University, and B16.F10 cells[235] were kindly provided by the Gajewski lab. 4T1 and B16.F10 cells were grown in Dulbecco's modified eagle medium (DMEM; Invitrogen) supplemented with 10% characterized fetal bovine serum (FBS; HyClone) and 1% penicillin/streptomycin (Pen/Strep; Invitrogen); 4T1 media was additionally supplemented with 1x minimal essential medium non-essential amino acids (MEM-NEAA; Invitrogen). 4T1 shRNA clones were grown in complete media supplemented with 4 µg/ml puromycin (Fisher) based on the minimum effective inhibitory concentration. All cells were grown in a 37°C humidified incubator with 5% CO_2.

Stable knockdowns

pLKO-puro plasmids expressing shRNA targeting mouse Atg7 (TRCN0000375444), p62 (TRCN0000098619), Nbr1 (TRCN0000238310), MAP1LC3B/Atg8 (TRCN0000120800), and paxillin (TRCN0000305025) and a pLKO-puro plasmid expressing non-targeting control shRNA

(SHC002) were purchased from Sigma. A custom-made pLKO-puro plasmid expressing shRNA to human/mouse ATG5/Atg5 (seed sequence: GCATTATCCAATTGGTTT) was purchased from Sigma. Plasmids were transfected into 4T1 cells using Lipofectamine 2000 (Invitrogen) in Opti-MEM I Reduced Serum Medium (Invitrogen), and selection was performed with 4 μg/mL puromycin (Fisher) based on the minimum inhibitory concentration. At least twenty-four single colonies per knockdown target were picked and expanded to for the validation of successful knockdown by western blot; at least two independent and validated stable knockdown cell lines were established for further analysis.

Paxillin siRNA

Non-targeting control (Santa Cruz sc-37007) or paxillin siRNA (Santa Cruz sc-36197) was transfected into cells at a concentration of 50 nM using Lipofectamine 2000 (Invitrogen) in Opti-MEM I Reduced Serum Medium (Invitrogen). All downstream assays were carried out starting at 48 hours post-transfection.

Plasmid transfections

Transient plasmid transfections were performed using Lipofectamine 2000 (Invitrogen) in Opti-MEM I Reduced Serum Medium (Invitrogen); the DNA/lipofectamine complexes were removed after 6 hours, after which the cells were returned to normal growth media for recovery and plasmid expression. DNA transfection amounts were normalized to ensure equal expression among different plasmid constructs (e.g., EGFP vs. EGFP-LC3B). All downstream assays were carried out starting at 24 hours post-transfection.

Plasmids and cloning

The EGFP-paxillin plasmid was kindly provided by Rick Horwitz (University of Virginia). The pSG5-Src^{Y527F} plasmid was a kind gift from Sara Courtneidge (OHSU). The Gardel lab (University of Chicago) provided the mApple-paxillin plasmid, and the Tang lab (University of Chicago) provided the EGFP-LC3B plasmid.

For the generation of paxillin mutants, polymerase chain reaction (PCR) mutagenesis was performed using the Expand High Fidelity^{PLUS} PCR system (Roche). The PCR products were separated on a 1% agarose gel, and the bands containing the correctly sized product were cut out and purified using the Wizard SV Gel and PCR Clean-Up System (Promega). A second-round PCR reaction was performed using the first-round products as templates. The PCR products were again separated on a 1% agarose gel, cut out, and purified. Products were then digested using restriction enzymes and were ligated back into the original plasmid. Plasmids were transformed into DH5α cells, which were plated onto LB plates supplemented with the appropriate antibiotic for overnight growth. Individual colonies were picked the following day and grown in overnight cultures. DNA was purified using an in-house miniprep protocol. Insertion was confirmed by restriction digest, and plasmids containing the correctly sized restriction product were submitted for DNA sequencing analysis at the University of Chicago Comprehensive Cancer Center DNA Sequencing & Genotyping Facility. Constructs containing the desired sequence were then midiprepped with the Nucleobond Xtra Midi Plus Kit (Clontech).

Transwell assays

For invasion assays, 24-well 8-µm pore cell culture inserts (BD) were pre-coated with 200 µl rat collagen I (BD) at 0.02 mg/ml in cold, sterile phosphate-buffered saline (PBS;

Invitrogen) and allowed to dry overnight in a sterile tissue culture hood. The following day, the inserts were rehydrated with 100 µl serum-free media at 37°C for at least 45 minutes. 4T1 cells in 200 µl serum-free media were seeded per well as follows: $1x10^5$ cells per collagen-coated insert for invasion assays, and $5x10^4$ cells per uncoated insert for migration assays, with 3-6 replicates per condition. Complete medium (10% FBS) was added outside of the insert, and plates were incubated at 37°C for 16-22 h. Cells were fixed by incubating the inserts in 4% paraformaldehyde/PBS for 30 minutes, followed by Giemsa-staining for 1.5 hours. Inserts were washed 3x in distilled water, and non-migrating cells were scraped from the inner side of the insert membrane with a cotton swab. After membranes dried overnight, the migrating/invading cells were counted in five 20x fields per well.

Western blotting

Cells were washed in PBS supplemented with PMSF (0.5 mM), sodium orthovanadate (1 mM), leupeptin (1 µg/mL), and aprotinin (1 µg/mL), harvested by scraping, and subsequently pelleted at 4000xg for 4 min at 4°C. Cell pellets were lysed on ice for 15 minutes by 1:1 suspension in RIPA buffer (1% sodium deoxycholate, 0.1% SDS, 1% Triton X-100, 10 mM Tris-HCl pH 8.0, 0.14 M NaCl) or 1:2 suspension in NP40 buffer (for LC3 western blots; 150 mM NaCl, 50 mM Tris-HCl pH 7.5, 1 mM EDTA, 1% NP40) supplemented with protease and phosphatase inhibitors as above. Lysates were clarified by centrifugation at 16300xg for 20 min at 4°C, supernatants were collected, and protein concentration was determined by DC protein assay (BioRad). SDS-PAGE (8%-15%) was used to separate 20-40 µg protein, depending on the protein being detected. After proteins were transferred to nitrocellulose or PVDF membranes (for LC3), membranes were blocked in 5% milk/PBS or 5% BSA/PBS and incubated at 4°C

overnight with primary antibody (Table 2.1). For LC3B westerns, membranes were cut to remove the >25 kDa portion prior to incubation with primary antibody. After washing, two-hour incubation with HRP-conjugated secondary antibodies (Table 2.1), and additional washes, detection was carried out by enhanced chemiluminescence.

All densitometry was performed on scanned images of films using the gel analysis tool in ImageJ. After measurement, band intensities were normalized to actin loading control band intensity, and normalized values are reported as fold change relative to the first lane of the blot unless otherwise noted.

Table 2.1: Primary antibodies used for western blot

Target	Source/Catalogue Number	Dilution
Atg5	Novus NB110-53818	1:500
Atg7	Sigma A2856	1:1,000
β-actin	Sigma A1978 (clone AC-15)	1:50,000
E-cadherin	Cell Signaling #3195	1:1,000
GABARAP	MBL M135-3	1:1,000
GABARAPL1	Proteintech 18721-1-AP	1:500
GATE16	MBL PM038	1:1,000
GFP	Santa Cruz sc-9996	1:1,000
LC3A	Proteintech 18722-1-AP	1:1,000
LC3B	Novus NB600-1384	1:3,000
Nbr1	Cell Signaling #9891	1:1,000
P62	Progen CP62-C	1:5,000
Paxillin	BD #610558 (clone 177) Millipore #2492134	1:2,000 1:10,000
Twist1	Abcam ab50887	1:50
Guinea pig IgG (HRP-conjugated)	Santa Cruz sc-2903	1:5,000
Mouse IgG (HRP-conjugated)	Dako P0260	1:5,000 (1:50,000 for β-actin)
Rabbit IgG (HRP-conjugated)	Dako P0217	1:4,000

Immunoprecipitation (IP) and *in vitro* binding assays

For Atg7 IP-westerns, RIPA lysates were incubated with 1.5 µg anti-Atg7 at 4°C overnight and subsequently with protein A beads (Pierce) at 4°C for 1 hour. The beads were washed four times with RIPA buffer and eluted in 2X SDS sample buffer (187.5 mM Tris pH 6.8, 6% w/v SDS, 30% glycerol, 150 mM DTT, 0.03% w/v bromophenol blue, 2% β-mercaptoethanol) by boiling at 100°C for 5 min for western blot analysis as described previously.

For co-immunoprecipitations, 4T1 cells were seeded at 4-8 x 10^5 cells per 10-cm plate. The following day, cells were transfected as described previously. The morning after transfection, the plates with cells at ~80% confluency were washed 1x with ice-cold PBS, followed by the addition of cold IP lysis buffer (50 mM Tris pH 8.0, 150 mM NaCl, 5 mM EDTA, 5% glycerol, 1% triton x-100, 25 mM NaF) supplemented with phosphatase (PhosSTOP; Roche) and protease inhibitors (cOmplete protease inhibitor cocktail without EDTA; Roche). Cells were incubated with IP lysis buffer for 30 min at 4°C with constant rocking. Cells were scraped from the dishes and subjected to sonication at 10% amplitude for four cycles of 5 sec on/5 sec off at 4°C, followed by centrifugation at 21130xg for 20 min at 4°C. The supernatants were recovered and assayed for total protein concentrations using a DC protein assay (BioRad), and a sample of the lysate was saved as an input control. Approximately 2 mg lysate was diluted to a 1 mL final volume in IP lysis buffer and was precleared for 1 h with binding control agarose beads at 4°C (Chromotek). Samples were centrifuged at 2500xg for 2 min to recover supernatant, and binding control agarose beads were discarded. The supernatant was then incubated with GFP-trap agarose beads overnight at 4°C. Samples were subsequently centrifuged at 2500xg, washed thrice in IP lysis buffer, and eluted in 2X SDS sample loading buffer (187.5 mM Tris pH

6.8, 6% w/v SDS, 30% glycerol, 150 mM DTT, 0.03% w/v bromophenol blue, 2% β-mercaptoethanol) by boiling at 100°C for 10 min. The samples were cooled on ice and centrifuged at 16300xg for 2 min, and the supernatants were recovered and store at -80°C until use.

Approximately 20 ug of each input sample was subjected to western blot to assess the level of expression of exogenous proteins (e.g., GFP-LC3, mApple-paxillin, etc.). The loading of subsequent input and IP samples was adjusted to normalize to the levels of exogenous proteins in the input samples. Western blot was performed as described previously, with the following change: the anti-paxillin antibody (BD) was used at a dilution of 1:250.

Immunofluorescence

For LC3B staining, cells were fixed in 4% paraformaldehyde (PFA) for 15 minutes at room temperature, permeabilized in 100% MeOH at -20°C for 20 minutes, and blocked in 2% FBS/1% goat serum/PBS for 30 minutes at room temperatures. Otherwise, cells were fixed and permeabilized (3.7% PFA/PBS in 100 mM PIPES pH 6.8, 10 mM EGTA, 1 mM MgCl2, and 0.2% Triton-X) for 10 minutes at room temperatures, washed in TBS/0.1% triton and blocked in TBS/0.1% BSA for 30 minutes. Cells were incubated with primary antibody diluted in blocking solution overnight at 4°C, followed by washing and incubation with fluorescence-labeled secondary antibodies (Invitrogen) diluted in blocking solution for two hours at room temperature in the dark (Table 2.2). Cells were mounted in Prolong gold with DAPI (Invitrogen) and protected from light until imaging. Cells were imaged with an Axiovert200m widefield fluorescence microscope (Zeiss). Image deconvolution was performed with Openlab software (PerkinElmer); all other image analysis was performed with ImageJ.

Table 2.2: Antibodies for immunofluorescence

Target	Source/Catalogue Number	Dilution
LC3B	Cell Signaling #2775	1:200
Paxillin	BD #610051 (clone 349)	1:500
Zyxin	Mary Beckerle, University of Utah, B71	1:6000
Rabbit IgG, Alexa-488-conjugated	Invitrogen A11008	1:500
Rabbit IgG, Rhodamine Red-X-conjugated	Invitrogen R6394	1:500
Mouse IgG, Alexa-488-conjugated	Invitrogen A11029	1:500
Mouse IgG, Rhodamine Red-X-conjugated	Invitrogen R6393	1:500

Live cell microscopy

Cells were seeded in 35-mm #1.5 glass-bottom dishes (MatTek) for 24 hours prior to imaging. Timelapse DIC and fluorescence imaging were carried out with an Olympus LCV110U VivaView microscope system maintained at 37°C and 5% CO_2. Confocal imaging of mApple-paxillin and EGFP-LC3B was performed on an Olympus DSU Spinning Disk confocal microscope. Colocalization was analyzed on background-subtracted Z-stacks (0.5-µm slices) in ImageJ using the JACoP object-based method (Bolte and Cordelieres, 2006) with 10-15 images (10-25 cells)/condition/experiment.

GABARAP immunohistochemistry

Neutral buffered formalin (10%)-fixed and paraffin-embedded sections of 4T1 primary tumors sections were provided to the University of Chicago Human Tissue Resource Center for GABARAP immunohistochemistry. Briefly, slides were incubated in xylenes, followed by rehydration in serial dilutions of ethanol to deionized water. After epitope retrieval, endogenous peroxidase activity was quenched. Sections were blocked (Vector Laboratories) for 30 minutes at room temperatures and were incubated in primary antibody diluted in blocking buffer for 1 hour at room temperature, followed by biotinylated-secondary antibody with avidin-biotin signal amplification (Vector Laboratories). The proteins were visualized by Elite kit (Vector Laboratories) and DAB (DAKO). The stained slides were digitized using an Allied Vision Technologies Stingray F146C color slide scanner at the Integrated Microscopy Core Facility at the University of Chicago and analyzed using Panoramic Viewer.

Statistics

Data were analyzed with GraphPad Prism. Data are presented as mean ± SE. Significance was determined by unpaired Student's t-test for 2-group comparisons and 1-way ANOVA for >2-group comparisons. A Tukey post-hoc test was used to identify significant pairwise differences when 1-way ANOVA identified a significant difference between means. *$p<0.05$, **$p<0.01$, ***$p<0.001$, ****$p<0.0001$

CHAPTER 3

TURNOVER OF THE FOCAL ADHESION PROTEIN PAXILLIN IN 4T1 METASTATIC MURINE MAMMARY CARCINOMA CELLS IS DEPENDENT ON INTACT AUTOPHAGY

Introduction

In the context of primary tumor growth, autophagy can serve both pro-tumorigenic and anti-tumorigenic roles (Figure 1.2). Early in tumor progression, autophagy can limit oxidative stress, aggregate formation, and the accumulation of damaged organelles, as well as promoting the degradation of oncogenic proteins or induction of senescence in response to oncogenic proteins. During growth of the primary tumor, autophagy can allow cancer cells to cope with metabolic stress, generate biosynthetic intermediates, maintain a CSC population, and survive challenges of hypoxia and anoikis[5,128–130]. These stage-dependent roles of autophagy have been extensively studied both *in vitro* and *in vivo*, and the generation of several mouse models seems to confirm that early inhibition of autophagy promotes malignant transformation and the development of early lesions, whereas autophagy is required in established tumors to progress to a more advanced phenotype[135–137,141,156–158].

The role of autophagy in metastasis is less well characterized, although it is likely that autophagy may similarly exhibit pro- and anti-cancer effects dependent on the stage, oncogene status, and tissue type[205]. In human tumors, increased expression of autophagic markers has been correlated with metastasis and a more aggressive phenotype, potentially suggesting that metastatic cells exhibit increased autophagic flux as a means to promote metastasis[150,202–204].

Experimental evidence supports role for autophagy in the response to metastatic stimuli[107,108,206–208]. Furthermore, autophagy may play a role in EMT, CSC maintenance, and as a means of coping with the stress of ECM detachment and growth factor deprivation (see Chapter 1). However, relatively little work has been done to explore the role of autophagy during *in vivo* metastasis, and whether the roles of autophagy in metastasis extend to other stages in the metastatic cascade remained unclear.

Previous work in our lab sought to address the role of autophagy in metastasis by examining the effect of autophagy inhibition on tumor cell metastasis using the 4T1 murine model of metastatic mammary carcinoma. In this model, highly metastatic cells derived from a spontaneous Balb/C mouse mammary tumor are injected into the mammary fat pad of syngeneic Balb/C mice. The mice develop palpable tumors within two weeks, which subsequently metastasize to the lung and liver by 4 weeks post-injection[234]. Autophagy was inhibited in 4T1 cells through stable shRNA-mediated knockdown of either *Atg5* or *Atg7*. Both Atg5 and Atg7 are core autophagy proteins required for PE conjugation of LC3B to localize LC3B to the phagophore membrane and promote autophagosome formation (Figure 1.1). Interestingly, the primary tumor growth of autophagy-deficient 4T1 cells expressing *Atg5*- or *Atg7*-specific shRNA did not differ from that of parental 4T1 tumors or tumors expressing scrambled control shRNA despite the tumors continuing to exhibit inhibition of autophagy as measured by a lack of LC3B-positive puncta. However, mice harboring autophagy-deficient tumors exhibited a significant reduction in the number of lung and liver metastases. Thus, in the 4T1 tumor murine mammary carcinoma model, autophagy is not required for primary tumor growth but is required for metastasis. Interestingly, when autophagy-deficient and autophagy-competent 4T1 cells were injected into the tail vein, thereby bypassing the early steps of the metastatic cascade (i.e., local

invasion and intravasation), there was no difference among the cells with respect to the ability to form metastases, suggesting that autophagy is required early in the metastatic processes in this model.

When the autophagy-deficient and autophagy-competent 4T1 cells were examined *in vitro*, they exhibited markedly different morphologies. Although cells expressing a scrambled shRNA spread out and formed the lamellipodia and pseudopodia characteristic of migratory cells and could be observed to move about on the plate, autophagy-deficient cells formed tight, rounded colonies without protrusions and failed to move around. Consistent with this observation, autophagy deficient cells exhibited impaired migration and collagen invasion in transwell assays. Given the critical role of the cytoskeleton and focal adhesions in cell motility, our lab examined focal adhesion morphology in the 4T1 cells. Scrambled shRNA-expressing control cells exhibited paxillin-positive focal adhesions that could be observed to assemble and disassemble over time. However, autophagy-deficient cells exhibited an accumulation of enlarged focal adhesions. Furthermore, when focal adhesion dynamics were examined, although autophagy-deficient cells were able to successfully assemble focal adhesions, they exhibited significantly impaired focal adhesion disassembly relative to control cells. These observations of impaired cell motility and the accumulation of enlarged focal adhesions that could not be turned over suggested that autophagy is required for proper focal adhesion dynamics in highly metastatic cells. Thus, we were interested in determining the mechanism underlying the *in vitro* motility and focal adhesion defects leading to *in vivo* metastasis inhibition of autophagy-deficient cells.

Altered focal adhesion morphology and motility in autophagy-deficient 4T1 cells do not reflect a change in EMT programming.

The change in the morphology of the autophagy-deficient cells, including decreased cell spreading, decreased protrusions, and decreased cell motility, suggested the possibility that the autophagy-deficient 4T1 cells were adopting a more epithelial cellular program, consistent with suggestions that 4T1 cells exist in a highly plastic state that primes them to interchange between a mesenchymal and epithelial phenotype[234,236]. Furthermore, recent work has suggested that the autophagy adaptor protein p62/Sqstm1 regulates the degradation of the metastasis-associated Twist1 transcription factor[224]. Therefore, we assessed the levels of Twist1 and E-cadherin in autophagy-deficient 4T1 cells. Elevated expression of E-cadherin in autophagy-deficient cell lines would reflect the adoption of a more epithelial and thus less motile phenotype. Similarly, downregulation of Twist1 could reflect suppression of an EMT transcriptional program. However, neither the levels of the Twist1 EMT transcription factor nor the levels of the epithelial marker E-cadherin differed in autophagy-deficient cells relative to autophagy-competent cells (Figure 3.1), suggesting that the morphological and focal adhesion changes in autophagy-deficient cells were not caused by changes in the mesenchymal cellular state.

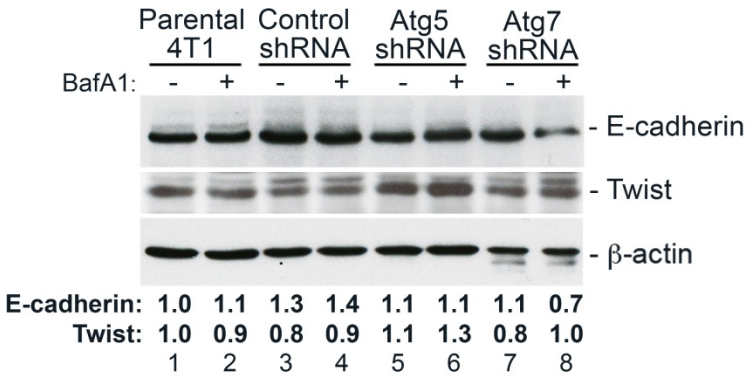

Figure 3.1 E-cadherin and Twist levels are unchanged in autophagy-deficient cells. Western blot for E-cadherin and Twist in parental 4T1 cells and clonal 4T1 cells stably expressing a scrambled control shRNA, Atg5 shRNA, or Atg7 shRNA in the presence or absence of BafA1 to inhibit lysosomal degradation, demonstrating no change in either E-cadherin or Twist levels upon autophagy inhibition.

Paxillin accumulation underlies the focal adhesion and motility defects in autophagy-deficient 4T1 cells.

Given that previous work our lab had established that autophagy-deficient cells exhibit impaired metastasis *in vivo* as well as impaired motility and focal adhesion disassembly *in vitro,* we sought to determine the mechanism underlying impaired focal adhesion disassembly. Interestingly, cells lacking FAK[196], catalytically active Src[199], or paxillin[237] exhibit decreased cell spreading and motility in association with increased focal adhesion size and number and impaired focal adhesion disassembly, phenocopying our observations in autophagy-deficient 4T1 cells. Although we did not observed any alterations in FAK or Src protein levels or phosphorylation status (data not shown), we observed significantly increased paxillin levels in 4T1 cells stably knocked down for Atg5 or Atg7 expression relative to both parental cells and cells stably expressing scrambled control shRNA (Figure 3.2A, 3.2B). Furthermore, treatment of parental and scrambled shRNA control 4T1 cells with BafA1, a potent and specific inhibitor of vacuolar H+ ATPase[68–70] that prevents the maturation of autophagic vacuoles and can be used to inhibit autophagy *in vitro*[71], similarly resulted in an accumulation of paxillin protein, suggesting that the autophagic regulation of paxillin levels is physiologic in 4T1 tumor cells (Figure 3.2A, 3.2B). This observation was also confirmed *in vivo*; lysates from autophagy-deficient 4T1 tumors exhibited accumulation of paxillin protein relative to control primary 4T1 tumors (data not shown). Finally, this increase in paxillin levels was due to increased protein stability, not increased mRNA levels, and was independent of proteasomal activity (data not shown).

To determine whether the accumulation of paxillin underlies the cell motility defects in autophagy-deficient 4T1 cells, siRNA was used to transiently knock down paxillin levels in 4T1 cells stably expressing Atg5 shRNA to levels similar to those in parental cells (Figure 3.3A).

Normalization of paxillin levels restored the focal adhesion morphology to that of control 4T1 cells, resulting in fewer and smaller focal adhesions (Figure 3.3B). Furthermore, knockdown of paxillin levels and normalization of focal adhesion morphology rescued the transwell migration and invasion defect observed in autophagy-deficient cells (Figure 3.3C, D). Taken together, these results provide strong evidence that paxillin levels in the highly metastatic 4T1 cells are regulated by autophagy and that the increase in paxillin protein levels in autophagy-deficient cells leads to the accumulation of abnormal focal adhesions and resultant motility defects.

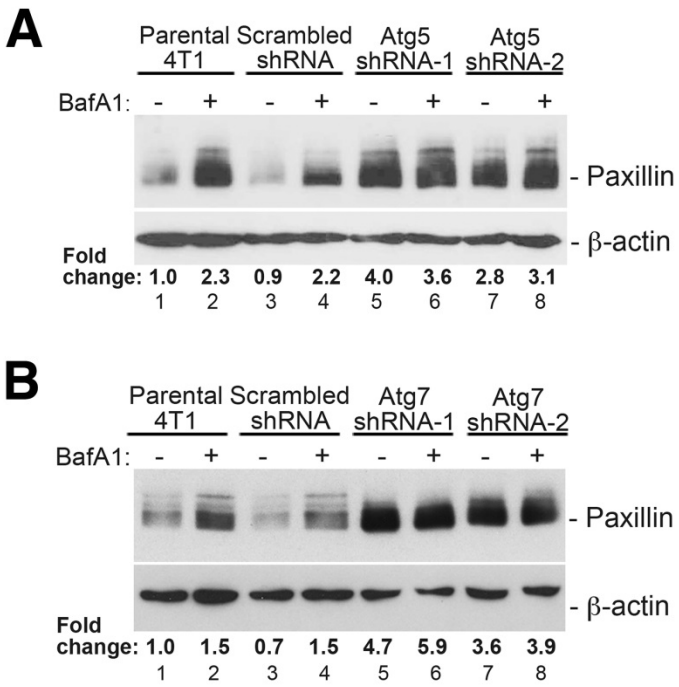

Figure 3.2 Paxillin accumulates in autophagy-deficient cells. (A, B) Western blot for paxillin in control 4T1 cells (parental and scrambled shRNA) and two different 4T1 clones stably expressing Atg5 shRNA (A) or Atg7 shRNA (B) in the presence or absence of BafA1. Data in panel (A) was generated by M. Sharifi.

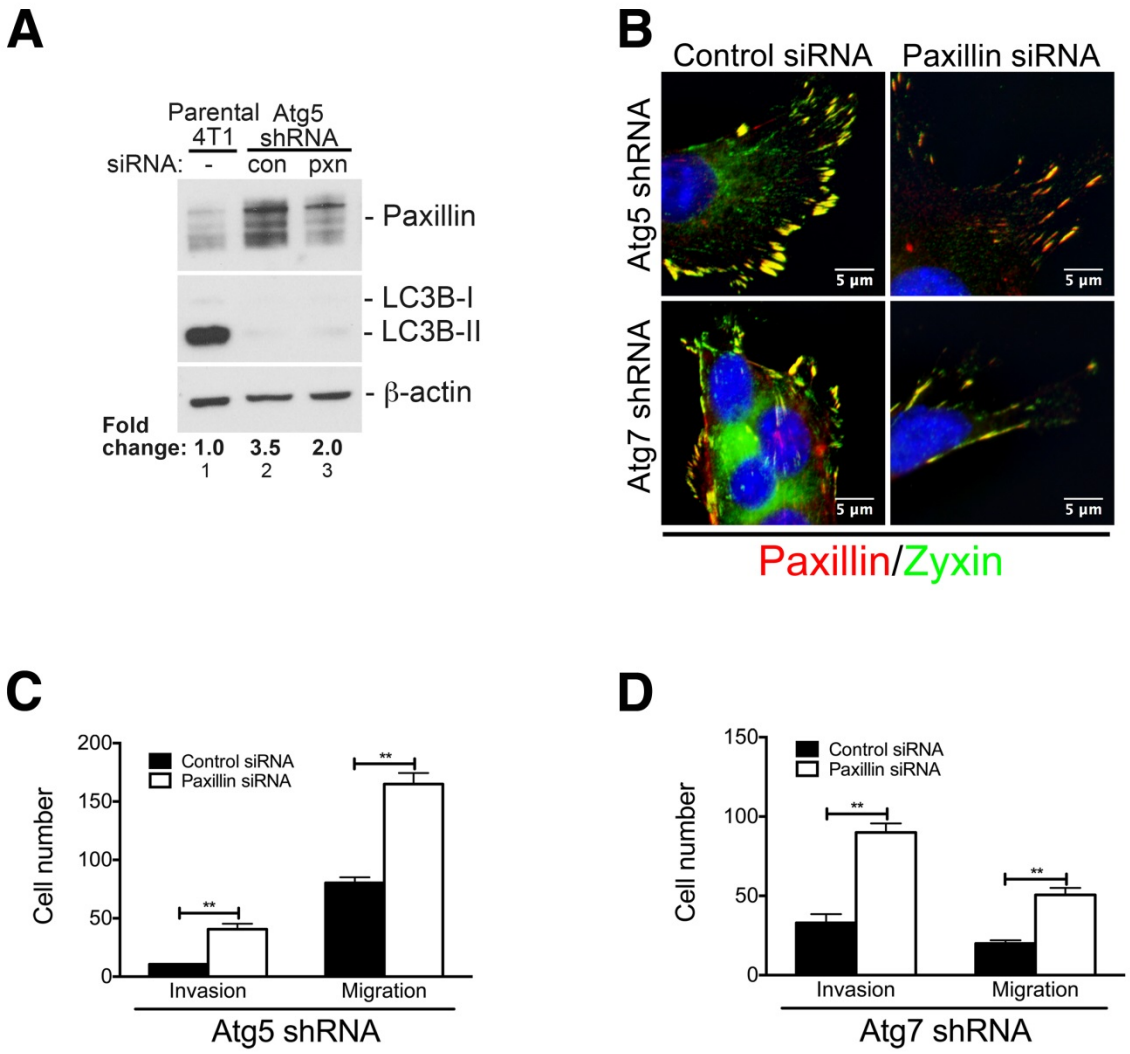

Figure 3.3 Restoration of paxillin levels rescues defects in focal adhesion morphology and cell motility. (A) Western blot confirming paxillin knockdown in autophagy-deficient 4T1 cells with no effect on impaired LC3B processing. (B) Immunofluorescent staining of paxillin and zyxin in 4T1 cells stably expressing Atg5 shRNA (top) or Atg7 shRNA (bottom) transiently transfected with control (left) or paxillin siRNA (right). (C, D) Quantification of the effects of siRNA-mediated paxillin knockdown on transwell migration (right) and invasion through collagen (left) in 4T1 cells stably expressing Atg5 shRNA (D) and Atg7 shRNA (D). **p<0.01. Data in panels B-D were collected by M. Sharifi.

Autophagic degradation of paxillin is not dependent on the p62/Sqstm1 or Nbr1 autophagy adaptor proteins.

We next focused our investigation on the mechanism underlying the autophagic degradation of paxillin. Selective targeting of proteins to the autophagosome can occur either through direct binding of the target protein to LC3 family members on the surface of the forming autophagosome or through binding to selective autophagy receptors that link the target protein to the autophagic machinery[238]. In the latter case, autophagic receptors recognize the target protein by binding molecular determinants; one common example is conjugated ubiquitin. Paxillin is known to be ubiquitinated *in vivo* by RNF5, and this ubiquitination serves to regulate cellular paxillin localization[239]. Two of the best-characterized autophagic adaptor proteins for ubiquitinated proteins include p62/Sqstm1 and Nbr1[75,83,238,240]. Both of these proteins have been implicated in the regulation of cell migration, with p62/Sqstm1 suggested to function in concert with Twist1[224] and Nbr1 suggested to regulate focal adhesion dynamics in Ras-transformed epithelial cells[241]. Therefore, we asked whether either of these two well-characterized autophagy adaptor proteins were involved in targeting paxillin to the autophagosome and subsequent cell motility changes.

We generated 4T1 cell lines in which the expression of p62/Sqstm1 or Nbr1 was stably knocked down by shRNA (Figure 3.4A, B). However, we failed to observe stabilization of paxillin under basal conditions in cells expressing p62/Sqstm1 or Nbr1 shRNA, and these cells failed to exhibit accumulation of paxillin upon BafA1 treatment to the same degree as parental or control shRNA cells (Figure 3.4A, B). On the contrary, paxillin levels seemed to be suppressed in both p62/Sqstm1 shRNA and Nbr1 shRNA cells. Furthermore, knockdown of p62/Sqstm1 or Nbr1 had no statistically significant effect on the ability of these cells to migrate or invade

through collagen in transwell assays, as would be expected if either autophagy adapter were involved in paxillin and focal adhesion regulation in this cell system (Figure 3.4C, D). Finally, our attempts to co-immunoprecipitate paxillin with either p62/Sqstm1 or Nbr1 were unsuccessful. Together, these data confirm that the autophagic degradation of paxillin and the motility defects observed in autophagy-deficient 4T1 cells are independent of the p62/Sqstm1 and Nbr1 autophagy adaptor proteins.

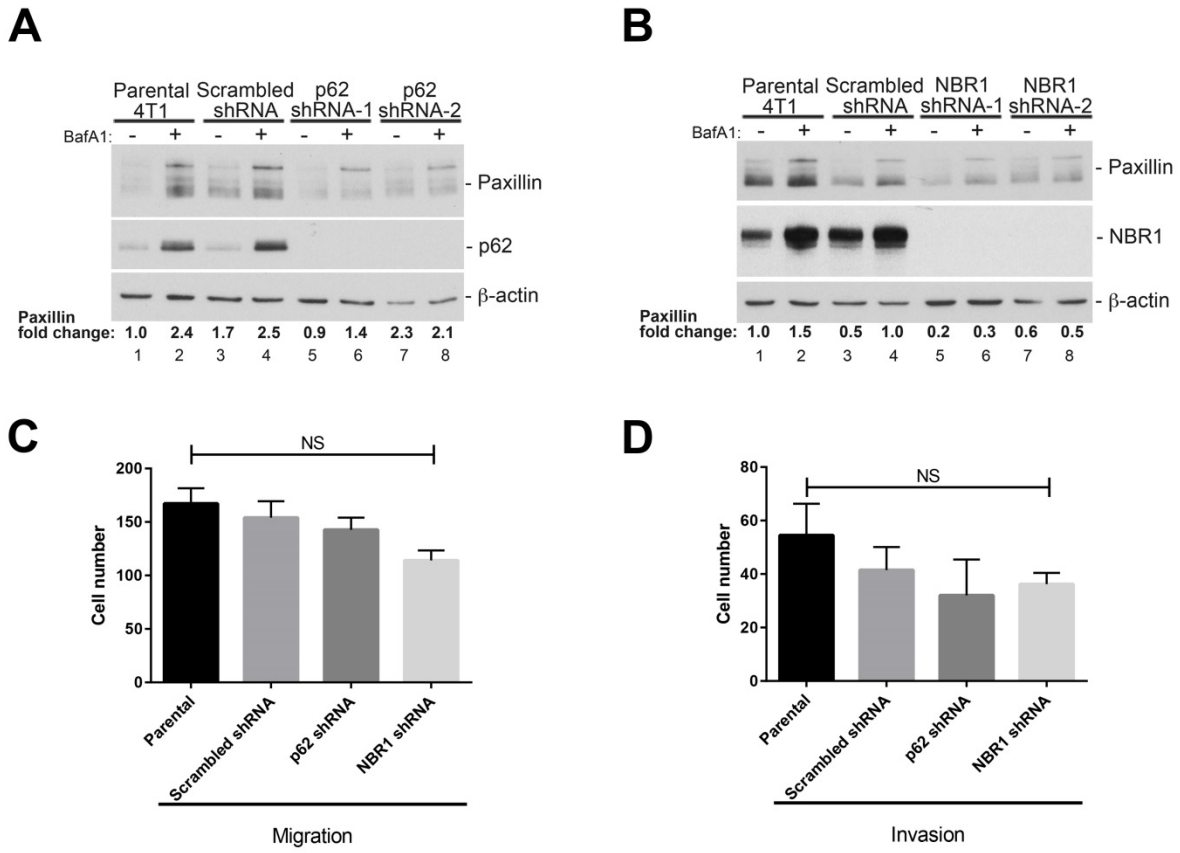

Figure 3.4 Neither p62/Sqstm1 nor Nbr1 are responsible for the accumulation of paxillin and consequent motility defects in autophagy-deficient cells. (A, B) Western blot for paxillin in control 4T1 cells (parental and scrambled shRNA) and two different 4T1 clones stably expressing p62 shRNA (A) or Nbr1 shRNA (B) in the presence or absence of BafA1. (C, D) Quantification of the transwell migration (C) and invasion through collagen (D) of parental 4T1 cells and 4T1 cells stably expressing scramble control shRNA, p62 shRNA, or Nbr1 shRNA. NS, not significant.

Knockdown of the Atg8 family member GABARAP phenocopies knockdown of Atg5 and Atg7

Given that neither p62/Sqstm1 nor Nbr1 were responsible for autophagic targeting of paxillin, we investigated whether paxillin could bind directly to the autophagic machinery by binding to Atg8 family proteins anchored in the phagophore membrane. Interestingly, paxillin possesses a putative LC3-interacting region (LIR) motif at amino acids 40-43 (Figure 3.5A). LIR motifs are defined by the core consensus sequence [W/F/Y]xx[L/I/V], where x represents any amino acid[72]. Most LIR motifs include a W or an F in the +1 aromatic position, although Y-containing LIRs, including Nbr1, are known and have been shown to bind in a manner similar to W-containing LIRs[72,85]. The presence of an acidic charge (e.g., E, D, S, or T) in the -1 or +2 position is also important to binding and can act as a site of regulation[72]. The putative LIR motif of paxillin is highly conserved from *Xenopus* through humans, suggesting that this region may have functional significance (Figure 3.5B).

As a clue into which Atg8 family member may bind paxillin, we examined the levels of several Atg8 family members in parental 4T1 cells (Figure 3.6). Atg8 family members are divided into two subgroups, LC3A-C and GABARAP, GABARAPL1, GATE16, and GABARAPL3, which may be expressed simultaneously and are believed to act at different stages in autophagosome biogenesis[56,57,242]. Although the levels of LC3A, GABARAPL1, and GATE16 were absent or barely detectable in 4T1 cells, both LC3B and GABARAP were expressed at high levels and increased upon BafA1 treatment (Figure 3.6). *In vivo,* GABARAP and LC3B were expressed in 4T1 control primary tumors (Figure 3.7 and data not shown, respectively). Interestingly, IHC for GABARAP revealed a striking accumulation of GABARAP

at the tumor periphery, where tumor cells would be most likely to adopt a more motile phenotype in the early stages of metastasis from the primary tumor.

To probe the potential role of GABARAP in the paxillin accumulation in autophagy-deficient cells, we stably transfected 4T1 cells with GABARAP shRNA and examined the levels of paxillin in cell lysates. As observed in Atg5 and Atg7 knockdown 4T1 cells, knockdown of GABARAP resulted in significant paxillin accumulation (Figure 3.8A). Furthermore, GABARAP knockdown cells exhibited reduced migration and invasion in transwell assays (Figure 3.8B). Thus, the phenotype of the GABARAP knockdown cells mimicked that of the Atg5 and Atg7 knockdown cells. This could suggest that GABARAP is the binding partner of paxillin responsible for its autophagic targeting and subsequent turnover. However, to date, we have been unable to generate co-immunoprecipitation or co-immunofluorescence data supporting such an interaction, potentially due in part to limitations on the available reagents for detecting GABARAP. Alternatively, the ability of GABARAP knockdown to phenocopy knockdown of Atg5 and Atg7 is consistent with reports that GABARAP is indispensable for autophagy[56], like Atg5 and Atg7, and could suggest that inhibition of the autophagic process either during phagophore elongation (i.e., Atg5 or Atg7 knockdown) or autophagosome maturation (i.e., GABARAP knockdown) is sufficient to block autophagic degradation of paxillin and cause abnormalities in focal adhesion morphology and cell motility.

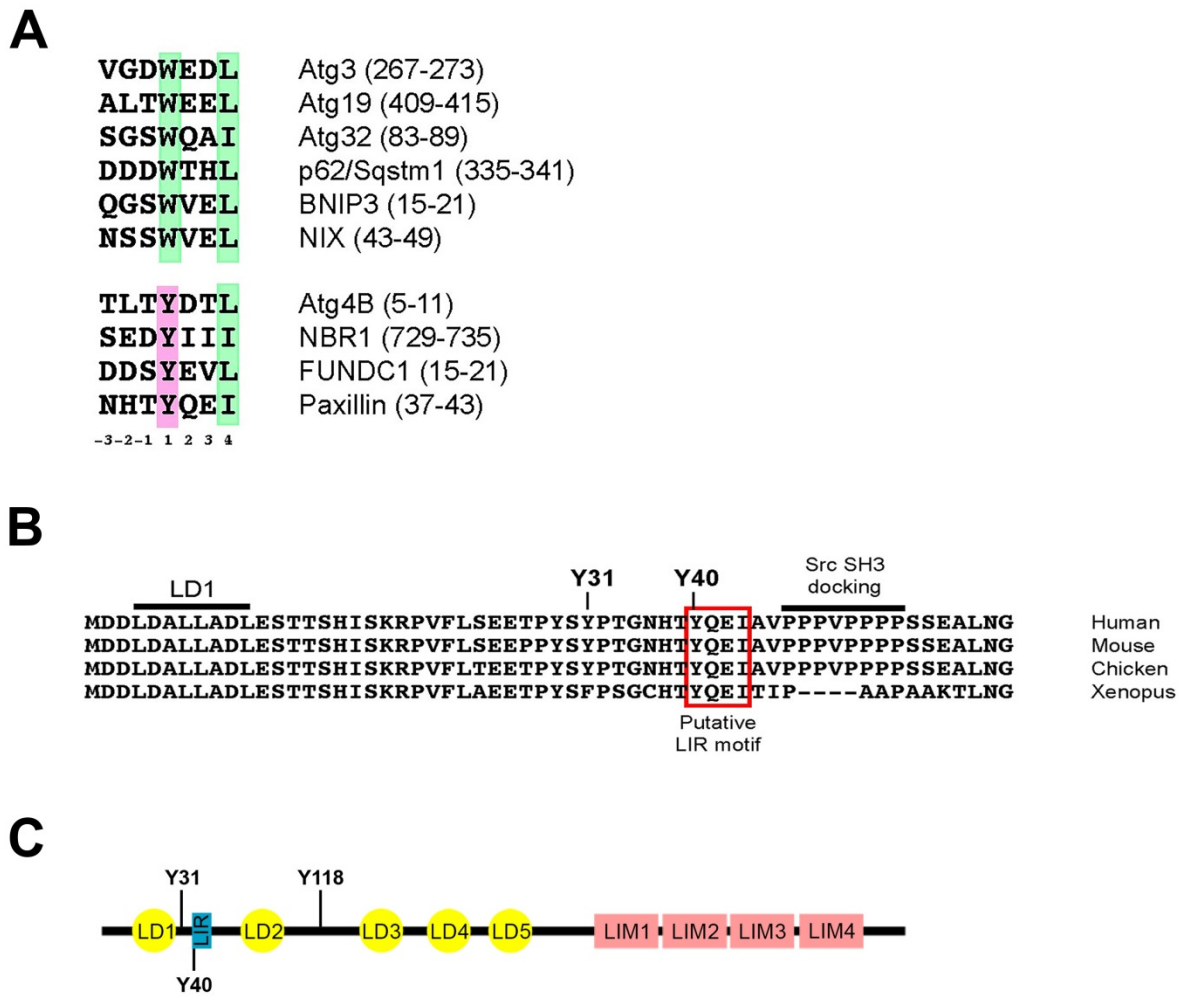

Figure 3.5 Paxillin possesses a putative LC3-interating region (LIR) motif. (A) Alignment of human paxillin residues 37-43 (last line) with the -3 to +4 residues of known tryptophan- (top) and tyrosine-containing LIR motifs (bottom). LIR motifs contain the sequence [W/F/Y]xx[L/I/V]. (B) Alignment of residues 1-60 of paxillin in human, mouse, chicken, and *Xenopus* containing the conserved putative LIR motif. (C) The putative paxillin LIR is located in the N-terminal regulatory region between LD1 and LD2. Src phosphorylation sitesY31, Y40, and Y118 are indicated.

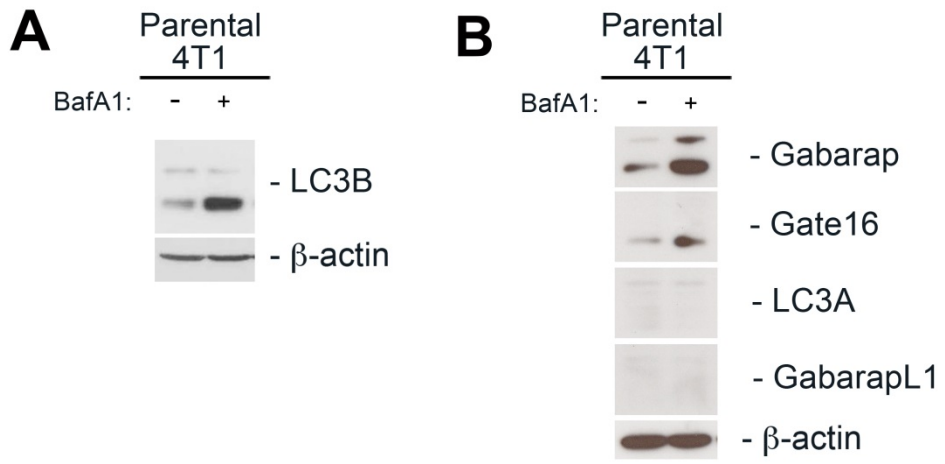

Figure 3.6 Expression of Atg8 family members in 4T1 cells. (A) Western blot for LC3B in parental 4T1 cells in the presence or absence of BafA1. (B) Western blot for GABARAP, GATE16, LC3A, and GABARAPL1 in parental 4T1 cells in the presence or absence of BafA1.

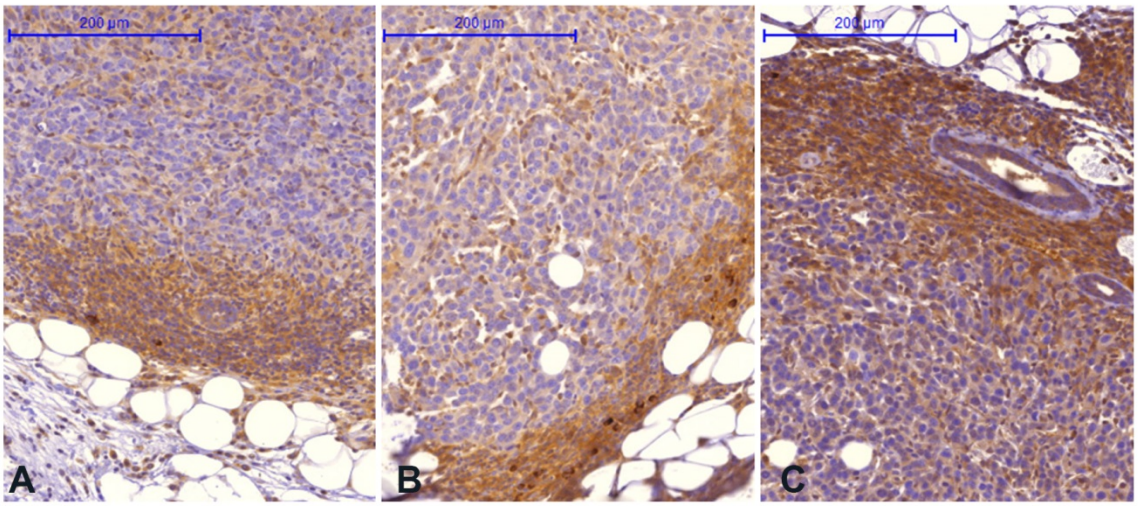

Figure 3.7 GABARAP accumulates at the periphery of 4T1 tumors. (A-C) Immunohistochemical staining for GABARAP in three examples of 3-week-old 4T1 control tumors expressing scrambled shRNA demonstrates increased staining at the tumor periphery. Scale bars are indicated.

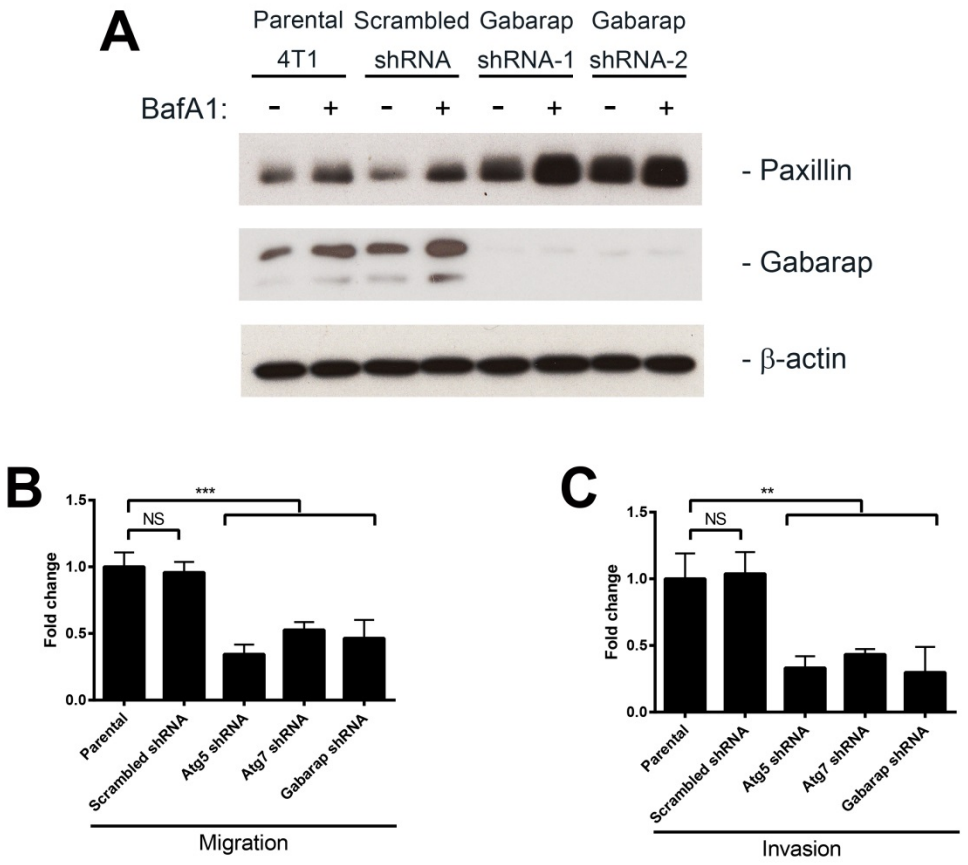

Figure 3.8 GABARAP knockdown results in paxillin accumulation and motility defects. (A) Western blot for paxillin in control 4T1 cells (parental and scrambled shRNA) and two different 4T1 clones stably expressing GABARAP in the presence or absence of BafA1. (B, C) Quantification of the transwell migration (B) and invasion through collagen (C) of parental 4T1 cells and 4T1 cells stably expressing scramble control shRNA, Atg5 shRNA, Atg7 shRNA, or GABARAP shRNA. NS, not significant; **p<0.01; ***p<0.001.

Conclusions

In this chapter, we have investigated the cause of the motility and focal adhesion defects in autophagy-deficient 4T1 mammary cancer cells. Despite previous reports of a role for p62/Sqstm1 in regulating EMT[224], these changes do not appear to be the result of a global change in an EMT phenotype. Instead, the elevated levels of paxillin observed in autophagy-deficient cells and upon pharmacologic inhibition of autophagy in control cells suggest that failure to autophagically degrade paxillin may underlie the phenotypes of Atg5 and Atg7 shRNA-expressing cells. In support of this hypothesis, knockdown of paxillin levels in autophagy deficient cells restores the focal adhesion and motility phenotype.

To determine the mechanism underlying autophagic degradation of paxillin, we first tested the hypothesis that the ubiquitinated protein adaptors p62/Sqstm1 or Nbr1 might promote delivery of paxillin to the autophagosome. Knockdown of either protein in autophagy-deficient cells, however, did not rescue paxillin levels or motility. Indeed, p62/Sqstm1 or Nbr1 knockdown had the opposite effect on paxillin levels – paxillin levels were actually slightly decreased in the absence of these adaptors. The reason for this is unclear. One possibility is that 4T1 cells are undergoing high levels of autophagic flux such that the recognition of LC3B by either cargo adaptors or direct interactions is rate-limiting in autophagic degradation. If this were the case, it is possible that the knockdown of a commonly used cargo adaptor (like p62/Sqstm1 or Nbr1) would liberate more potential LC3B molecules for binding to other adaptors or directly to proteins, thereby allowing increased autophagic degradation of paxillin and decreased paxillin levels in these cells. However, this explanation remains speculative. It is equally possible that the mechanism connecting knockdown of cargo adaptor levels with slight decreases in paxillin levels is more indirect; p62/Sqstm1 or Nbr1 may control the autophagic degradation of other proteins

that somehow affect paxillin levels in an autophagy-independent manner. Nonetheless, it appears that neither p62/Sqstm1 nor Nbr1 are directly involved in paxillin degradation, and as such, we did not pursue the more tentative, indirect connection between these adaptors and paxillin. It is important to note that we only tested the role of these two cargo adaptors; many other adaptors are known to exist, and it is possible that another adaptor mediates the autophagic degradation of paxillin either through direct binding or by facilitating the interaction.

The identification of a putative LIR in paxillin suggests that a direct interaction between paxillin and an Atg8 family member, not an autophagy adaptor, is responsible for autophagic degradation of paxillin. We determined that both GABARAP and LC3B are highly expressed in 4T1 cells, although it remains possible that the lack of detection of the other Atg8 family members was due to issues with antibody detection. The ability of GABARAP knockdown to phenocopy knockdown of Atg5 and Atg7 and, in particularly, the unique immunohistochemistry staining pattern of GABARAP at the tumor periphery, suggested that GABARAP might be directly responsible for paxillin binding. However, we have been unable to detect co-localization of GABARAP and paxillin by immunofluoresence, and our co-immunoprecipitates have failed to demonstrate an interaction. Whether this reflects the true biology or the limitations of GABARAP -specific reagents, which are less developed than those for LC3B, remains unclear. Future experiments should continue to test for a possible GABARAP /paxillin interaction using the co-immunoprecipitation system described and successfully employed in Chapter 4. Although the ability of paxillin to bind GABARAP cannot be established at this time, we can conclude that inhibition of autophagy either upstream of PE conjugation of Atg8 by Atg5 or Atg7 or downstream of phagophore elongation but upstream of phagophore closure by GABARAP is

sufficient to induce paxillin accumulation and leads to impaired 4T1 tumor cell motility. In the following chapter, we explored the possibility that LC3B is a direct binding partner of paxillin.

CHAPTER 4

PAXILLIN INTERACTS WITH LC3B THROUGH AN LC3-INTERACTING REGION MOTIF

Introduction

Autophagic can promote the bulk degradation of cytosol or the selective degradation of organelles and proteins. During selective autophagy of proteins, proteins are targeted to the autophagosome through cargo adaptors that recognize a molecular pattern on the protein (e.g., ubiquitin) or may directly bind to LC3/Atg8. Structurally, LC3/Atg8 proteins are referred to as ubiquitin-like proteins and contain two domains; the C-terminal tail is covalently linked to the membrane, whereas the N-terminal domain forms a β-grasp fold responsible for protein-protein ineractions[243]. Binding to LC3/Atg8 is mediated through a LIR motif in the target protein. LIR motifs are defined by the core consensus sequence [W/F/Y]xx[L/I/V], where x represents any amino acid[72]. The +1 and +4 position are most critical for binding, and these residues in the target protein become buried within two pockets within LC3/Atg8[243]. Nearby acidic residues can aid in the interaction by binding basic side chains adjacent to the LIR binding pockets[72,243].

There are several variations on the canonical WxxL LIR motif. For example, the aromatic +1 position may be occupied by a tyrosine residue[72,85]. Alternatively, LC3C is able to accommodate non-aromatic residues in the +1 position in an alternative binding location[93]. Noncontiguous three-dimensional LIR motifs have also been suggested[244]. A structural study of GABARAP with a 12-amino acid high-affinity peptide even revealed binding in an inverse orientation to canonical LIR sequences, with a C-terminal tryptophan in the +6 position binding

in the pocket usually occupied by the +1 aromatic residue; in this case, the +1 aromatic residue docked in another pocket conserved among Atg8/LC3 family members[243,245]. Finally, phosphodependent LIRs have been reported to regulate interactions with Atg8/LC3[87,243,90,246].

In Chapter 3, we described the identification of an evolutionarily conserved putative LIR motif in paxillin. Given the high levels of LC3B expression in 4T1 cells, we hypothesized that paxillin might bind LC3B directly to promote the autophagic targeting of paxillin. In this chapter, we test this hypothesis through the generation of LC3B-knockdown cells as well as through co-localization and co-immunoprecipitation experiments.

The Atg8 family member LC3B co-localizes with paxillin and is required for normal focal adhesion morphology and cell motility in 4T1 cells

Given our failure in detecting an interaction between GABARAP and paxillin, we next focused on LC3B, the best-studied of the Atg8 family member proteins. Live cell confocal imaging was used to examine the localization of mApple-paxillin and EGFP-LC3B in 4T1 cells. Within the cytosol, EGFP-LC3B exhibited punctate staining consistent with autophagosomes. mApple-paxillin co-localized to these punctate cytosolic structures, indicating that paxillin associates with autophagosomes in parental 4T1 cells (Figure 4.1A). Furthermore, when we examined mApple-paxillin-positive focal adhesions in the cell periphery, we noted EGFP-LC3B co-localization, demonstrating that autophagosomes co-localize to focal adhesions in autophagy-competent cells, as has been reported previously (Figure 4.1B)[247]. This intimate interaction can also be appreciated using three-dimensional reconstruction of live cell imaging, where EGFP-LC3B autophagosomes can be observed surrounding and engulfing cytoplasmic and focal adhesion-associated mApple-paxillin (Figure 4.1C, D).

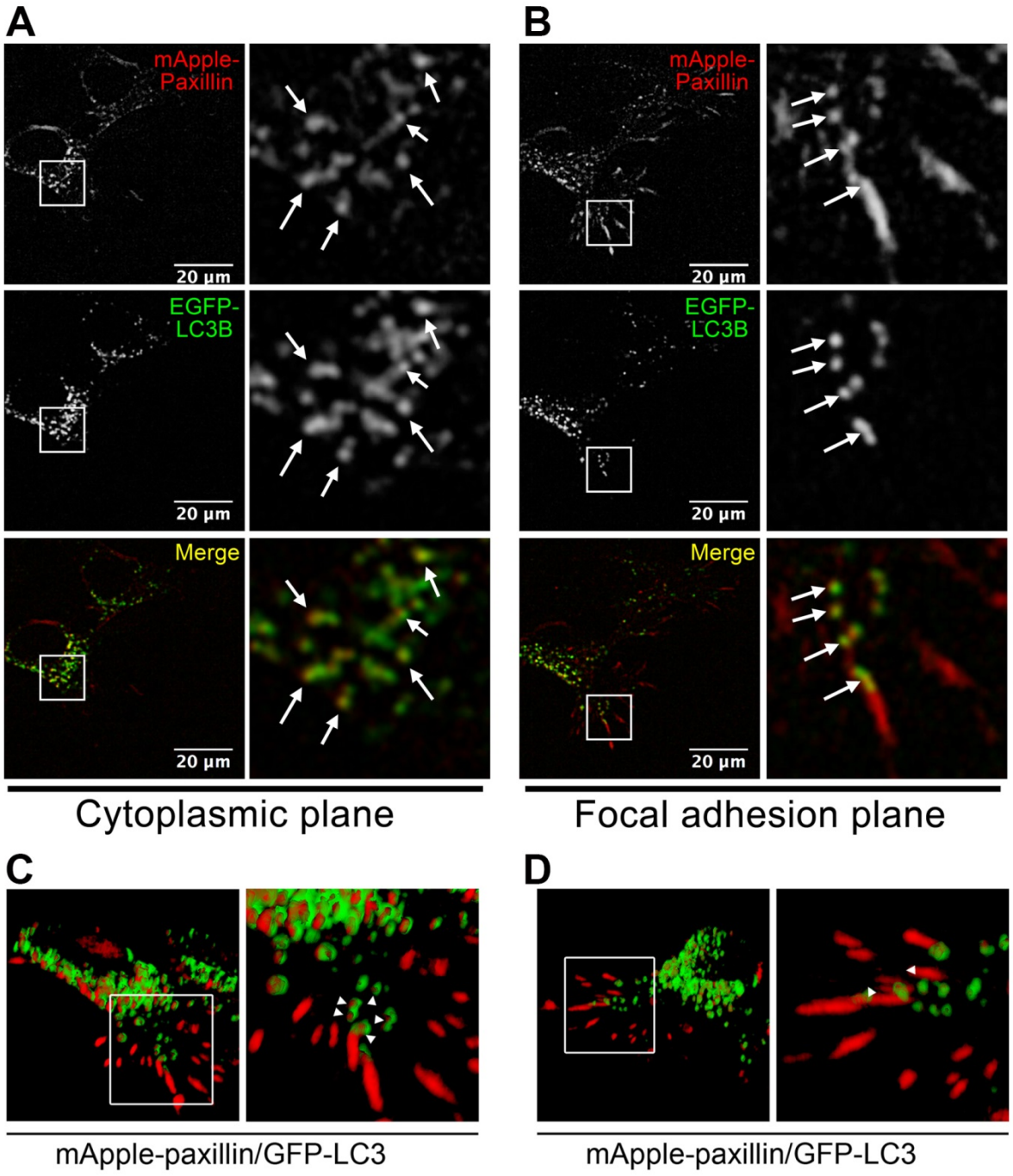

Figure 4.1 Paxillin co-localizes with LC3B at autophagosomes and focal adhesions. (A, B) 4T1 cells expressing mApple-paxillin and EGFP-LC3B were treated with BafA1, and live cells were imaged by confocal microscopy. mApple-paxillin colocalizes with EGFP-LC3B (arrows) in punctate cytosolic structures representing autophagosomes (A) and at focal adhesions (B). (C,D) Three-dimensional reconstruction of 4T1 cells treated and imaged as in (A, B) demonstrating colocalization (arrowheads) of mApple-paxillin (red) and EGFP-LC3B (green) at autophagosomes (C) and focal adhesions (D). Data in panels A-D were generated in cooperation with M. Sharifi.

To further test the possibility that LC3B was responsible for the autophagic regulation of paxillin levels, we generated 4T1 cells stably expressing LC3B shRNA (Figure 4.2A). Consistent with a critical role for LC3B in determining paxillin levels, we observed increased total paxillin levels in LC3B-knockdown 4T1 cells (Figure 4.2A). The levels of paxillin in these cells were elevated relative to basal levels in control cells and were even higher than the paxillin levels observed upon BafA1 treatment of control cells. Furthermore, 4T1 cells stably expressing LC3B shRNA exhibited altered focal adhesion morphology. Relative to scrambled control shRNA-expressing 4T1 cells, LC3B shRNA-expressing cells exhibited enlarged mature focal adhesions, as evidenced by staining for both paxillin and the late focal adhesion marker zyxin; these focal adhesions were also increased in number relative to control cells (Figure 4.2B). LC3B knockdown cells also exhibited decreased migration and invasion through collagen in transwell assays relative to parental and scrambled control shRNA cells (Figure 4.2C, D). These findings, which are similar to those observed for the Atg5, Atg7, and GABARAP knockdown lines, are consistent with a role for LC3B in regulating paxillin levels and subsequent cell motility as a necessary component of the autophagic machinery and, potentially, as a direct binding paxillin binding partner.

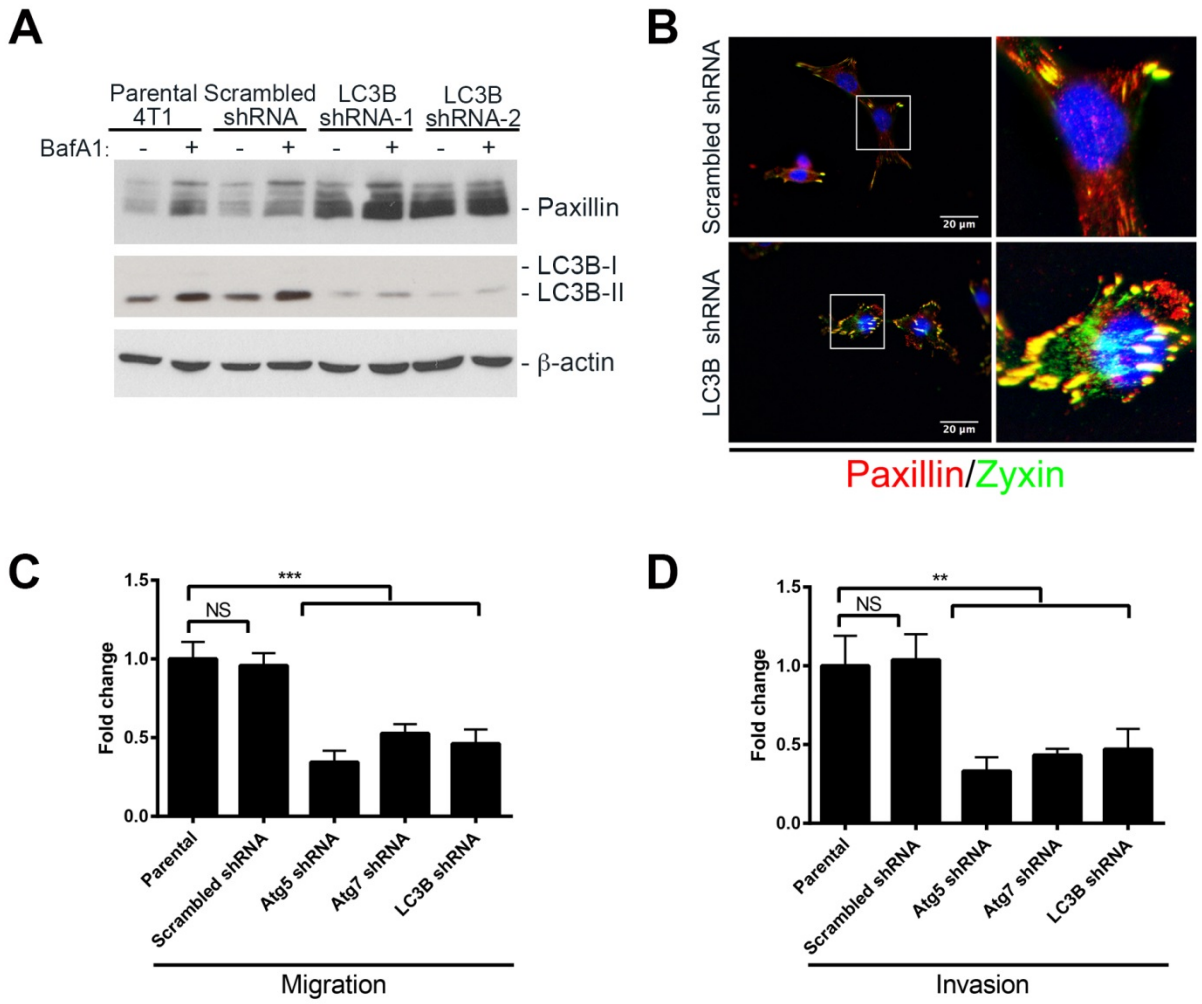

Figure 4.2 Knockdown of LC3B results in paxillin accumulation, abnormal focal adhesion morphology, and motility defects. (A) Western blot for paxillin in control 4T1 cells (parental and scrambled shRNA) and two different 4T1 clones stably expressing LC3B shRNA in the presence or absence of BafA1.(B) Immunofluorescence for paxillin (red) and zyxin (green) to visualize focal adhesions in 4T1 cells expressing scrambled or LC3B shRNA. (C, D) Quantification of the transwell migration (C) and invasion through collagen (D) of parental 4T1 cells and 4T1 cells stably expressing scramble control shRNA, Atg5 shRNA, Atg7 shRNA, or LC3B shRNA. NS, not significant; **p<0.01; ***p<0.001. Data in panel B were collected in cooperation with M. Sharifi.

Paxillin directly binds LC3B

Having observed EGFP-LC3B/mApple-paxillin co-localization by live-cell imaging, we tested for the ability of EGFP-LC3B to bind mApple-paxillin in co-immunoprecipitation experiments. Pulldown of EGFP using agarose beads coupled to GFP-specific nanobodies in 4T1 cells transiently expressing EGFP and mApple-paxillin failed to co-immunoprecipitate mApple-paxillin. However, GFP pulldown of EGFP-LC3B in 4T1 cells did successfully co-immunoprecipitate mApple-paxillin, demonstrating that these two proteins interact within cells. Furthermore, we detected endogenous paxillin in the co-immunoprecipitation as well, suggesting that the binding is not merely the result of exogenous protein expression (Figure 4.3A). We observed similar findings in B16.F10 cells, a murine melanoma cell line that exhibits a highly malignant and metastatic phenotype similar to 4T1 cells (Figure 4.3B)[235,248]. Together, these results indicate that paxillin binds LC3B in metastatic tumor cells, although the data cannot distinguish between a direct and an indirect interaction.

We attempted to enrich the co-immunoprecipitation of EGFP-LC3B and mApple-paxillin by transiently inhibiting autophagic flux by four-hour BafA1 treatment, hypothesizing that a temporary inhibition of autophagy would increase the amount of mApple-paxillin bound to available EGFP-LC3B. However, we failed to observe enrichment of mApple-paxillin levels in the co-immunoprecipitation (Figure 4.4). It is possible that in response to the exogenous expression of high levels of EGFP-LC3B and mApple-paxillin, the cells were already experiencing peak LC3B/paxillin binding, although our ability to further augment co-immunoprecipitation in other experiments (see Chapter 5) suggests otherwise. Alternatively, it may be that although transient autophagy inhibition is sufficient to cause paxillin accumulation and, presumably, increased binding of endogenous LC3B/paxillin, inhibition of autophagy for

longer than is possible with BafA1 treatment may be required in the case of high levels of exogenous EGPF-LC3B and mApple-paxillin.

To test for a direct interaction between paxillin and LC3B, we performed *in vitro* binding assays. GST-trap agarose beads were incubated with either GST or GST-LC3B purified from *E. coli*, following by incubation with myc/DDK-tagged paxillin purified from HEK293 cells; no other proteins were present to participate in binding. Paxillin was successfully pulled down with GST-LC3B but not GST, thereby demonstrating that LC3B is able to directly bind paxillin in the absence of any adaptor protein (Figure 4.5). Together with our observation of co-localization and co-immunoprecipitation of EGFP-LC3B and mApple-paxillin, these data demonstrate that LC3B and paxillin are able to directly bind one another and that this binding has physiological relevance.

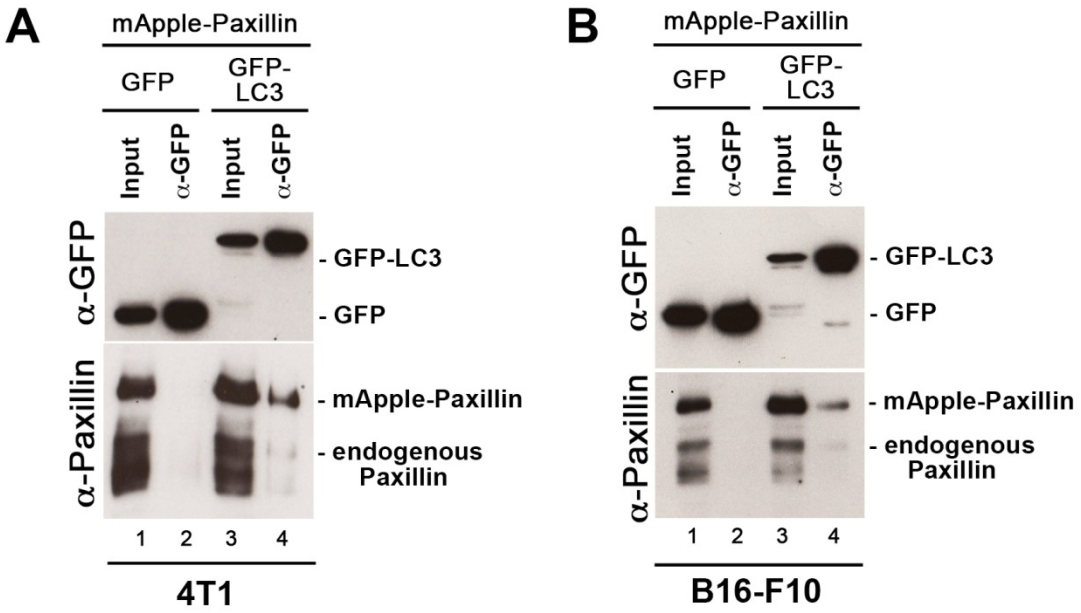

Figure 4.3 mApple-paxillin co-immunoprecipitates with EGFP-LC3B. (A, B) mApple-paxillin and EGFP (lanes 1-2) or EGFP-LC3B (lanes 3-4) were co-expressed in parental 4T1 (A) or B16.F10 cells (B). GFP pulldown was able to successfully co-immunoprecipitate mApple-paxillin and endogenous paxillin (lane 4).

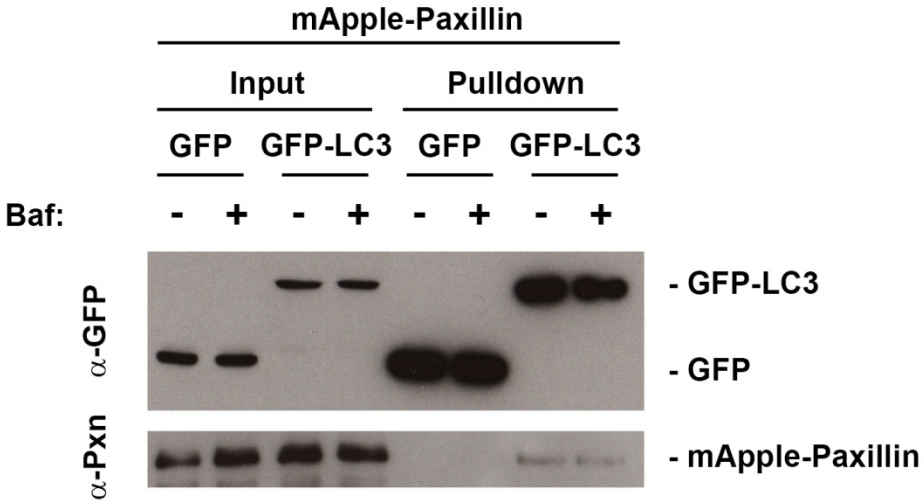

Figure 4.4 Transient lysosomal inhibition does not enrich the association of mApple-paxillin with EGFP-LC3B. 4T1 cells were transfected with mApple-paxillin and either EGFP or EGFP-LC3B and were treated or not with BafA1 to inhibit lysosomal degradation. Cell lysates were subjected to GFP pulldown, and western blots for GFP and paxillin were performed.

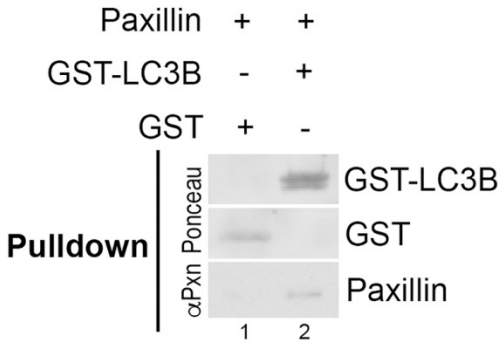

Figure 4.5 Paxillin binds directly to LC3B. *In vitro* binding assay of recombinant purified paxillin with recombinant purified GST (lane 1) or GST-LC3B (lane 2). GST pulldown demonstrates that pulldown of GST-LC3B but not GST is able to co-immunoprecipitate paxillin.

The paxillin LIR is required for interaction with LC3B and subsequent motility

To determine whether the interaction of paxillin with LC3B requires the putative N-terminal paxillin LIR motif, we generated a mutant version of mApple-paxillin in which the critical tyrosine at the +1 position of the putative LIR was mutated to alanine (Y40A) as well as a mutant in which positions +2 through +4 were mutated to alanine (QEI^{AAA}). In order to minimize the potential confounding effects of wildtype paxillin expression, we generated 4T1 cell lines stably expressing paxillin shRNA, in which wildtype paxillin protein levels were nearly undetectable (Figure 4.6A), and transiently expressed the mApple-paxillin mutants in these cells. Both the Y40A and QEI^{AAA} mutants localized appropriated to focal adhesions, indicating than an intact LIR is not required for trafficking of paxillin to focal adhesions (Figure 4.6B). However, both mutants exhibited decreased co-localization with EGFP-LC3B by live-cell confocal imaging in cytosolic autophagosomes (Figure 4.7A). This decreased colocalization was observed with respect both to the percentage of cells exhibiting mApple-paxillin/EGFP-LC3B co-localization as well as to the number of co-localization events observed per cell (Figure 4.7B, C).

Consistent with our microscopy observations, co-immunoprecipitation of mutant mApple-paxillin with EGFP-LC3B was significantly blunted in 4T1 cells stably expressing paxillin shRNA (Figure 4.8A). This effect was particularly evident for the Y40A mutant, highlighting the critical importance of the aromatic +1 position. To test whether the putative paxillin LIR motif is sufficient for binding to LC3B, we also generated a paxillin mutant in which the C-terminal end of paxillin was deleted (Δpaxillin), leaving only N-terminal LD1 and LD2 domains with the intervening LIR motif. However, although we could detect this truncation mutant in input samples, indicating that the truncation mutant is expressed at levels similar to wildtype mApple-paxillin in paxillin knockdown cells, the mutant failed to co-

immunoprecipitate with EGFP-LC3B (Figure 4.8B). It is possible that the interaction between paxillin and LC3 is not restricted to the putative LIR motif and requires additional binding interactions in the C-terminal region of paxillin. Alternatively, given that the four C-terminal LIM domains of paxillin, particularly LIM3, are required for targeting paxillin to focal adhesions[191,194], it is possible that the failure of the Δpaxillin mutant to localize to the focal adhesions abrogated any potential interaction with the autophagic machinery.

Having confirmed the important of the putative LIR motif in the interaction of LC3B and paxillin, we sought to determine its functional relevance. Paxillin knockdown 4T1 cells transiently expressing either the Y40A or QEI^{AAA} mutants exhibited decreased transwell migration and invasion (Figure 4.9). As in the co-immunoprecipitation assay, the Y40A mutant exhibited a stronger phenotype than the QEI^{AAA} mutant. Combined with our microscopy and immunoprecipitation investigations of the mutants, our data definitively confirm that the putative paxillin LIR motif is required for the binding of paxillin to LC3B and that abrogation of this motif impairs the functional motility of 4T1 tumor cells. Furthermore, our data is suggestive that the Y40 residue at the +1 LIR position in particular is critical to the paxillin/LC3B interaction.

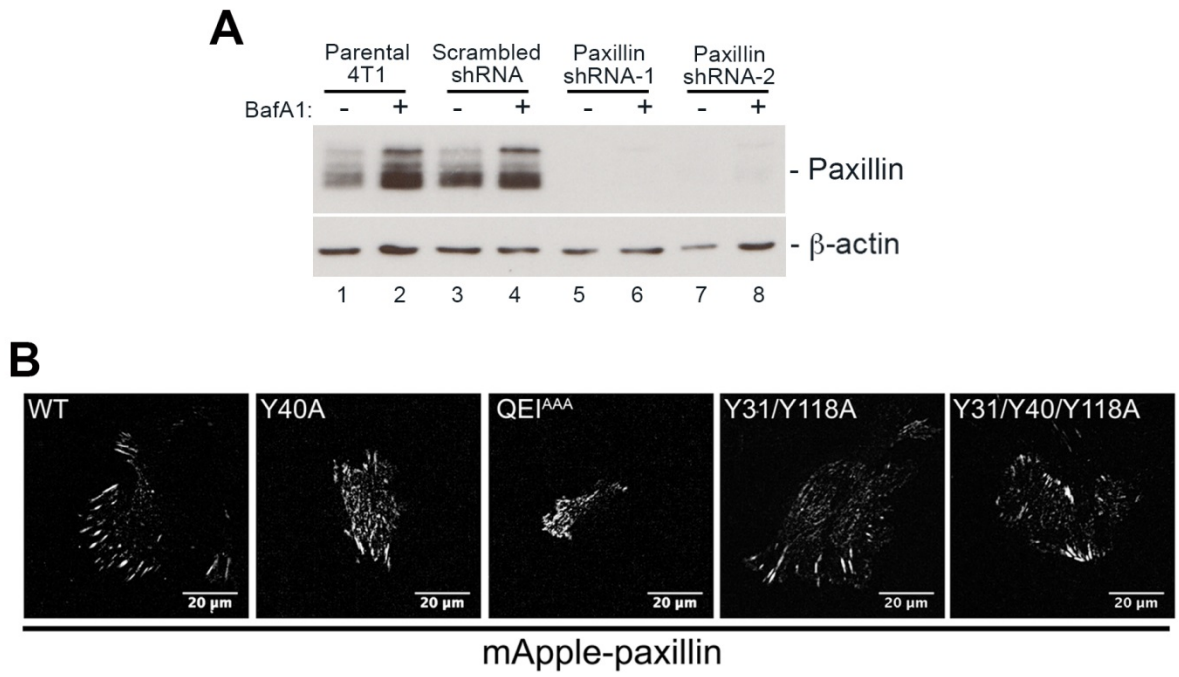

Figure 4.6 mApple-paxillin mutants localize to focal adhesions in paxillin-knockdown cells. (A) Western blot for paxillin in control 4T1 cells (parental and scrambled shRNA) and two different 4T1 clones stably expressing paxillin shRNA in the presence or absence of BafA1. (B) 4T1 cells stably expressing paxillin shRNA were transiently transfected with wildtype mApple-paxillin or the indicated mutants. Live cell confocal imaging was performed to demonstrate focal adhesion localization of all paxillin mutants.

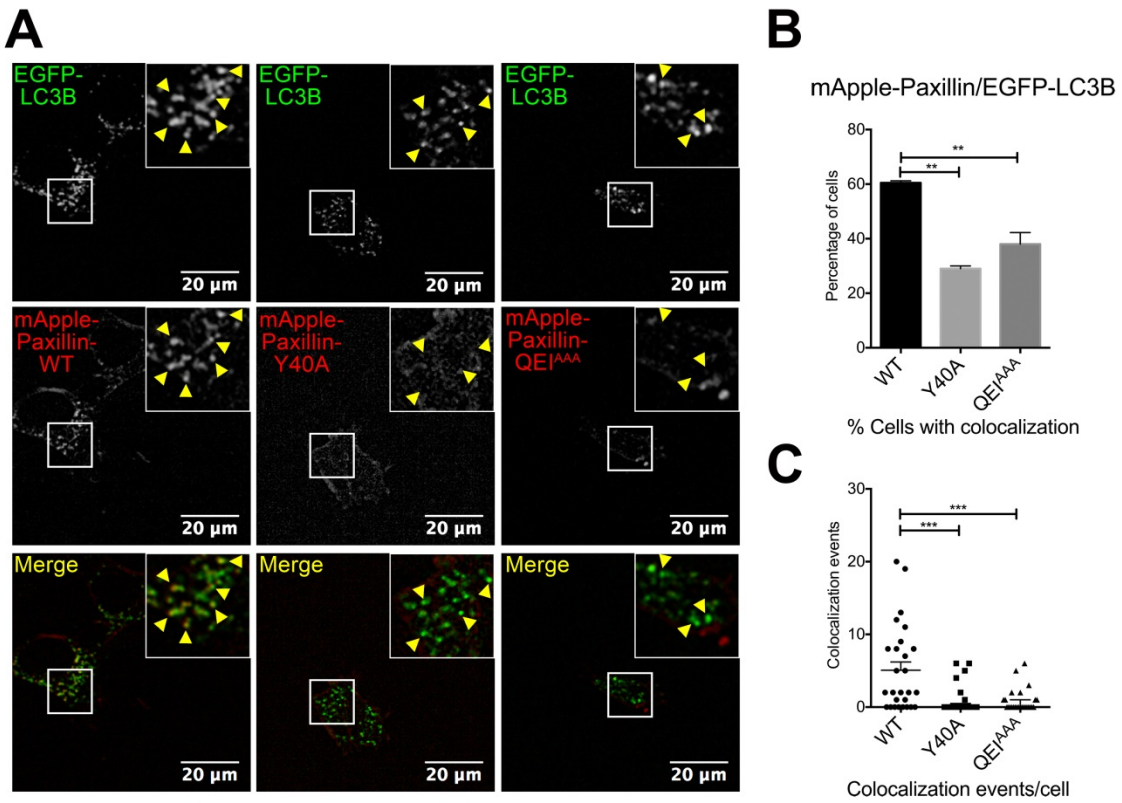

Figure 4.7 mApple-paxillin LIR mutants exhibit decreased localization with EGFP-LC3B. (A) Live cell confocal imaging of 4T1 paxillin knockdown cells expressing EGFP-LC3B (green) with mApple-paxillin wildtype, Y40A or QEI^{AAA} (red). Colocalization events are indicated by arrowheads; scale bar is indicated. (B, C) Quantification of colocalization of cells depicted in (A). (B) %Cells with colocalization (**$p<0.01$): Mean ± SEM, n=2, 15-20 cells/condition/experiment. (C) Colocalization events per cell (***$p<0.001$): Mean ± SEM, n=30. Data in panels A-C were generated in cooperation with M. Sharifi.

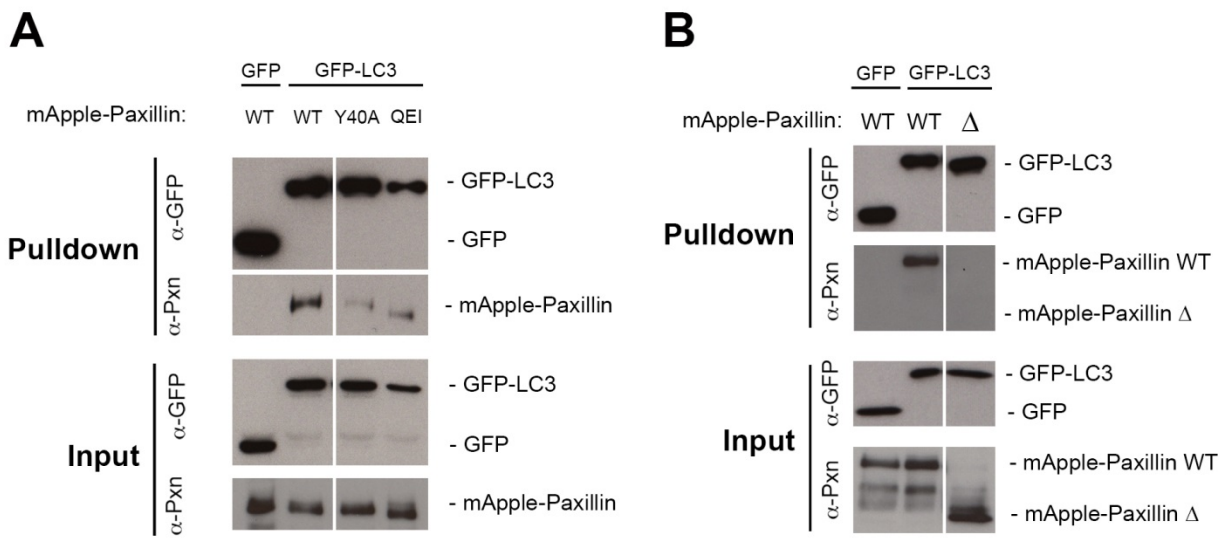

Figure 4.8 The paxillin LIR is necessary but not sufficient for co-immunoprecipitation of mApple-paxillin with GFP-LC3B. (A) 4T1 paxillin knockdown cells were transfected with EGFP or EGFP-LC3B and mApple-paxillin wildtype (WT), Y40A, or QEI^{AAA} and were subject to GFP-pulldown to assess co-immunoprecipitation of mApple-paxillin. (B) 4T1 paxillin knockdown cells were transfected with EGFP or EGFP-LC3B and either mApple-paxillin wildtype (WT) or a truncation mutant (Δ) containing only the LD1-LD2 region. Pulldown was performed as in (A).

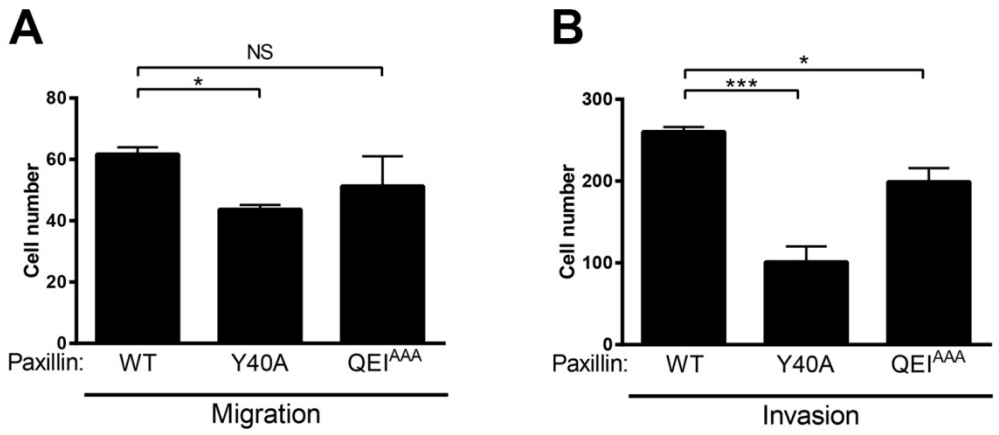

Figure 4.9 The paxillin LIR is required for cell motility. (A, B) Quantification of the transwell migration (A) and invasion through collagen (B) of paxillin knockdown 4T1 cells transfected with mApple-paxillin wildtype (WT), Y40A, or QEI^{AAA}. NS, not significant; *p<0.05; ***p<0.001.

Conclusion

In this chapter, we have explored the possibility that LC3B binds paxillin to target it for autophagic degradation. GFP-LC3B and mApple-paxillin co-localization was observed at both autophagosomes and at focal adhesions in 4T1 cells. Furthermore, stable knockdown of LC3B using shRNA reproduced the phenotype of autophagy-deficient cells with respect to increased paxillin levels in cell lysates, the accumulation of enlarged focal adhesions, and impaired migration and invasion in transwell assays. Furthermore, co-immunoprecipitation demonstrated that GFP-LC3B could co-immunoprecipitate both mApple-paxillin as well as endogenous paxillin in the two metastatic cell lines tested, 4T1 mammary carcinoma cells and B16.F10 melanoma cells. Our *in vitro* binding assay demonstrated that GST-LC3B and paxillin were able to bind one another in the absence of any intermediary protein. Finally, we probed the requirement of the putative paxillin LIR through the generation of paxillin LIR mutants and demonstrated that mutation of the +1 tyrosine residue and, to a lesser extent, the +2 through +4 residues significantly decreased co-immunoprecipitation, decreased co-localization of paxillin at autophagosomes, and impaired transwell migration and invasion.

Although we attempted to demonstrate an interaction between endogenous LC3B and paxillin, we have been unable to do so either by co-localization or by co-immunoprecipitation. It should be noted, however, that we did observe that GFP-LC3B was able to pull down some endogenous paxillin in addition to mApple-paxillin. The failure to demonstrate an endogenous interaction may reflect binding of the commercially available antibodies suitable for immunoprecipitation to regions of either LC3B or paxillin that are involved in the interaction, thereby occluding the binding site. Furthermore, within the literature, there is very little evidence of direct protein-protein interactions of paxillin with its accepted binding partners; most require

expression of exogenous tagged paxillin. It is important to remember that paxillin functions as a scaffolding protein with many interaction partners, which could hamper the ability to detect any one interaction using endogenous protein[187,194]. The highly globular and hydrophobic nature of paxillin may also explain the difficulty of an endogenous co-immunoprecipitation. Although the ability to detect an endogenous interaction might suggest the possibility of an indirect interaction, we have shown through GST pulldown of GST-LC3B and paxillin that paxillin can bind LC3B directly in the absence of any other intermediaries. However, this finding does not preclude the possibility that *in vivo*, an adaptor protein or other scaffold or chaperone might facilitate the paxillin/LC3B interaction to promote strong binding.

We have demonstrated that an intact LIR motif is required for paxillin/LC3B co-immunoprecipitation, co-localization, and functional outcomes. However, the finding that a truncation mutant of paxillin lacking LD3-4 and the C-terminal LIM domains was not co-immunoprecipitated with GFP-LC3B suggests that the proper localization of paxillin to focal adhesions is required for its association with the autophagic machinery. The possibility that regions other than the LIR (e.g., those located C-terminally and missing from the truncation mutant) participate in paxillin/LC3B binding cannot be excluded.

Although the effect of the paxillin LIR point mutants was strong, some residual association could still be detected in the Y40A and QEI^{AAA} mutants by co-immunoprecipitation. One possibility is that the trace levels of endogenous wildtype paxillin present in the paxillin knockdown cells helped facilitate the co-immunoprecipitation of the mutants with GFP-LC3B. *In vitro* binding assays of GST-LC3B with the paxillin LIR mutants would lend stronger support to the implied necessity of the LIR in paxillin/LC3B binding. However, such mutants are not

commercially available, unlike wildtype paxillin, and would require the development of protein purification protocols for these paxillin mutants in mammalian cells.

Given that both the +1 and +4 positions are known to be critical anchors of LIR motif binding, it is also possible that replacing both the +1 tyrosine and the +4 isoleucine, or indeed mutating the entire YQEI motif, might be required to completely eliminate binding. Alternatively, nearby residues up- or downstream of the LIR might also promote LIR binding, as is the case in binding of p62/Sqstm1 to LC3B[75,249]. However, while further mutational analyses could shed light on additional residues important to the binding interaction, only a crystal or NMR structure would be able to truly answer these questions.

CHAPTER 5

ONCOGENIC SRC REGULATES THE INTERACTION OF PAXILLIN AND LC3B TO PROMOTE AUTOPHAGY-DEPENDENT CELL MOTILITY

Introduction

Cellular motility requires polarization and cellular protrusion in the direction of movement, actin polymerization, the formation of focal adhesions to serve as tractions sites, cytoskeletal contractility, and focal adhesion disassembly[180]. Focal adhesion dynamics can be regulated by a number of proteins, and some of these proteins have been implicated in human cancers. Indeed, the cellular form of *v-src*, which was the first confirmed oncogene and was identified as the transforming gene of the Rous Sarcoma virus[250], is a proto-oncogene that is required for proper focal adhesion dynamics. Cells lacking c-Src, hereafter referred to as Src, exhibit enlarged focal adhesions, impaired motility, and decreased spreading[195]. Src is a non-receptor tyrosine kinase, and its kinase activity is required for focal adhesion disassembly[198,199]. In addition to its ability to modulate cell motility, Src kinase activity can alter cell cycle progression, differentiation, survival, angiogenesis, and metastasis; these effects can vary depending on the cell type and signaling upstream of Src[201,251].

The ability of Src to have wide-ranging effects makes it unsurprising that Src has been reported to be activated or overexpressed in more than 50% of colon, liver, lung, breast, and pancreatic tumors[251]. Src hyperactivation can be correlated with cancer cell proliferation and ability to migrate and invade[252–254]. Although Src is not a primary driver of tumorigenesis, inhibition of Src may represent an important aspect of combinatorial cancer therapeutics[255].

Several inhibitors of Src, most of which also target Abl kinase, are available; many are currently in clinical trials. In solid tumors, these inhibitors, notably dasatinib, can suppress migration *in vitro* and metastasis *in vivo*[201]. Although the majority of trials involving Src inhibitors are in the early phases, many indicate that Src inhibition is insufficient as monotherapy[256–259]; however, there is hope that the use of new biomarkers to identify appropriate patient populations or the use of Src inhibitors in combination chemotherapies will produce clinical benefit[201,259,260]. To what degree these effects reflect the ability of Src to regulate focal adhesion turnover or other signaling effects is unknown.

In Chapter 4, we demonstrated that the focal adhesion protein paxillin can bind directly to the autophagy protein LC3B. When cells are deficient for autophagy, they exhibit elevated paxillin levels and impaired focal adhesion disassembly. In this chapter, we sought to explore how autophagic targeting of paxillin might be regulated. Intriguingly, the focal adhesion accumulation and disassembly defects observed in autophagy-deficient cells are similar to those observed in Src-null or Src kinase-inactive cells[195,198,199]. Furthermore, paxillin is a tyrosine phosphorylation target of Src[187]. In this chapter, we explore the possibility that Src tyrosine kinase activity regulates the interaction of paxillin with LC3B.

Src promotes the interaction of paxillin with LC3B

A tyrosine in the +1 position is less commonly found in LIR motifs than the canonical +1 tryptophan residue[72]. In Chapter 4, we observed that the Y40A paxillin mutant exhibited a stronger phenotype than the QEI^{AAA} triple mutant. Intriguingly, the Y40 reside of paxillin is a known phosphorylation target of Src tyrosine kinase, although its functional significance is not well established (Figure 3.5)[261,262]. Furthermore, phosphorylation of residues within and around

LIR motifs is a known method of regulating interactions with Atg8 proteins[87,90,263]. Therefore, we sought to determine whether Src activity could modulate the interaction of paxillin with LC3B.

The expression of a constitutively active Src mutant, Src^{Y527F}, in paxillin knockdown 4T1 cells strongly stimulated the co-immunoprecipitation of mApple-paxillin and EGFP-LC3B (Figure 5.1A). The augmentation of co-immunoprecipitation was independent of mApple-paxillin levels, as the expression of mApple-paxillin was consistent among the input samples, and the presence of active Src had no effect on EGFP-LC3 levels. Similar results were observed in B16.F10 cells (Figure 5.1B). Interestingly, both unphosphorylated and phosphorylated paxillin, detected as an up-shifted band on the western blot, were observed in the co-immunoprecipitation. It is possible that the phosphorylation of paxillin by Src increases binding of LC3B to paxillin and thus increases recruitment of LC3B-decorated autophagosomes to focal adhesions, further stimulating an interaction of available LC3B with non-phosphorylated paxillin as well.

To test whether the ability of Src to stimulate the interaction of EGFP-LC3B and mApple-paxillin is a result of Src kinase activity or whether Src acts to facilitate the interaction by serving as an adaptor or through some non-kinase function, we treated transfected 4T1 cells with PP2, a potent inhibitor of Src family tyrosine kinases[264], and performed pulldown experiments as described previously (Figure 5.1C). As before, transfection with Src^{Y527F} resulted in the appearance of an up-shifted phosphorylated paxillin band in input samples. Active Src had no effect on GFP or GFP-LC3 levels, and no co-immunoprecipitation of mApple-paxillin with GFP was observed in either the presence or absence of active Src. The inhibition of Src activity by PP2 was confirmed by absence of the up-shifted phospho-paxillin band in input lanes from

PP2-treated samples. In cells expressing only endogenous Src, PP2 treatment inhibited co-immunoprecipitation of mApple-paxillin with EGFP-LC3B. Similarly, PP2 treatment inhibited co-immunoprecipitation of mApple-paxillin in cells expressing active Src^{Y527F}. In these cells, the level of mApple-paxillin co-immunoprecipitating with EGFP-LC3B approached the levels observed in cells not expressing active Src, suggesting that the ability of Src to phosphorylate paxillin was directly responsible for the augmentation in the paxillin/LC3B interaction.

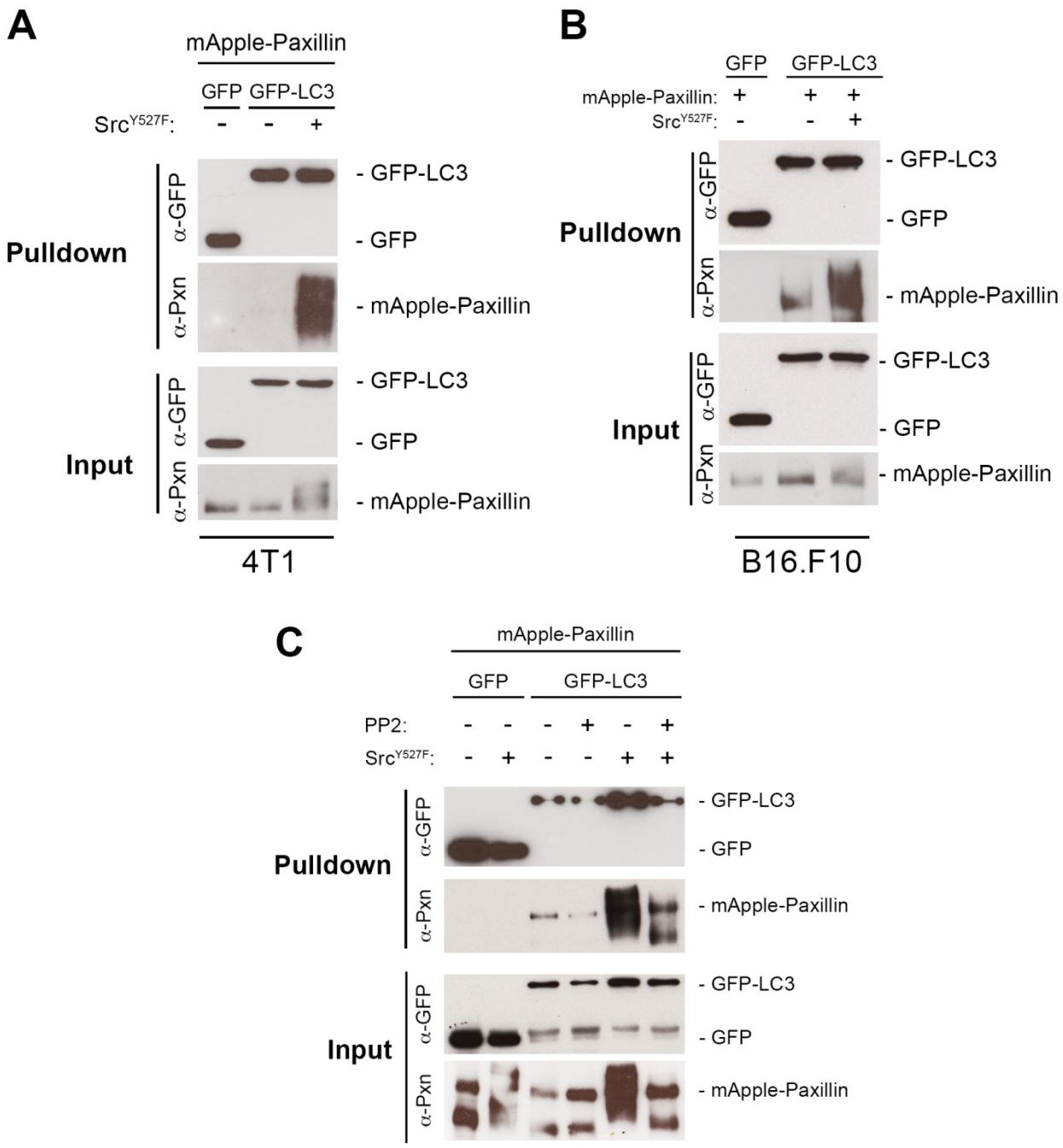

Figure 5.1 Oncogenic Src promotes the co-immunoprecipitation of mApple-paxillin with EGFP-LC3B. (A, B) mApple-paxillin and EGFP or EGFP-LC3B were co-expressed in parental 4T1 (A) or B16.F10 cells (B) in the presence of absence of oncogenic Src^{Y527F} transfection. Co-immunoprecipitation of mApple-paxillin with GFP-LC3B was strongly stimulated in the presence of oncogenic Src. (C) 4T1 cells were transfected with mApple-paxillin; EGFP or EGFP-LC3B; and Src^{Y527F} or vector in the presence or absence of the Src kinase inhibitor PP2. Lysates were subjected to GFP-pulldown to co-immunoprecipitate mApple-paxillin.

The effects of Src on the paxillin/LC3B interaction require an intact LIR motif

Given that the expression of paxillin LIR mutants inhibits the interaction of mApple-paxillin and EGFP-LC3 in immunoprecipitation experiments and our hypothesis that phosphorylation of the Y40 residue in the +1 LIR position by Src promotes the association of mApple-paxillin and EGFP-LC3B, we co-expressed the mApple-paxillin mutants with EGFP or EGFP-LC3B and Src^{Y527F} and performed co-immunoprecipitation experiments. As observed previously, under basal conditions, the QEI^{AAA} mutant blunted the interaction with EGFP-LC3B, whereas the Y40A mutant nearly completely abrogated the interaction (Figure 5.2). A similar pattern was observed in the presence of active Src^{Y527F}; the QEI^{AAA} mutant exhibited moderately reduced pulldown with LC3B relative to wildtype mApple-paxillin, and the Y40A mutant exhibited a strong reduction in co-immunoprecipitation samples (Figure 5.2). Although the level of co-immunoprecipitated mApple-paxillin QEI^{AAA} in the presence of active Src was higher than the level of co-immunoprecipitated mApple-paxillin wildtype in the absence of active Src, the level of co-immunoprecipitated mApple-paxillin Y40A was much more similar to the level of wildtype mApple-paxillin pulled down with EGFP-LC3B in the absence of Src. These immunoprecipitation experiments demonstrate that the LIR motif is critical for the Src-stimulated interaction of LC3B and paxillin, both with respect to binding through the +2 through +4 QEI residues and to the Src phosphorylation target Y40 in the +1 position.

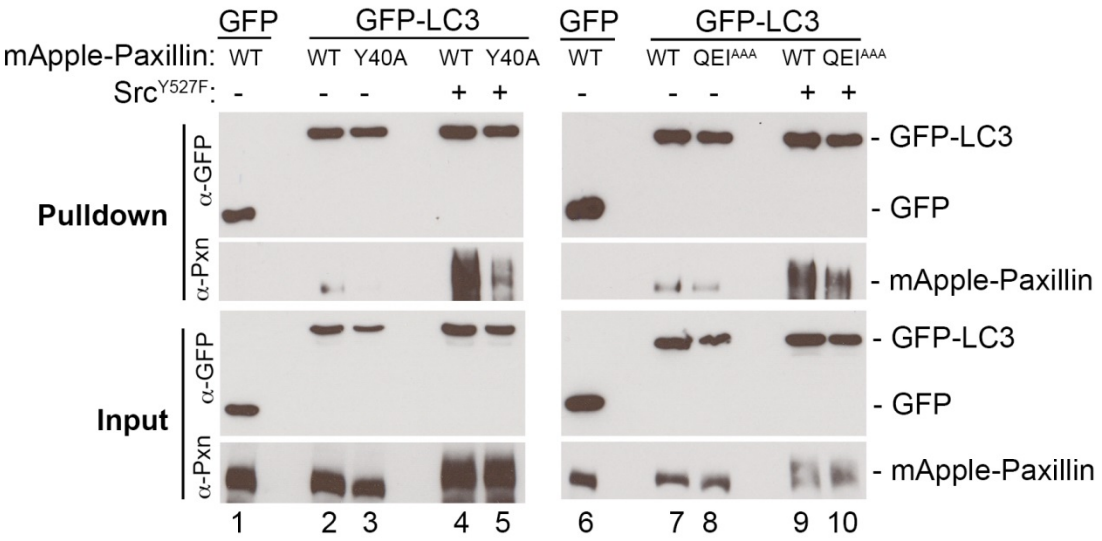

Figure 5.2 The effects of oncogenic Src on co-immunoprecipitation of EGFP-LC3B and mApple-paxillin require an intact LIR motif. 4T1 paxillin knockdown cells were transfected with GFP (lanes 1, 6) or EGFP-LC3B (lanes 2-5, 7-10); mApple-paxillin wildtype (lane 1, 2, 4, 6, 7, 9), Y40A (lanes 3,6), or QEI^{AAA} (lanes 8, 10); and either oncogenic Src (lanes 4, 5, 9, 10) or vector control (lanes 1-3, 6-8). mApple-paxillin was co-immunoprecipitated from cells by GFP pulldown.

The Src-stimulated interaction of mApple-paxillin and EGFP-LC3B is independent of the canonical Src phosphorylation sites

As mentioned previously, the function of the Y40 Src phosphorylation site is not well established; research has focused on the role of the two classical Src phosphorylation sites, Y31 and Y118[187]. Therefore, we wondered whether the ability of Src to regulate the paxillin/LC3B interaction involved either of these two residues in addition to Y40, as previously established. We thus generated two additional mApple-paxillin mutants, including a mutant in which both canonical tyrosine phosphorylation sites were mutated to alanine (Y31/Y118A) and a mutant in which all three tyrosine sites were mutated to alanine (Y31/Y40/Y118A). As observed with our earlier mApple-paxillin mutants, these mutants localized appropriately to focal adhesions (Figure 4.6). Although pulldown of both mApple-paxillin Y40A and the triple mutant by EGFP-LC3B were strongly inhibited, we observed no change in the ability of the Y31/Y118A double mutant to interact with EGFP-LC3B (Figure 5.3). Therefore, the effects of active Src on the paxillin/LC3B interaction are not dependent on the canonical Y31 and Y118 Src phosphorylation sites but do require the Y40 residue in the LIR motif.

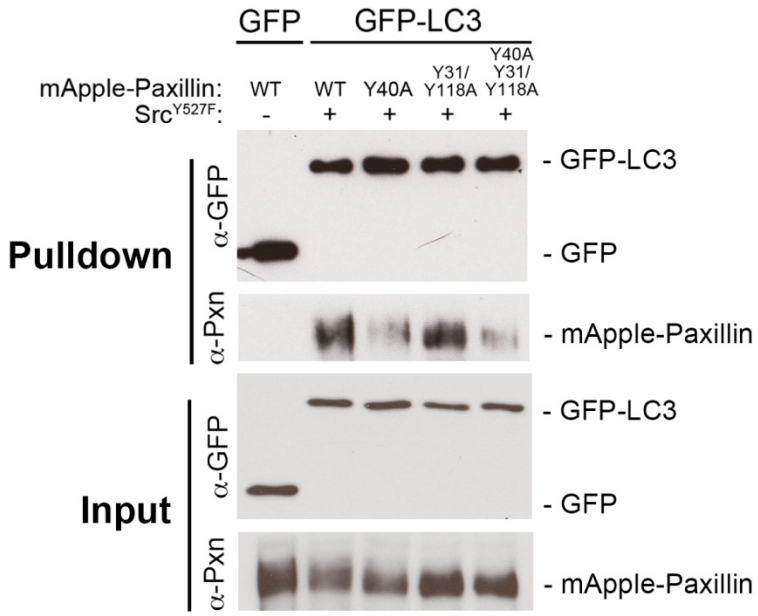

Figure 5.3 The Src-stimulated interaction between EGFP-LC3B and mApple-paxillin is independent of the canonical Src phosphorylation sites. 4T1 paxillin knockdown cells were transfected with EGFP and mApple-paxillin or EGFP-LC3B; mApple-paxillin wildtype, Y40A, Y31/Y118A, or Y31/Y40/Y118A; and oncogenic Src. mApple-paxillin was co-immunoprecipitated by GFP-pulldown.

Autophagic degradation of paxillin is required for Src-stimulated motility

To determine whether the Src-regulated interaction of paxillin and LC3B underlies to motility defects of autophagy-deficient cells, we performed transwell migration and invasion assays. Consistent with the known role of Src kinase in promoting cell motility[199], expression of Src^{Y527F} strongly stimulated the transwell migration and invasion of 4T1 cells stably expressing control scrambled shRNA (Figure 5.5A). However, strikingly, Src^{Y527F} expression had absolutely no effect on the migration or invasion of autophagy-deficient 4T1 cells (Figure 5.5A). These data demonstrate that intact autophagy is required for Src-stimulated motility and are consistent with our model that Src phosphorylation of the Y40 residue of paxillin promotes the paxillin/LC3B interaction and subsequent paxillin degradation, focal adhesion turnover, and cell motility.

Finally, to confirm the functional relevance of the LIR motif to Src-stimulated motility, we expressed the mApple-paxillin LIR mutants in 4T1 paxillin knockdown cells and subjected the cells to transwell motility assays. In cells expressing wildtype mApple-paxillin, the expression of Src^{Y527F} caused a two-fold increase in cellular migration and invasion (Figure 5.5B). However, the effect of active Src on cells expressing mApple-paxillin Y40A or QEI^{AAA} was significantly blunted, and the difference in the migration and invasion of Src-stimulated mApple-paxillin wildtype and LIR mutants was statistically significant (Figure 5.5B). These data thus demonstrate that stimulation of the interaction between paxillin and LC3B by oncogenic Src and the subsequent autophagic degradation of paxillin promote cellular motility in the metastatic 4T1 cell line.

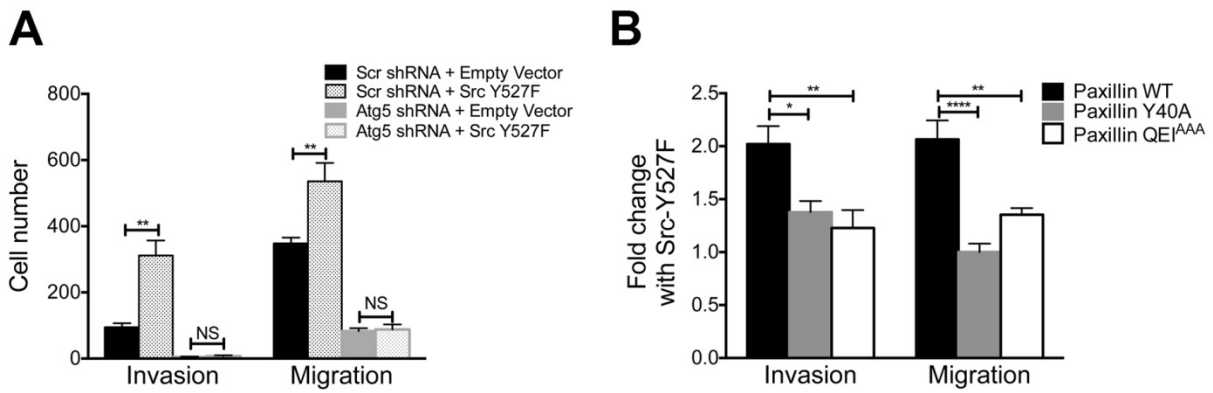

Figure 5.4 Src-stimulated cell motility requires intact autophagy and the paxillin LIR motif. (A) Quantification of the transwell migration (right) and invasion through collagen (left) of 4T1 scramble shRNA and Atg5 shRNA cells transfected with Src^{Y527F} or empty vector. (B) Quantification of Src^{Y527F}-stimulated fold change in the transwell migration (right) and invasion through collagen (left) of 4T1 paxillin knockdown cells expressing with mApple-paxillin wildtype (WT), Y40A, or QEI^{AAA}. NS, not significant; *p<0.05; **p<0.01; ****p<0.0001.

Conclusions

In this study, we have examined the mechanism underlying why autophagy-deficient cells exhibit impaired metastasis *in vivo* and impaired motility and focal adhesion disassembly *in vitro*. We have demonstrated that the aberrant elevation of paxillin in autophagy-deficient cells underlies the focal adhesion accumulation and that paxillin is turned over by autophagy. Autophagic targeting of autophagy is accomplished by direct binding of paxillin to LC3B through a conserved N-terminal LIR motif (YQEI, residues 40-43) located in a region of paxillin known to be important in signaling and regulation. Abrogation of the paxillin/LC3B interaction through LIR mutations, particularly the Y40A mutant, produces the functional consequences of decreased localization of autophagosome to focal adhesions and decreased cell migration and invasion.

In this chapter, we have explored the oncogenic Src-mediated regulation of the interaction of paxillin with LC3B. Our interest in Src was motivated by the observation that the focal adhesion and motility phenotypes of the autophagy-deficient cells were similar to those reported for *Src*-null or catalytically inactive Src[195,198,199]. Furthermore, the Y40 residue of the paxillin LIR motif has been demonstrated to be a Src phosphorylation site[261,262]. Expression of the constitutively active Src^{Y527F} in 4T1 or B16.F10 cells strongly promoted the ability of EGFP-LC3B to co-immunoprecipitate mApple-paxillin. Furthermore, both the basal and Src^{Y527F}-stimulated co-immunoprecipitation of mApple-paxillin could be inhibited by treatment with PP2, a Src kinase inhibitor. The effects of Src, both with respect to co-immunoprecipitation and cellular migration/invasion, were eliminated by mutation of the Y40 site within the paxillin LIR motif, but mutation of the canonical Src tyrosine phosphorylation sites Y31/Y118 had no effect.

These data led us to conclude that Src phosphorylation of the Y40 residue within the paxillin LIR motif promotes the interaction of paxillin with LC3B and the subsequent autophagic degradation of paxillin, focal adhesion turnover, and cell motility. However, although our data are strongly suggestive, we have not directly demonstrated either the ability of Src to phosphorylate Y40 or the direct effect of Src phosphorylation on paxillin/LC3B binding. This would best be accomplished by *in vitro* binding assays complementing our demonstration of a direct interaction of paxillin and GST-LC3B in Chapter 4. Incubation of recombinant paxillin with (1) either catalytically active or catalytically inactive Src and (2) the appropriate ATP levels, followed by additional incubation with GST-LC3B, would be required to directly demonstrate that phosphorylated paxillin exhibits increased binding to LC3B.

Although our assays comparing the ability of GFP-LC3B to co-immunoprecipitate mApple-tagged single (Y40A), double (Y31/118A), or triple (Y31/40/118A) demonstrate that only the Y40 residue is required for the Src-stimulated pull-down of paxillin, we have not eliminated the possibility that other potential tyrosine phosphorylation sites are involved. Indeed, in addition to Y31, Y40, and Y118, paxillin Y76, Y88, Y182, Y377, and Y436 have been identified as phosphorylation sites using mass spectrometry of immunoprecipitated FLAG- or FLAG-GFP-tagged paxillin expressed in HEK cells[262]. Of these sites, only Y31, Y40, Y88, and Y118 are predicted targets of Src by NetPhos 2.0 and Scansite[262]; these residues have all been experimentally validated[261,265,266]. Y182 is a predicted but not experimentally validated target of EGFR and PDGFR[262]. Therefore, it is possible that phosphorylation of any of these additional residues may contribute either directly or indirectly to paxillin/LC3B binding.

A novel finding of our study is the observation that Src^{Y527F}-stimulated cell motility required intact autophagy; Atg5-deficient 4T1 cells, in contrast to control cells, failed to migrate

or invade in transwell assays irrespective of Src status. To the best of our knowledge, this is the first report of a requirement for autophagy in response to oncogenic Src-mediated motility. Whether this reflects a unique co-option of autophagy by highly metastatic 4T1 cells in response to oncogenic Src signaling or a general cellular requirement is unclear. Src has been reported to be degraded by autophagy through binding to c-Cbl, although only in the context of FAK deficiency[247]. It is at this time not possible to distinguish between a requirement for autophagy in Src-stimulated motility that is dependent on autophagic degradation of paxillin or one that is dependent on autophagic degradation of Src. Future experiments should examine the effect of genetic or pharmacologic autophagy inhibition on Src-stimulated motility in other cell systems, including other highly metastatic lines like B16.F10, malignant but non-metastatic cells, and non-tumorigenic cells.

The results of this study, in combination with previous work in the 4T1 model of mammary metastasis, demonstrate that failure of paxillin degradation in autophagy-deficient cells leads to impaired focal adhesion disassembly and cell migration *in vitro* that is consistent with the observation of impaired metastasis *in vivo*. We have identified a previously unreported LIR motif in the N-terminal region of paxillin. Targeting of paxillin to the autophagosome is mediated through direct binding of paxillin to LC3B through this LIR motif. This interaction can be regulated by oncogenic Src on the Y40 residue of the LIR motif with function consequences. Finally, in this system, the motility-promoting effects of oncogenic Src require intact autophagy, highlighting the potentially critical role of autophagy in Src-stimulated focal adhesion turnover and resultant cell migration.

CHAPTER 6

DISCUSSION

Summary and significance

Although the role of autophagy in primary tumor growth is generally held to be tumor suppressive prior to malignant transformation and tumor-promoting after the establishment of the primary tumor, autophagy's role in metastasis is less well characterized. However, clinical data suggest that metastases may exhibit increased autophagic flux relative to primary tumors[150,202–204]. Furthermore, *in vitro* and *in vivo* experiments have implicated a role for autophagy in overcoming several challenges that metastasizing cells face, including EMT, anoikis, and CSC maintenance (Chapter 1). As autophagy may ultimately been viewed as an adaptive (or, in the case of certain pathologies, maladaptive) response to stress, there has been increasing interest in the role of autophagy during all stages of the metastatic cascade.

One of the challenges in answering this question lies in untangling the role of autophagy in the primary tumor from its role in metastatic cells and metastatic outgrowth. As has become abundantly clear over the past decade, the role of autophagy in cancer is highly context-dependent, and eliminating confounding variables can greatly aid in the interpretation of results. In our study of autophagy, we made use of the 4T1 murine model of metastatic breast cancer. Unlike many other reports, the inhibition of autophagy in these cells has no effect on primary tumor growth; furthermore, autophagy-deficient 4T1 cells are able to effectively colonize the lung when injected directly into the circulation. The inability of autophagy inhibition to alter these phenotypes may be related to the highly aggressive nature of 4T1 cells, which exhibit rapid

proliferation both *in vitro* and *in vivo*. However, 4T1 cells do exhibit impaired metastasis from the primary tumor and exhibit impaired motility and defects in focal adhesion disassembly. Thus, this model is ideally suited to studying the role of autophagy in metastasis in an isolated fashion independent of the canonical effects of autophagy as a cellular response to stress.

We determined that the accumulation of focal adhesions in autophagy-deficient cells was accompanied by an accumulation of paxillin, and that restoration of paxillin levels reversed the motility phenotype of autophagy-deficient cells. Inhibition of autophagy either upstream of Atg8/LC3 conjugation (i.e., knockdown of *Atg5* or *Atg7*) or downstream of conjugation during phagophore closure (i.e., knockdown of *GABARAP*) produced similar phenotypes. The autophagic degradation of paxillin was not due to the p62/Sqstm1 or Nbr1 adaptors (Chapter 3). The presence of a putative LIR motif in paxillin led us to explore a role for LC3B in binding paxillin directly. Indeed, paxillin binds GST-LC3B directly *in vitro*, and GFP-LC3B and mApple-paxillin were co-immunoprecipitated from cells. Mutation of the LIR motif inhibited co-immunoprecipitation, co-localization, and cell motility, validating the sequence as a bona fide LIR motif (Chapter 4). Paxillin's role in focal adhesions is not merely structural but also reflects its presence as a signaling hub. We noted that the paxillin LIR contained an experimentally validated but uncharacterized tyrosine phosphorylation site that is a target of Src, one of the modulators of paxillin and focal adhesion turnover. Expression of oncogenic Src strongly promoted the paxillin/LC3B co-immunoprecipitation in a manner dependent on an intact LIR motif and intact autophagy (Chapter 5).

The work presented in this thesis has led to the generation of a model explaining the role of autophagy in highly metastatic cells (Figure 6.1). In this proposed model, oncogenic Src promotes the direct binding of the paxillin LIR motif with LC3B-II. Paxillin is thus targeted to

the autophagosome and degraded, promoting the disassembly of focal adhesions and cellular motility. Under this model, inhibition of autophagy results in the accumulation of paxillin, abrogates the motility-promoting effects of Src, and causes impaired focal adhesion disassembly, thereby leading to the inhibition of cellular migration and invasion *in vitro* and the inhibition of metastasis *in vivo*.

This work is the first demonstrating direct binding between LC3B and paxillin as a means of targeted autophagic degradation of paxillin. Furthermore, the necessity of intact autophagy in oncogene Src-stimulated migration and invasion has never before been reported. Finally, this work adds to the growing recognition that post-translational modifications in or around LIR motifs can regulate binding to Atg8/LC3.

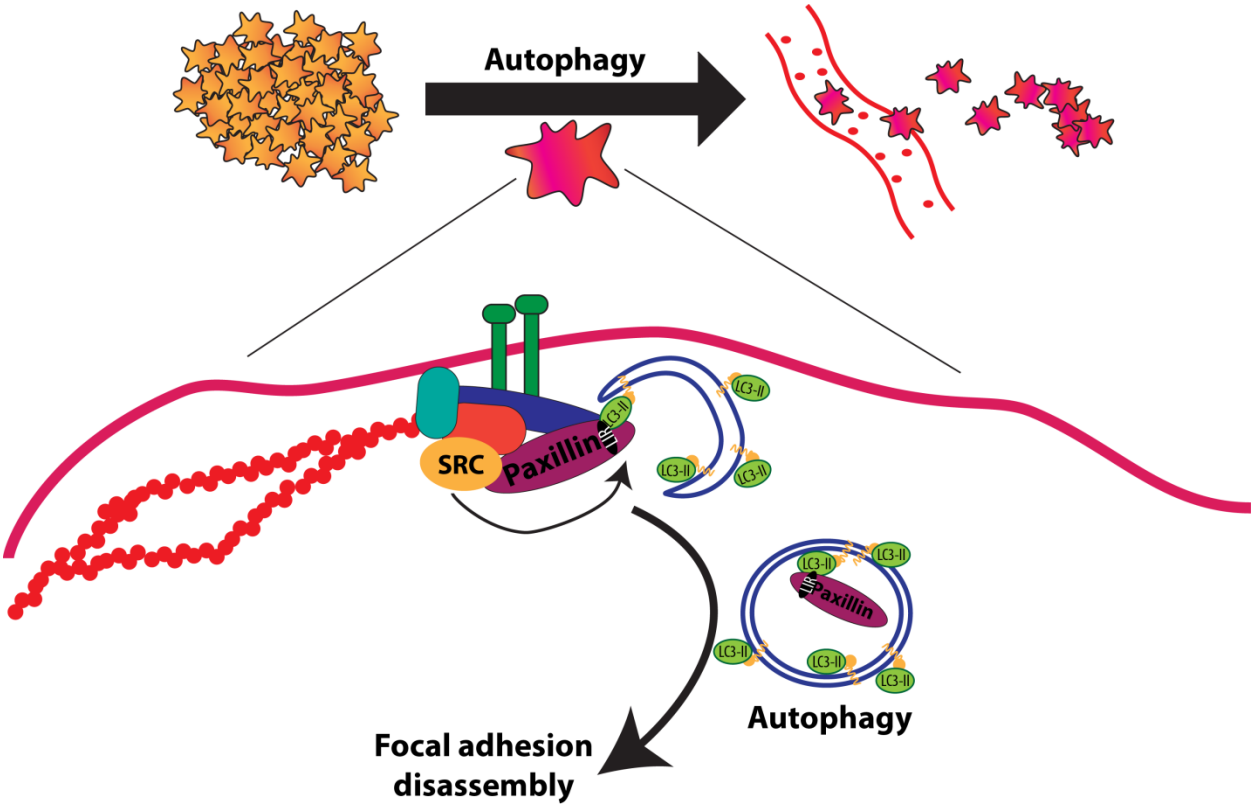

Figure 6.1 Proposed model of the requirement for autophagy in focal adhesion disassembly. Autophagy is required in the early stages of the metastatic cascade in highly metastatic cells. SRC promotes the interaction of the focal adhesion protein paxillin with LC3B through paxillin's LC3 interacting region (LIR) motif. Paxillin is subsequently degraded by autophagy, thereby promoting focal adhesion disassembly and subsequent cell motility and cancer cell metastasis.

Does autophagy directly participate in focal adhesion disassembly?

Focal adhesions represent the link between the intracellular cytoskeleton and the ECM. As cells migrate, focal adhesions are formed towards the leading edge and as used as sites of traction for the cytoskeleton to pull the cell along the ECM. Disassembly of focal adhesions at the rear of the cell and release from the ECM is necessary for the next forward wave of cell migration. Although the assembly of focal adhesions has been well-studied, the signaling involved in focal adhesion disassembly is less well characterized; focal adhesion disassembly is not merely the reversal of focal adhesion formation, which is largely dependent on Rho family GTPases and integrin engagement. FAK, Src, p130CAS, paxillin, ERK, and myosin light-chain kinase (MLCK) are known to be important for focal adhesion turnover in cell protrusions[198]. Microtubules also play a role in stimulating disassembly through clathrin-mediated endocytosis of focal adhesion integrins, which requires the catalytic activity of FAK and Src and the guanosine 5'-triphosphatase dynamin[267–269].

In this thesis, we have demonstrated that paxillin is degraded by the autophagosome, to which it is targeted by interaction with LC3B (Chapter 4). Another group has also reported the presence of LC3B and Atg7, which is involved in the two conjugation reactions required for phagophore elongation, at focal adhesions[96]. The observation of Atg7 at focal adhesions may suggest that elongating phagophores are directed to and form around focal adhesions; thus, autophagy may be responsible for the degradation of multiple focal adhesion proteins. Indeed, Src is targeted for autophagic degradation by c-Cbl in *FAK*-null or detached cells in a manner requiring Src kinase activity[96]. Past work in our lab has identified co-localization of dsRed-zyxin with GFP-LC3B as well as increases in the levels of zyxin and vinculin, two focal adhesion proteins, in autophagy-deficient cells, although the phenotype is not as striking as the paxillin

accumulation. Recently, Kenific *et al* reported that in *HRas*^{V12}-transformed MCF10a cells, inhibition of autophagy impaired focal adhesion assembly and disassembly. The authors attributed this phenotype to Nbr1 and suggested that Nbr1 acts as a cargo adaptor for delivery of several focal adhesion proteins to the autophagosome[241]. Thus, there are reports of autophagic degradation of several focal adhesion proteins, and the ability of autophagosomes to engulf and degrade large protein complexes makes autophagic degradation of focal adhesions an attractive hypothesis. However, it will be necessary to further assess the levels of other focal adhesion proteins in our 4T1 model to further substantiate this claim. Confirmation would beg the question whether other focal adhesion proteins are degraded because they also bind LC3B or an adaptor or whether they are degraded by autophagy indirectly by virtue of their association with paxillin and paxillin's association with the autophagosome. Measuring the levels of these focal adhesion-associated proteins in cells expressing paxillin LIR mutants could clarify this point.

An alternative hypothesis to the engulfment of paxillin by autophagosomes at focal adhesions is the autophagic degradation of non-focal adhesion-associated paxillin. Given the scaffolding function of paxillin and its numerous binding partners, dissociation of paxillin from the focal adhesion might be required for its LC3B binding site to be accessible. Under this model, autophagy would directly degrade only paxillin, thereby siphoning it away from focal adhesions and promoting focal adhesion disassembly. Indeed, our observation that siRNA-mediated knockdown of paxillin in autophagy-deficient cells rescues the focal adhesion phenotype is consistent with this hypothesis (Chapter 3). However, we have also shown that a paxillin truncation mutant containing only the N-terminal LD1-LD2 domains (including the LIR motif) but not the LIM domains implicated in focal adhesion association fails to co-immunoprecipitate with GFP-LC3B. This could indicate that localization of paxillin at the focal

adhesion is critical to its autophagic degradation, possibly because of additional interactions between autophagosomes and other focal adhesion proteins. Thus, whether autophagic degradation of paxillin represents a unique method of regulation in metastatic 4T1 cells or a general requirement for autophagy in the degradation of focal adhesion proteins remains to be determined.

By what mechanism does Src activity modulate paxillin degradation?

Based on our observations that the focal adhesion accumulation and impaired motility in autophagy-deficiency in 4T1 cells was similar to the phenotype reported in cells null for *Src* or expressing catalytically inactive Src[195,198,199] as well as our observation that the Y40 residue within the paxillin LIR is a known Src phosphorylation target[261,262], we investigated a role for Src in mediating the interaction between paxillin and LC3B. Indeed, oncogenic Src promoted the interaction of mApple-paxillin and GFP-LC3B, and mutation of the Y40 residue but not the canonical Src tyrosine phosphorylation sites Y31 and Y118 abrogated this interaction (Chapter 5).

There have been previous reports of phospho-dependent regulation of Atg8/LC3 interactions. The autophagy adaptor OPTN is phosphorylated on the -1 serine relative to the LIR motif by TBK1 to promote binding to LC3 and subsequent autophagic clearance of cytosolic *Salmonella enterica* bacteria[90]. Similarly, binding of Bnip3, a mitochondrial protein that acts as a cargo adaptor for autophagic degradation of mitochondria, to LC3B and GATE-16 is promoted by phosphorylation of the serine residues located in the -1 and +7 positions relative to the LIR sequence. This phosphorylation-promoted binding stimulates pro-survival mitophagy downstream of Bcl-x_L[263]. In both of these cases, phosphorylation of sites surrounding the LIR

promotes Atg8/LC3 binding. However, there has also been a report of binding regulated by phosphorylation within the LIR motif. Like paxillin, the integral mitochondrial outer membrane protein FUNDC1 possesses a tyrosine residue in its +1 LIR motif position. Under basal conditions, the residue is phosphorylated by Src, but upon hypoxia exposure, the +1 residue is dephosphorylated, promoting interaction with LC3 and subsequent mitophagy[87]. Thus, phosphorylation of residues in and around LIR motifs is an established strategy to regulation Atg8/LC3 interactions.

Although our data due strongly support a role for oncogenic Src in regulating the interaction of paxillin and LC3B, we have not directly demonstrated that Src catalytic activity is required. An *in vitro* binding assay demonstrating increased binding of GST-LC3B and paxillin in the presence of active Src relative to the binding in the presence of catalytically inactive Src would confirm that Src kinase activity is the driving force behind increased binding. The demonstration that neither active nor inactive Src promote binding would suggest that Src phosphorylation of targets other than paxillin indirectly promotes the binding of paxillin with LC3B, possibly by destabilizing the interaction of paxillin with other binding partners to free paxillin for binding to LC3B.

Phosphorylation of paxillin on Y31 and Y118 is well-established to be important for cellular migration. However, we have demonstrated that these two Src phosphorylation sites are not required for paxillin/LC3B binding (Chapter 5). In contrast, the Y40 site is required for binding. This suggests two competing hypotheses for Src regulation of the paxillin/LC3B interaction. First, Src phosphorylation of the Y40 residue within the LIR motif may promote binding. Alternatively, Src phosphorylation of another uncharacterized tyrosine residue, like the experimentally validated Y88[261] or the identified but uncharacterized Y76, Y182, Y377, or

Y436[262], may be indirectly responsible for the paxillin/LC3B interaction. Under this model, mutation of the Y40 residue would abrogate binding to LC3B irrespective of Src status simply because it disrupts the LIR motif, not because it is a Src phosphorylation target.

The first hypothesis is made somewhat less likely in light of the fact that in the case of FUNDC1, Src-stimulated tyrosine phosphorylation in the +1 position is destabilizing[87]. Furthermore, the +1 LIR position typically occupies a highly conserved hydrophobic binding pocket on Atg8/LC3; the addition of a highly negatively charged phosphate group would therefore be predicted to inhibit, not promote, binding. However, Atg8/LC3 binding of tyrosine-containing LIR-motifs is less well characterized than tryptophan-containing motifs. It is possible that positively charged residues or ions located near the phosphotyrosine in three-dimensional space might somehow stabilize the negative charge. Alternatively, perhaps the phosphotyrosine does not occupy the canonical hydrophobic pocket, as has been reported in a phage-display study involving GABARAP-binding peptides in which a peptide was observed to bind in an inverse orientation relative to the canonical LIR sequence[245]. Interestingly, our attempts to generate a phosphomimetic LIR using a Y40E substitution were unsuccessful because the mutant was very unstable when expressed in 4T1 cells, consistent with increased autophagic degradation of pY40.

Future experiments should focus on the generation of mutants of the other potential Src phosphorylation sites within paxillin. Tyrosine 377 and 436 are located in the C-terminal region of paxillin between LIM1 and LIM2 and between LIM2 and LIM3, respectively. As this is the region generally believed to be involved in localization to the focal adhesions but less implicated in regulation or signaling interactions, these are less likely to be involved in Src-regulated autophagic targeting of paxillin. Of the N-terminally located sites, Y76, Y88, and Y182, Y88 is particularly interesting. Src phosphorylation of Y88 has been experimentally validated[261],

whereas the other two sites are not predicted Src targets[262]. Furthermore, its close proximity to the LIR motif may suggest that it could act as a distal site promoting binding directly or could destabilize interactions between paxillin and other proteins in this region to make the LIR motif available for LC3B binding. Finally, among the four experimentally validated Src phosphorylation sites (Y31, Y40, Y88, and Y188), Y88 is believed to be the strongest contributor to the retarded electrophoretic mobility characteristics of tyrosine-phosphorylated paxillin; mutation of this site eliminates the heterogeneous electrophoretic mobility of phosphorylated wildtype paxillin and results in a tight down-shifted band[261]. Interestingly, our co-immunoprecipitations indicated that oncogenic Src stimulated binding of LC3B with the up-shifted paxillin band with retarded electrophoretic mobility (Chapter 5), suggesting that perhaps Y88 phosphorylation is a strong contributor to the binding interaction. Using co-immunoprecipitation experiments involving a variety of paxillin tyrosine mutants, it will be possible to identify which sites are involved in Src-stimulated phosphorylation. Subsequently, these mutants can be used in *in vitro* binding assays in the presence and absence of active Src to determine whether they affect binding directly (i.e., active Src stimulates *in vitro* binding of GST-LC3B to wildtype but not Tyr-mutant paxillin) or whether they affect binding indirectly (i.e., Tyr-mutant paxillin has no effect on *in vitro* binding to GST-LC3B). These series of experiments will open avenues to further characterize other players involved in the regulation of paxillin/LC3B binding and may shed light on whether autophagosomes are targeted to focal adhesion-associated paxillin or to free paxillin.

What is the role of autophagy in cell motility?

Our discovery that autophagy can promote cell migration and invasion through focal adhesion disassembly downstream of autophagic degradation adds to a growing body of work implicating autophagy and the Atg proteins in cell motility. As discussed in Chapter 1, autophagy has been implicated in migration, invasion, and metastasis in cancer cells. Interestingly, a systems biology analysis linked overexpression of 108 "autophagy prime genes", which include autophagy-related genes determined to be most critical for the functional aspects of autophagy regulation and execution, to cells from the germinal center, neuronal cells, and macrophages, all cells in which cellular motility represents a critical function, potentially suggesting that the role of autophagy in cell motility is a physiologic or developmental one that is co-opted by cancer cells[270].

Our findings are not the first to link autophagy and paxillin. In *Drosophila*, genetic studies identified a connection between Atg1/Ulk1 and paxillin, and *in vitro* assays confirmed that Atg1 could phosphorylate paxillin. Upon nutrient deprivation of mouse embryonic fibroblasts (MEFs), paxillin was redistributed from focal adhesions, and cells deficient in paxillin exhibited defects in autophagosome formation[34]. However, we did not observe any changes in autophagy in paxillin-deficient cells, which may be a reflection of differences in normal versus cancerous cells. However, these findings and our own indicate that autophagy may regulate paxillin at multiple levels.

A very recent paper confirms our findings that autophagy promotes focal adhesion disassembly and also suggests that it may promote focal adhesion assembly as well; however, the group linked regulation of focal adhesion dynamics to the selective autophagy cargo receptor Nbr1[241]. In our system, Nbr1 has no effect on either cell motility or paxillin levels (Chapter 3),

possibly due to the cell systems used; here, we employed metastatic 4T1 and B16.F10 cells, whereas the aforementioned paper employed *HRas*^{V12}-transformed MCF10a cells. Nonetheless, taken together, our and others' work suggests a conserved role for autophagy in cell motility through focal adhesion regulation.

Although we did not observe any changes in FAK phosphorylation status or levels in our system (data not shown), FAK has also been linked to autophagy. Indeed, FIP200, a member of the Ulk1 complex regulating autophagosome formation, was originally identified as an inhibitor of FAK leading to decreased cell spreading, decreased migration, and inhibition of cell cycle progression[271]. FIP200 activity lies downstream of starvation-induced AMPK-dependent activation of the ULK1 complex, and release of FAK from FIP200-mediated inhibition can enhance cellular invasion and metastatic dissemination in mouse models and is correlated with shortened overall survival in patients[272]. Given that FAK, like Src, is also implicated in focal adhesion disassembly[196,198,267], these findings may suggest a method by which the upstream autophagy machinery can help coordinate downstream focal adhesion disassembly.

There have been several reports linking autophagy or Atg proteins with the Rho family of GTPases and cytoskeletal dynamics, which largely function in the earlier stages of cell migration at the leading edge. Autophagy has been shown to inactive Rac1, which promotes lamellipodia formation, in favor of Rab7 activation and subsequent stimulation of autophagosome-lysosomal fusion[273]. In *Drosophila*, autophagy is required for cell spreading and the production of Rho1-induced cell protrusions, and loss of autophagy impairs the ability of hemocytes to migration to epidermal wounds[274]. The observation that cellular spreading was depending on the *Drosophila* homolog of p62 suggested a role for selective autophagy in this process[274]. Consistent with this finding, p62/Sqstm1 was reported to target active RhoA, the mammalian homolog of *Drosophila*

Rho1, to the autophagosome; failure of autophagy led to impaired cytokinesis and aneuploidy[275]. Autophagy has also been implicated in cytoskeleton regulation downstream of Rho. Using an siRNA screen for genes that modulate autophagy, Chan *et al* identified Rho-associated kinase 1 (ROCK1), a downstream effector of Rho that regulates migration and cytoskeletal dynamics, as a regulator of starvation-induced but not basal autophagy[276]. Inhibition of ROCK1 elevated autophagic flux and led to the accumulation of enlarged early autophagosomes, leading the authors to speculate that ROCK1 inhibition controls autophagosome size by extending the phagophore elongation stage through increased association of the Ulk1 complex with autophagosmes[277]. Interestingly, another group reported that activation of ROCK1 under metabolic stress promoted autophagy by binding and phosphorylating Beclin1 at Thr199. This phosphorylation resulted in dissociation of Bcl-2 from Beclin1 without affecting UVRAG/Beclin1 interactions to promote autophagy[278]. Finally, a Rho GTPase module has been identified within an autophagy-centered gene interaction network, and Cdc42 was experimentally validated as a protein that fine-tunes autophagic responses to environmental conditions[270].

Autophagy has also been implicated in ECM-related aspects of cell motility. Inhibition of autophagy through *Beclin1* knockdown has been shown to inhibit collagen degradation, suggesting that autophagy may play a role in intracellular degradation of ECM components[279]. Furthermore, autophagy has been implicated in degradation of β1 integrin. Inhibition of autophagy in MEFs can slow lysosomal degradation of internalized integrins to promote integrin membrane recycling and thereby increase cell migration[280].

Thus, autophagy has been implicated at nearly every stage of cell migration, from interactions with the Rho GTPase family to focal adhesions to ECM regulation. Whether the Src-

regulated autophagic degradation of paxillin represents a generalized characteristic of non-neoplastic cells or a unique adaptation of highly metastatic cells like the 4T1 and B16.F10 cells investigated in this study remains to be determined. Paxillin degradation has been shown to be required for focal adhesion turnover and mesodermal cell motility during *Xenopus* gastrulation[281], and in mice, paxillin is required for proper development of mesodermally derived structures[237]. Furthermore, paxillin phosphotyrosine levels are related to developmental stage in both chicken and rat[282]. However, as both *Atg5*-null and *Atg7*-null embryos survive until birth[283,284], autophagic degradation of paxillin does not seem to be a requirement during mammalian morphogenesis. Nonetheless, autophagy may play a post-developmental role in the motility associated with wound healing or migratory immune cells. Indeed, autophagy may represent a key regulatory node allowing cells to respond to extracellular conditions or internal conditions by balancing cell movement to areas of greater nutrient concentrations or metastatic niches with motility arrest and either pro-survival autophagy or cellular death. Future work exploring autophagy in the context of either physiological or pathologic cell migration will likely reveal many more connections between autophagy and cell motility.

What is the clinical feasibility of autophagy therapy?

Both repression and stimulation of autophagy have been suggested as therapeutic approaches to cancer. Excessive autophagy could impede cell recovery and survival, thereby promoting autophagic cell death. This may represent a particularly useful approach in cancer cells defective for apoptosis. Alternatively, inhibition of autophagy may prevent its use as a survival mechanism that allows tumors to combat stress or its utility in specific processes like cell motility. Whether autophagy is acting largely as a pro-death mechanism or a pro-survival

mechanism will vary by tumor type and stage. Of course, it is also important to consider the effects of autophagy therapies on non-cancer cells. For example, given that autophagy is believed to be tumor suppressive early in cancer progression, systemic inhibition of autophagy may predispose patients to the development of new lesions even as their original tumor is treated effectively.

Many of the currently available chemotherapy compounds result in autophagy induction[285–287]. For example, mTOR inhibitors are attractive candidates to inhibit the PI3K/Akt/mTOR pathway, which is deregulated in many cancers, but inhibition of mTOR may stimulate pro-survival autophagy. The fact that so many different classes of chemotherapeutic agents (e.g., proteasome inhibitors, tyrosine kinase inhibitors, HDAC inhibitors, monoclonal antibodies, etc.) induce autophagy could suggest that autophagy may represent a generalized escape mechanism from chemotherapy. In contrast, relative few inhibitors of autophagy are currently available. Most of these agents, like chloroquine and hydroxychloroquine, target acidic compartments and can affect both autophagy and generate lysosomal activity. Thus, they may have significant non-autophagic and non-tumor effects. Indeed, it is not clear whether the *in vitro* effects observed in response to these agents will be relevant at the concentrations used clinically or within a systemic context. Furthermore, under certain conditions, autophagy inhibitors may become autophagy inducers. For example, chloroquine has been shown to stimulate autophagy and lysosomal biogenesis downstream of upregulation of the TFEB transcription factor[114], and compounds that inhibit class I and class III PI3Ks can be either autophagy-inhibiting or autophagy-promoting at different concentrations[288].

As has become a general theme in cancer therapeutics, combination therapies may be necessary. Autophagy inhibitors are being combined with established cancer therapies, many of

which induce autophagy, in a number of ongoing phase 1 trials[287]. The combination of autophagy inhibitors with radiotherapy is also an attractive option[286]. However, with combination treatments, the choice of autophagy inhibitor may be of critical importance. There have been several reports of different autophagy inhibitors having opposing effects when combined with the same chemotherapeutic agent[289,290]. Some authors have suggested that this may reflect differences in targeting both macroautophagy and chaperone-mediated autophagy using late-stage autophagy inhibitors (e.g., chloroquine) and in targeting only macroautophagy using early-stage autophagy inhibitors (e.g., 3-methyladenine).

Does autophagy inhibition represent a viable chemotherapeutic target? Although there is significant excitement and ongoing clinical trials modulating autophagy in the therapeutic setting, it seems that our understanding of autophagy is as-of-yet insufficient to answer that question. Our findings here that autophagy promotes migration and invasion could imply that autophagy inhibition may prevent clinical metastasis; however, given that these events occur at the initial and non-rate-limiting steps of the metastatic cascade, this type of therapy may be of limited utility in patients with advanced disease. Furthermore, it remains to be determined whether systemic autophagy inhibition, either in hopes of preventing metastasis or halting primary tumor growth, will negatively affect other motile cell types, including immune cells. We have yet to understand precisely when and where autophagy is pro- versus anti-tumorigenic, and targeting autophagy pharmacologically has revealed unanticipated complications.

What is the future of autophagy research?

Klionsky reported that in 2000, someone suggested to him, “Autophagy will be the wave of the future”[14]. Indeed, from its humble beginnings as a description of new electron microscopy

findings, autophagy is now widely recognized to affect fields as diverse as developmental biology, microbiology, metabolism, immunology, neurology, aging, and cancer. Our molecular understanding of autophagy is relatively new; the first autophagy-related gene, *ATG1*, was cloned less than twenty years ago[18]. Since that time, the number of autophagy publications in PubMed has grown almost exponentially[14]. The number of Atg genes now exceeds thirty, whereas the genes involved in the human autophagy interaction network number 1222[270].

Within the field of cancer research, we have come to appreciate that the term autophagy refers to a very general phenomenology that can manifest in highly unique manners under different conditions. Although the general consensus is that autophagy is initially tumor-suppressive but eventually becomes tumor-promoting, there are certainly exceptions to the rule. With respect to metastasis, most studies support a tumor-promoting role. The work presented in this thesis describes a specific role for autophagy in focal adhesion disassembly and subsequent cell motility and tumor cell metastasis. In metastatic tumor cells, the focal adhesion protein paxillin binds to LC3B in a Src-regulated manner to target paxillin for autophagic degradation.

The initial enthusiasm of the field and the clinical potential of autophagy has mellowed somewhat as we have begun to appreciate that we cannot easily predict what effect autophagy will have in which contexts or, indeed, in what direction our manipulations will modulate it. Future research must focus on clarifying what factors regulate the outcomes of autophagy induction and on identifying which autophagy-regulated processes are common among all cell types, which are specific to malignant cells, and which are specific to select tumor types. Given autophagy's many roles, it is likely that clinical inhibition or induction of autophagy will require tissue- or tumor-specific targeting to avoid unintended effects. For example, acute system inhibition of autophagy has been shown to cause neurodegeneration and premature death as well

as overwhelming starvation-induced liver, muscle, and brain damage upon fasting, suggesting that systemic autophagy therapy may have many unintended side effects[291]. Furthermore, specific autophagy inhibitors or inducers that do not have broad effects (e.g., effecting all PI3K signaling or all acidic compartments) are urgently needed. Combination of autophagy regulators with other chemotherapies may be needed to achieve optimal therapeutic success.

Despite these challenges, the field of autophagy research marches on. Whether the next twenty years will reveal as many adjustments to our current model of autophagy in cancer as the past twenty years have remains to be seen. However, when it comes to autophagy, the old adage is certainly true: “The more we learn, the more we realize how little we know.”

APPENDIX:

THE ROLE OF AUTOPHAGY IN TUMOR PROGRESSION IN A MOUSE MODEL OF CARCINOGEN-INDUCED HEAD AND NECK SQUAMOUS CELL CARCINOMA

ABBREVIATIONS

4NQO	4-nitroquinoline 1-oxide
DMBA	7,12-dimethylbenz[a]anthracene
GEMM	Genetically engineered mouse model
HNSCC	Head and neck squamous cell carcinoma
K5	Keratin 5
K14	Keratin 14
LCM	Laser-capture microdissection
OSCC	Oral squamous cell carcinoma
PCR	Polymerase chain reaction
SCC	Squamous cell carcinoma
TSCC	Tongue squamous cell carcinoma

CHAPTER A1

INTRODUCTION

Head and neck cancer: Pathogenesis and clinical course

Head and neck squamous cell cancer (HNSCC) is the sixth most common cancer worldwide and typically arises in the oral cavity, although tumors may also be found in the oropharynx, nasal cavity, paranasal sinuses, larynx, and hypopharynx[292–294]. The most important risk factors of HNSCC include tobacco use and alcohol consumption, which exert a synergistic effect, as well as infection with high-risk types of human papillomavirus (HPV)[292–294]. Indeed, Llewellyn *et al* have estimated that the risk of oral and pharyngeal cancer in adults under the age of 46 is increased 20-fold for chain smokers, 5-fold for heavy drinkers, and nearly 50-fold for individuals exhibiting both risk factors[295]. Although the five-year survival rate of HNSCC patients diagnosed in the earlier stages is 80%, approximately two-thirds of patients are diagnosed with late-stage disease and have a five-year survival rate of only 19%[292,293,296].

The low survival rate of HNSCC is affected by the high incidence of recurrence of multiple primary tumors, which develop at a rate of 3-5% every year[293]. The development of multiple primary tumors may be the result of exposure of the entire mucosal surface of the upper aerodigestive tract to the same carcinogen[294]. The concept of "field cancerization" was first introduced in 1953 by Slaughter *et al* to explain the persistence of abnormal tissue after surgery[297]. Under this model of carcinogenesis, a stem cell acquires genetic alterations, typically mutations in *TP53,* and forms a patch of genetically altered daughter cells. Further genetic alterations result in the escape of the stem cell from normal growth control and expansion of the

patch into a field of related cells at the expense of normal tissue. This field, which is often characterized by *CDKN2A* loss and alterations in *TP53* in approximately 70-80% and 60-80% of HNSCC cases, respectively[292,293], may be considered "primed" for transformation after clonal divergence and selection of multiple related neoplastic lesions[298]. Several studies have demonstrated that in approximately one-third of patients in whom a primary tumor was removed with clear margins, cells with tumor-associated genetic alterations are left behind undetected in the patient and are poised to undergo transformation[292,298].

Attempts to define subclasses of HNSCC to better predict therapeutic treatment and response have largely focused on HPV positivity and high/low chromosomal instability[292], although some researchers have noted that HNSCC tumor pO_2 exhibits a strong prognostic significance[299]. *EGFR* overexpression was one of the first identified alterations in HNSCC, and since then, point mutations, although rare, and amplifications have been reported[292,300–304]. The PI3K/ATK/mTOR pathway is frequently altered in HNSCC, with an estimated 50% of cases of HNSCC exhibiting activating mutations in ATK or loss of PTEN expression[305,306]. Studies within the past decade suggest that mTOR inhibition exerts a potent anti-tumorigenic effect in HNSCC cell lines and *in vivo* models[305,307–310]. Recent whole-exome sequencing data in HNSCC from two independent groups identified *Notch1* as frequently mutated in human HNSCC cancer, in addition to confirming previously known mutations in *TP53*, *CDKN2A*, *PIK3CA*, *HRas*, and *PTEN* [311,312]. *Notch1* mutation was part of a significantly mutated gene set also including *IRF6* and *TP63*, which are involved in renewal of basal keratinocytes and squamous differentiation[312]. Both groups confirmed that HPV-associated tumors were genetically distinct from HPV-negative tumors, although the groups reported conflicting information concerning whether HNSCC exhibited the G/C → T/A transversions characteristic of tobacco-associated lung cancers.

However, gene expression analysis of smokers with lung or HNSCC indicates that distinct gene signatures differentiate smoking-associated and smoking-independent cancers[313]. Future studies should focus on identifying prognostic biomarkers and therapies targeted at the characteristics of different tumor subclasses in HNSCC.

Symptoms of early HNSCC may be vague, including pain, non-healing ulcers, and hoarseness, and early leukoplakia lesions may be identified upon close inspection[294]. The majority of patients with HNSCC are treated with surgery or radiation therapy, and chemotherapy may be added for locally advanced cases[293]. Chemotherapy typically includes platinum compounds, antimetabolites, and taxanes, although targeted therapies, notably the EGFR antibody cetuximab and PI3K pathway inhibitors, are also being explored[125,293]. Despite the introduction of new targeted therapies, survival rates in HNSCC have stagnated in recent decades[292]. Thus, the field has begun to turn towards other pathways for intervention.

Mouse models of HNSCC

Mouse models of HNSCC can be classified into three broad groups: (1) chemically induced models, (2) xenografts and orthotopic models, and (3) GEMMs[314]. Perhaps the best studied among these models are the chemically induced models. One traditionally used model is the carcinogenic 7,12-dimethylbenz[a]anthracene (DMBA)-induced Syrian hamster cheek pouch model[315]. Although the animals develop premalignant lesions and SCCs after repeated application of the carcinogen and exhibit genetic changes reflective of the human pathophysiology, the lesions differ in their anatomic location and do not grossly or histologically resemble human HNSCC. A more faithful model of human disease is the 4-nitroquinoline 1-oxide (4NQO) model. 4NQO is a water-soluble carcinogen that binds preferentially to guanine

residues to promote the formation of DNA adducts and induce intracellular oxidative stress, mutations, and DNA strand breaks; these changes mimic the damage induced by tobacco and alcohol, the most prevalent risk factors for HNSCC[316,317]. Unlike other carcinogen HNSCC models that have been proposed, including DMBA and other polycyclic aromatic hydrocarbons, 4NQO exhibits the distinct advantage of not inducing an excessive inflammatory response[316]. The ability of 4NQO to dissolve in water means that the compound can be administered chronically in the drinking water of immune-competent mice, thereby closely replicating tobacco-induced oral carcinogenesis. The mice develop pre-malignant lesions as well as SCCs of the tongue and oral cavity that resemble human HNSCC histologically as well as molecularly, including alterations in cytokeratin expression, the PI3K/ATK pathway, *p53* status, and cell cycle proteins[296,308,316–319]. The model is thus highly attractive as a physiologically relevant model that is ideal for use as a preclinical model in HNSCC to address the stagnation in HNSCC patient survival.

Xenograft models of HNSCC, in which human HNSCC cells are injected subcutaneously, suffer from a failure to appropriately model the environment of HNSCC and thus do not support locoregional invasion or metastasis[320]. An improvement on this model has been the development of patient-derived xenografts. Primary tumors harvested from human patients can be implanted subcutaneously into nude mice. These tumors tend to recapitulate the original histology of the patient tumor and exhibit expression patterns more similar to the original tumor than cells in culture[321]. Compared with xenograft models, orthotopic models in which HNSCC cells are injected into the tongues of mice are better able to recapitulate human HNSCC histology and exhibit the predicted lymph node invasion pattern[320,322].

Relatively few HNSCC-specific GEMMs exist. The very first HNSCC GEMM involved

expression of cyclin D1 downstream of the Epstein-Barr virus lytic promoter to drive expression in the tongue, esophagus, and forestomach. Although the mice did develop dysplasias, they failed to progress to tumors[323]. An improvement on the model came with its combination with *TP53* heterozygous mice, which did develop invasive cancer, although the mice also developed tumors in other organ systems due to the systemic nature of *TP53* heterozygosity[324]. Transgenic approaches have also been attempted to limit off-target expression. For example, Lu *et al* generated an inducible model of TGFβ expression under the control of a keratin 5(K5)-driven GLp65 transactivator in which TGFβ is expressed specifically in basal epithelial cells upon application of the synthetic steroid antagonist RU486[325]. Although the model induced hyperproliferation in and inflammation of the oral epithelial, no tumors were observed[325]. Several groups have used either K5-driven Cre[326] or tetracycline-inducible Cre[327] to drive activation of oncogenic $KRas^{G12D}$ and the production of benign papillomas. However, given the etiology of human HNSCC, chemical carcinogenesis models, particularly the 4NQO model, may provide the most faithful model of the full clinical course of HNSCC.

The role of autophagy in HNSCC

There is emerging evidence that autophagy may play a role in HNSCC. First, smoking has been reported to induce autophagy in a *SIRT-1-PARP-1*-dependent manner[328], and autophagy may act to mitigate the effects of oxidative stress and chronic inflammation associated with smoking[329]. Autophagy inhibition has also been shown to promote the infectivity of HPV-16[330]. Furthermore, several clinical studies have correlated the expression of autophagy-related genes with HNSCC progression and survival.

In oral squamous cell carcinoma (OSCC), increased immunostaining for Atg16L1 has been observed in malignant cells and surrounding stroma and is associated with lymphovascular invasion and lymph node metastasis[331]. Similarly, elevated LC3 expression is correlated with poor overall OSCC survival after controlling for grade, stage, and the consumption of alcohol, betel, and tobacco[332]. This finding is supported by another study by the same authors correlating positive *Beclin-1* and *ATG5* expression with reduced overall and recurrence-free survival in OSCC[333]. However, instances of reduced *Beclin-1* mRNA have also been reported in OSCC[334], and in tongue squamous cell carcinoma (TSCC), downregulation of Beclin-1 and LC3 is observed and is associated with stage and differentiation status[335]. Furthermore, an immunohistochemical study of 195 OSCCs reported higher levels of cytoplasmic p62/SQSTM1; however, the authors also noted that increased levels of LC3-II were associated with poor outcomes[336]. This apparently conflicting result may reflect re-activation of autophagy in advanced-stage cancers.

The use of inhibitors of the PI3K/Akt pathway in HNSCC therapies provides correlative evidence that targeting autophagy might represent a useful therapeutic strategy. Indeed, mouse models of HNSCC have demonstrated that mTOR activation is an early event in HNSCC development and that mTOR inhibition can halt malignant transformation[308]. A more direct link between autophagy and HNSCC has recently been reported by Kuo *et al* in HNSCC cell lines and human tissue samples[125]. In HNSCC cell lines, resistance to PI3K/AKT inhibitors was positively associated with loss of autophagy through down-regulation of *Atg7* and accumulation of p62/SQSTM1, and modulation of autophagy could restore PI3K/AKT inhibitor sensitivity[125]. Furthermore, a tissue microarray of normal, dysplasic, and malignant human oral tissues demonstrated progressive accumulation of p62/SQSTM1, and alterations of the *Atg7* gene

resulting in down-regulation or deletion were detected in TCGA HNSCC samples[125].

In this appendix, the role of autophagy in HNSCC was further explored using a combination of the 4NQO model of carcinogenesis with K14-driven deletion of key autophagy genes. In Chapter A3, we describe the characteristics of control 4NQO-induced lesions, which exhibit basal cell markers and downregulation of autophagy in advanced lesions. In Chapter A4, we discuss a potential role for autophagy in the progression of 4NQO-induced lesions. The limitations of this model and currently available tools for analysis, as well as remaining questions and future experiments, are addressed in Chapter A5.

CHAPTER A2

MATERIALS AND METHODS

Mice

All mouse protocols and procedures were approved the University of Chicago Institutional Animal Care and Use Committee under the terms of animal protocol 71155. Mice were housed up to five adult mice per cage in the Animal Resource Facility, a temperature- and humidity-controlled, specific pathogen-free barrier facility with a 12 hour:12 hour light:dark cycle. Animals were fed standard chow and autoclaved drinking water *ad libitum*. Breeding schemes employed both paired and harem breeding to generate mice of the desired genotype.

129Sv-Tg(K14-Cre) mice were originally generated in the Fuchs laboratory[337] and were kindly provided by Xiaoyang Wu (University of Chicago). The 129Sv-Tg(K14-Cre) mice were subsequently backcrossed to C57BL/6 mice to achieve an inbreeding coefficient greater than 0.996. C57BL/6-Tg(Atg5-flox), C57BL/6-Tg(Atg7-flox), and C57BL/6-Tg(GFP-LC3) mice were initially generated in the laboratory of Mizushima[162,283,338] and were kindly provided by Seungmin Hwang (University of Chicago), Eileen White (Rutgers), and Eugene Chang (University of Chicago), respectively. C57BL/6-Tg(Rosa26-LSL-tdTomato) mice were obtained from The Jackson Laboratory.

Genotyping

Genomic DNA was isolated by isopropanol precipitation from tail snips following overnight digestion at 55°C in lysis buffer (100 mM Tris pH 8.0, 5 mM EDTA pH 8.0, 0.2%

SDS, 200 mM NaCl) containing 100 nM proteinase K. Genotyping polymerase chain reactions (PCRs) were performed in a thermocycler according to the developer's protocols under conditions appropriate for the genotyping primers (Table A2.1).

Table A2.1: Genotyping primers

Gene	**Primers**	**Expected band size**
Atg5-flox	Check2: 5'-acaacgtcgagcacagctgcgcaagg-3' Exon3-1: 5'-gaatatgaaggcacacccctgaaatg-3' Short2: 5'- gtactgcataatggtttaactcttgc-3' 5L2: 5'-cagggaatggtgtctcccac-3'	Wildtype: 350 bp Floxed-in: 650 bp Cre-deleted: 300 bp
Atg7-flox	Ex14F: 5'-tctcccaggacaagacagggtgaa-3' Pst-rv: 5'- gtggagctgatggtctctgtcctg-3'	Wildtype: 200 bp
	Fl_5.1: 5'-ccttttccctgtcactctgc-3' Fl_3.1: 5'-cagagaccatcagctccaca-3'	Floxed-in: 200 bp
	Hind-Fwd: 5'-tggctgctacttctgcaatgatgt-3' Ex14R: 5'-aagccaaaggaaaccaagggagtg-3'	Cre-deleted: 600 bp
Cre	Cre-Fwd: 5'-ggacatgttcagggatcgccaggc-3' Cre-Rev: 5'-cgacgatgcagcatgtttagctg-3'	Transgene: 200 bp
Rosa26-LSL-tdTomato	Wt-Fwd: 5'-aagggagctgcagtggagta-3' Wt-Rev: 5'-ccgaaaatctgtgggaagtc-3' Tg-Fwd: 5'-ggcattaaagcagcgtatcc-3' Tg-Rev: 5'-cgacgatgcagcatgtttagctg-3'	Wildtype: 297 bp Transgene: 196 bp

Administration of 4-nitroquinoline 1-oxide

4-nitroquinoline-1-oxide (4NQO) was purchased from Sigma-Aldrich. Stock aliquots of 4NQO were stored at 50 mg/ml in DMSO at -20°C until use. On the days of 4NQO administration, stock 4NQO solution was diluted to 12.5 mg/ml in propylene glycol (Sigma) and then further diluted in fresh autoclaved water to a final treatment concentration of 100 µg/ml. A fresh bottle of 4NQO drinking water was prepared every week for each of the 8 weeks of carcinogenic treatment. Normal autoclaved drinking water was resumed at the end of the 8-week carcinogenic treatment period.

For 4NQO tumor studies, 6- to 8-week-old male and female mice of the following genotypes on C57BL/6 backgrounds were used: *K14-Cre*, *Atg5-flox*, and *Atg7-flox* (control); and *K14-Cre;Atg5-flox* and *K14-Cre;Atg7-flox* (experimental). K14-Cre was maintained in heterozygosity; floxed alleles were maintained in homozygosity. For each control group, six mice were assigned to each of six experimental endpoints; for each experimental group, 12 mice were assigned to each endpoint. Mice were treated for 8 weeks with 4NQO drinking water prepared as described above. After 8 weeks of treatment, normal autoclaved drinking water was resumed. Mice were sacrificed by CO_2 asphyxiation and cervical dislocation at 4, 8, 12, 16, 20, or 24 weeks after cessation of 4NQO treatment. Mice dying prior to their pre-assigned experimental endpoint were not included in the final analysis.

For histological diagnosis of tongue lesions, at least two hematoxylin and eosin-stained sections of bisected tongues taken 90 µm apart were examined by an experienced pathologist (Mark Lingen; University of Chicago). The animals were scored according to the most advanced lesion present on the tongue sections.

Preparation of mouse tissues

Tongues isolated from sacrificed mice were cut so as to bisect any macroscopic lesions and were subsequently fixed for 24 hours in 10% neutral-buffered formalin, followed by transfer to 70% ethanol. All samples for histology were processed, embedded in paraffin, and sectioned (5 μm) by the University of Chicago Tissue Resource Center.

Tissues from *K14-Cre;Rosa26-LSL-tdTomato* mice for frozen histology were fixed in 4% paraformaldehyde for 4 hours at room temperature. The tissues were transferred to a 10% sucrose/PBS solution and left at 4°C for 24 hours, followed to two additional 24-hour incubations at 4°C in 20% sucrose/PBS and 30% sucrose/PBS. The tissues were gently dabbed on a Kimwipe to remove excess moisture and were placed in Tissue-Tek O.C.T. Compound (Sakura) in a cryomold. The cryomolds were frozen over a methyl butane/dry ice bath until the O.C.T. Compound turned completely white and were incubated in the bath for five minutes thereafter. The cryomolds were wrapped in foil and stored at -80°C until further processing and sectioning (8 μm) by the University of Chicago Tissue Resource Center.

Immunohistochemistry

Immunohistochemistry for Ki67, p63, K14, and LC3B was performed by the University of Chicago Human Tissue Resource Center (Table A2.2). Staining for Atg7 was performed manually using similar methods. Briefly, paraffin-embedded sections were incubated in two washes of xylenes, followed by rehydration in serial dilutions of ethanol to deionized water. After heat-induced epitope retrieval in a pressure cooker, endogenous peroxidase activity was quenched by incubation in 10% methanol/3% hydrogen peroxide for 30 minutes. Sections were blocked in 1.5% goat serum (Vector Laboratories) for 30 minutes at room temperatures and were

incubated in primary antibody diluted in blocking buffer overnight at 4°C (Table A2.2), followed by biotinylated-secondary antibody with avidin-biotin signal amplification (Vector Laboratories), and the proteins were visualized by Elite kit (Vector Laboratories) and DAB (DAKO). The stained slides were digitized using an Allied Vision Technologies Stingray F146C color slide scanner at the Integrated Microscopy Core Facility at the University of Chicago and analyzed using Panoramic Viewer.

Table A2.2: Immunohistochemistry antibodies

Target	Source/Catalogue number	Dilution	Epitope retrieval
Atg7	Sigma HPA007639	1:125-1:250	0.01 M citrate buffer, pH 6.0
K14	Biolegend PRB-155P-100	1:1,000	Antigen retrieval buffer (DAKO)
Ki67	Labvision #RM-9106-s	1:300	Antigen retrieval buffer (DAKO)
LC3B	Nanotools #0231-100	1:100	Antigen retrieval buffer (DAKO)
P63	Santa Cruz sc-8431	1:100	Antigen retrieval buffer (DAKO)
P62	Biomol #pw9860	1:500	Antigen retrieval buffer (DAKO)

Visualization of tdTomato fluorescence

Frozen tissue slides were allowed to warm to room temperature for 10 min, followed by washing in PBS. Coverslips were mounted on the slides using Vectashield mounting media with DAPI to prevent photobleaching (Vector Laboratories). The slides were visualized on an Olympus DSU Spinning Disk confocal microscope in the Integrated Microscopy Core Facility at the University of Chicago.

CHAPTER A3

CARCINOMAS ARISING IN THE 4-NITROQUINOLINE 1-OXIDE MOUSE MODEL OF HEAD AND NECK SQUAMOUS CELL CARCINOMA ARE CHARACTERIZED BY BASAL CELL MARKERS AND LOSS OF AUTOPHAGY

Introduction

In exploring the complex role of autophagy in cancer, researchers have sought to distinguish the context-dependent effects of autophagy using mouse models with tissue-specific *Atg* deletion. Recent work has focused on differentiating the contributions of autophagy in early vs. late tumorigenesis in the presence of specific genetic alterations. The current consensus is that autophagy acts as a tumor suppressor during malignant transformation but promotes the growth and metastasis of established tumors. The generation of genetically engineered mouse models (GEMMs) to explore the role of autophagy in cancer has recently expanded to include lung cancer[135,136,141], pancreatic cancer[137], breast cancer[158], prostate cancer[157], and melanoma[156]. The majority of these models involve the use of strong oncogene drivers (*Kras*^{G12D}, *Braf*^{V600E}, and *MMTV*), which are known to modify numerous processes, most notably tumor metabolism, which may complication the interpretation of autophagy deficiency or lead to an over-interpretation of the metabolic-specific effects of autophagy deficiency.

We were interested in expanding the autophagy mouse models to include HNSCC. Autophagy has recently been implicated in HNSCC progression clinically[331–336] as well as in the response to therapy[125]. To characterize the role of autophagy in the natural progression of HNSCC, we decided to make use of the 4NQO model of carcinogen-induced HNSCC. 4NQO is

a water-soluble carcinogen that binds preferentially to guanine residues to promote the formation of DNA adducts and induce intracellular oxidative stress, mutations, and DNA strand breaks; these changes mimic the damage induced by tobacco and alcohol, the most prevalent risk factors for HNSCC[316,317]. Although numerous other carcinogens for HNSCC cancer models have been proposed, 4NQO exhibits the distinct advantage of not inducing an excessive inflammatory response[316]. The ability of 4NQO to dissolve in water means that the compound can be administered chronically in the drinking water of immune-competent mice, thereby closely replicating tobacco-induced oral carcinogenesis. The mice develop pre-malignant lesions as well as oral squamous cell carcinoma (SCC) of the tongue and oral cavity that resemble human HNSCC histologically as well as molecularly, including alterations in cytokeratin expression, the PI3K/ATK pathway, *p53* status, and cell cycle proteins[296,308,316–319]. The model is thus highly attractive as a physiologically relevant model that is ideal for use as a preclinical model in HNSCC to address the stagnation in HNSCC patient survival.

In this chapter, we validate the use of the 4NQO model as a mouse model of carcinogen-induced HNSCC. Six- to eight-week old C57BL/6 mice were treated with 100 µg/ml 4NQO in autoclaved water for 8 weeks and were sacrificed 4-24 weeks after the cessation of treatment. We explored the cell of origin of HNSCC in this model and began to characterize the autophagic flux over the natural course of lesion progression in this model.

The 4NQO mouse model recapitulates human HNSCC progression

The utility of the 4NQO mouse model lies in its reliable onset of lesions, the ability to observe lesion progression over a predictable timecourse, and the similarity of lesions to human pathology. As expected, control autophagy-competent mice in our study developed 4NQO-

induced lesions over the 24-week post-treatment timecourse (Figure A4.4). Lesions ranged in gross appearance from undetectable (i.e., diagnosed only upon histopathological examination) to large growths occupying the majority of the oral cavity. Lesions were diagnosed histopathologically by an experienced pathologist as follows: histologically normal, hyperkeratosis, epithelial dysplasia, and squamous cell carcinoma (SCC), listed in order of malignant progression. Frequently, a single mouse tongue exhibited multiple lesions (e.g., an SCC and two focal dysplasias in a field of hyperkeratosis); in such cases, the histological diagnosis was based on the most advanced lesion (i.e., SCC in the example above).

As anticipated, the majority of the 4NQO-treated mice exhibited some degree of histopathological progression, with a relative low incidence of histologically normal tongues observed. Normal mouse tongue histology was characterized by a very clearly defined epithelium with a single layer of basal cells (Figure A3.1A). Hyperkeratosis was defined by either a focal or global thickening of the keratinized layer with or without a thickened spinous layer (acanthosis); no nuclear or cellular atypia was associated with hyperkeratotic lesions (Figure. A3.1B). Hyperkeratotic lesions predominated early in the time course and began to decrease in incidence around 16 weeks post-4NQO treatment, with no cases of hyperkeratosis observed at 24 weeks (Figure A4.4). Dysplasias exhibited the inverse pattern, with some cases appearing early in the time course but generally increasing in incidence beginning at week 16 (Figure A4.4). The dysplastic lesions ranged in size from small focal lesions to lesions sufficiently large to affect the mouse's ability to eat and drink. These lesions reflected a wide range of appearances and severities but were grouped together due to the subjective nature of assigning severity descriptors; all of the dysplastic lesions were characterized generally by a loss of epithelial organization but failure to invade the underlying tissue. The histopathological

alterations of the dysplasias included cellular and nuclear enlargement, prominent nucleoli, increased nuclear to cytoplasmic ratio, nuclear hyperchromatosis, dyskeratosis, increased or abnormal mitotic figures, bulbous or teardrop-shaped rete ridges, and loss of polarity (Figure A3.1C). SCCs, which were identified in the majority of lesions at 24 weeks (Figure A4.4), were characterized by frank invasion into the underlying connective tissue stroma (Figure A3.1D). The identification of histological lesions of varying severity and over a timecourse comparable to those published in the literature[296,317,318,339] validate the application of the 4NQO-induced HNSCC model in our hands.

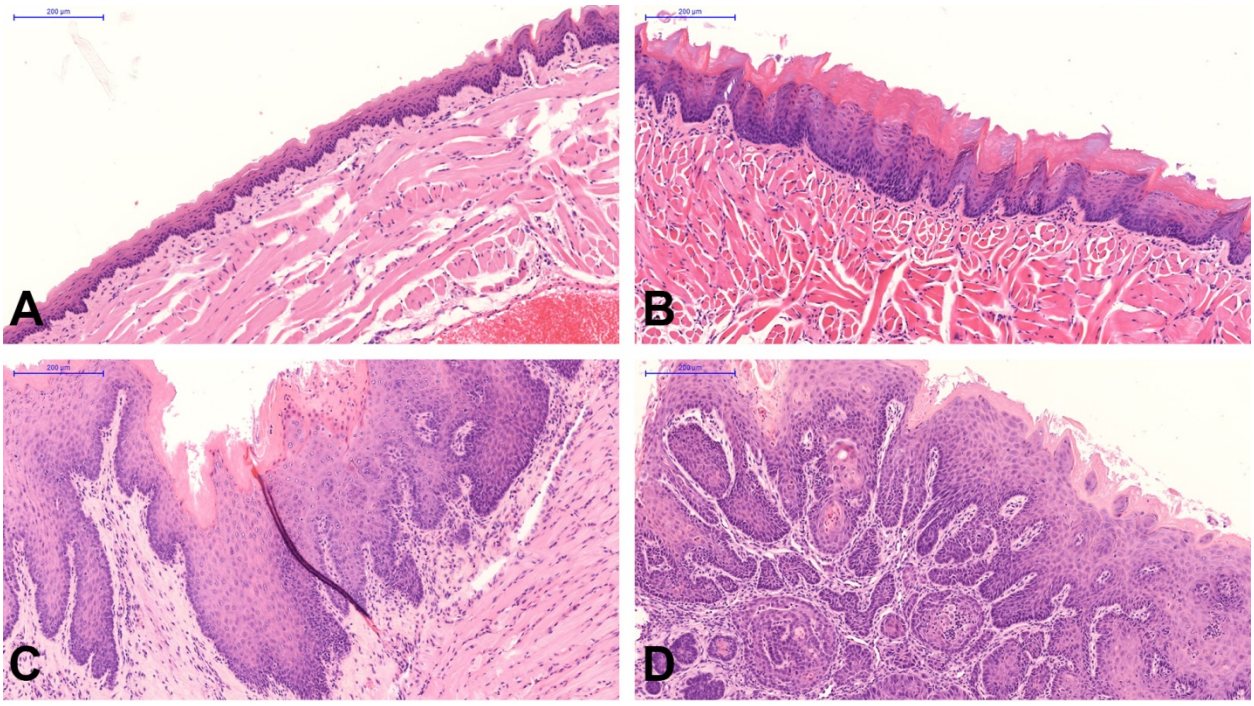

Figure A3.1 Histopathology of 4NQO-induced oral lesions in the mouse tongue. (A-D) Photomicrographs demonstrating the histopathologic progression in the carcinogen-induced model of HNSCC. (A) Histologically normal. (B) Hyperkeratosis. (C) Dysplasia. (D) Squamous cell carcinoma. Scale bar = 200 µm.

4NQO-induced lesions arise from basal epithelial cells and continue to exhibit basal cell markers

To confirm that the histopathological lesions arising in mice after 4NQO treatment arose from the proliferating stem/progenitor cell population in the basal layer of the keratinized tongue epithelium, we examined the expression patters of two basal/stem cell makers: keratin 14 (K14) and p63. K14 is a member of the type I keratin family of intermediate filaments and is expressed by basal cells of keratinized epithelium[340]; its expression is downregulated as cells differentiate[341]. K14 expression has been correlated with progression of carcinomas of the oral cavity and esophagus in both mice and humans[342–344]. P63 is a p53 homolog that is essential for epithelial cell regenerative proliferation and is specifically expressed by stem keratinocytes but not by their immediate progeny[345]; mutations in the gene encoding p63 have been observed in human HNSCC[312].

K14 expression was observed only in the basal epithelial layer of the 4NQO-treated tongues with normal histology, with loss of K14 staining as the cells moved upward and differentiated (Figure A3.2A). K14 staining was altered and expanded as lesions progressed through hyperkeratosis, dysplasia, and carcinoma (Figure A3.2B-D). In particular, K14 was expressed in the suprabasal layers of the tongue epithelium, and both the level and area of K14 staining increased with lesion progression. Most importantly, SCCs continued to exhibit strong K14 expression throughout the lesion (Figure A3.2D). P63 expression was confined to the nucleus, as expected, and decreased rapidly as differentiating cells progressed upwards from the basal cell layer (Figure A3.3A). With increasing lesion progression, a greater population of p63-positive cells was observed. P63 staining in hyperkeratotic lesions was largely confined to basal layer cells, with a few select suprabasal layer cells exhibiting p63 staining (Figure A3.3B). The

majority of cells in dysplastic lesions stained positive for p63, although the level of p63 expression varied from intense to pale (Figure A3.3C). A similar p63-staining pattern was observed in SCCs, with more invasive nests of cells staining most strongly for p63 (Figure A3.3D).

Because K14 and p63 are markers of basal epithelial cells, which are the proliferative subset of cells in the keratinized epithelium, we performed Ki67 IHC to examine the number of actively cycling cells (Figure A3.4)[346,347]. Broadly, Ki67 staining correlated with staining for K14 and p63. In normal epithelium, Ki67 expression was limited to the basal cell layer, with approximately half to two-thirds of the cells exhibiting positive nuclear Ki67 staining (Figure A3.4A). A mild increase in Ki67 staining was observed in hyperkeratotic lesions, with some suprabasilar staining (Figure A3.4B), whereas a large expansion in the number and a concurrent alteration in the organization of Ki67 cells were observed in dysplastic lesions, with many examples or nests of suprabasilar proliferating cells (Figure A3.4C). SCCs exhibited a high proportion of Ki67 cells, consistent with the identity of these lesions as highly proliferative (Figure A3.4D).

The persistence of K14 and p63 staining in 4NQO-induced lesions in conjunction with widespread Ki67 staining provides strong evidence that the lesions in these mice arise from the basal layer of proliferating stem cells. The high degree of proliferation and uniform basal cell expression of SCCs, in conjunction with the clear delineation of lesions among a field of normal or less-progressed cells may suggest that these lesions represent clonal populations of cells arising from a single stem cell within the basal layer. This feature of the 4NQO model makes it particularly attractive to genetic manipulation of these basal stem cells (see Chapter A4).

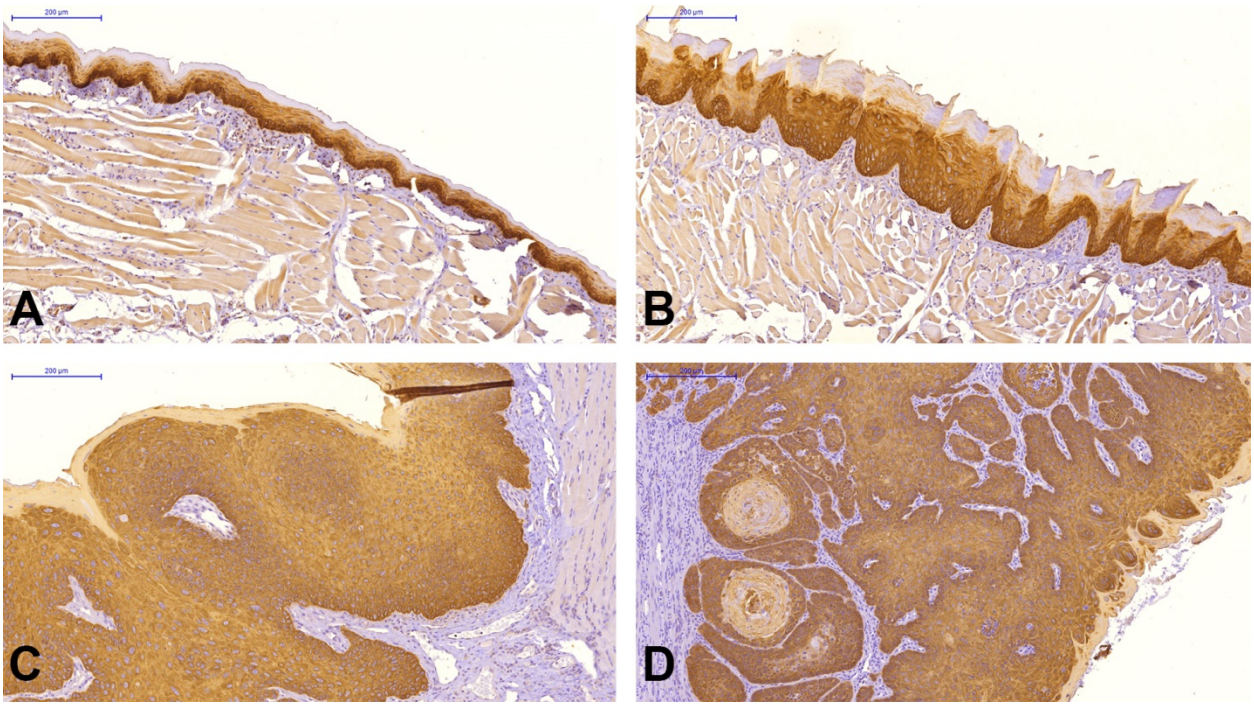

Figure A3.2 Immunohistochemical staining of K14 in the 4NQO mouse model of HNSCC. (A-D) Tissue sections from 4NQO-treated mice containing areas of normal (A), hyperkeratosis (B), dysplasia (C), and squamous cell carcinoma (D) were immunohistochemically stained for K14. Scale bar indicates 200 µM.

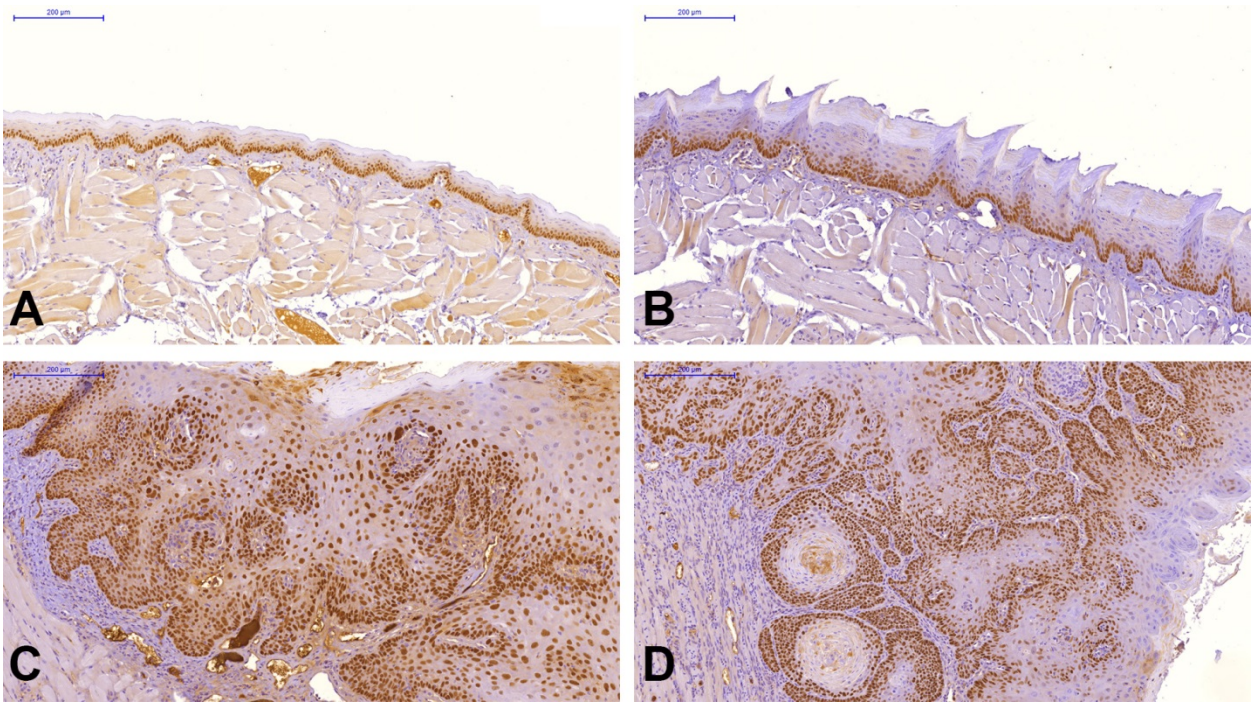

Figure A3.3 Immunohistochemical staining of p63 in the 4NQO mouse model of HNSCC. (A-D) Tissue sections from 4NQO-treated mice containing areas of normal (A), hyperkeratosis (B), dysplasia (C), and squamous cell carcinoma (D) were immunohistochemically stained for p63. Scale bar indicates 200 µM.

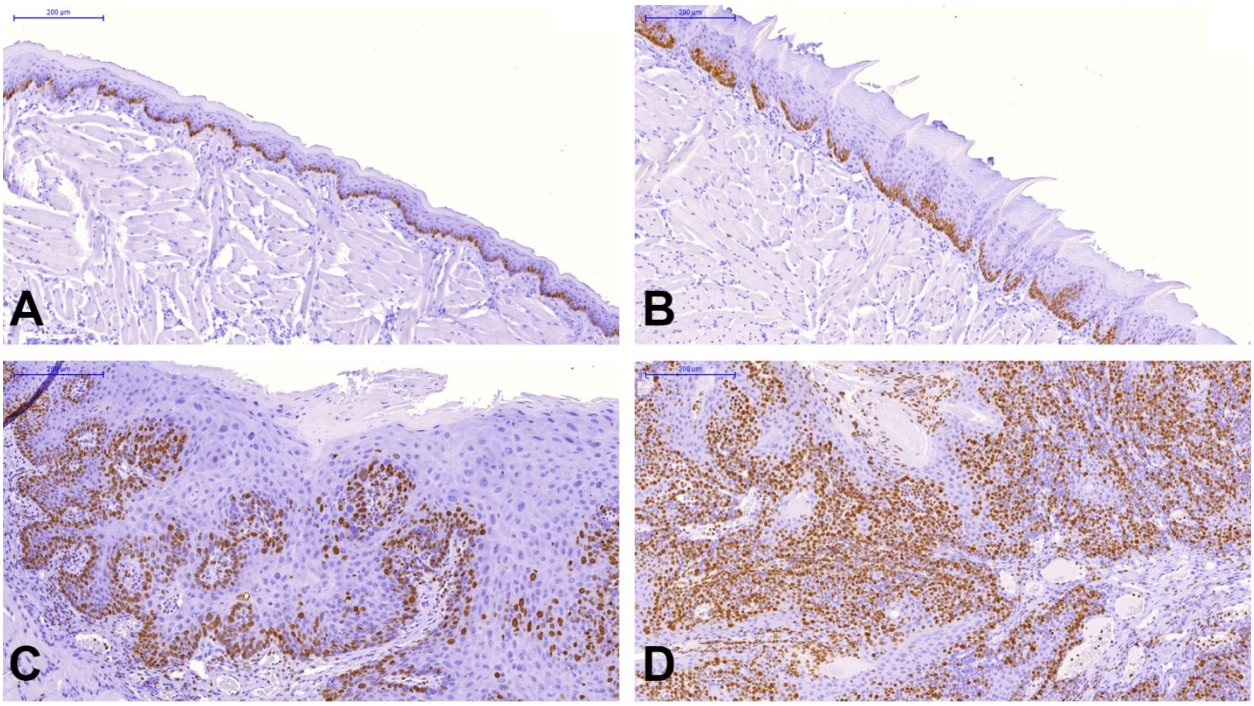

Figure A3.4 Immunohistochemical staining of Ki67 in the 4NQO mouse model of HNSCC. (A-D) Tissue sections from 4NQO-treated mice containing areas of normal (A), hyperkeratosis (B), dysplasia (C), and squamous cell carcinoma (D) were immunohistochemically stained for Ki67. Scale bar indicates 200 μM.

Advanced lesions in the 4NQO model exhibit down-regulation of autophagy

Autophagy is generally believed to be tumor-suppressive early in malignant progression but tumor-promoting during later stages (Figure 1.2). To date, there is no available autophagy mouse model in HNSCC despite reports linking autophagy to HNSCC progression. Furthermore, a subset of human HNSCC cases exhibit silencing of the key autophagy gene Atg7 and subsequent inhibition of autophagy[125]. Therefore, we were interested in assessing the role of autophagy in the evolution of 4NQO-induced oral lesions.

The ability to assess autophagic flux in tissues remains a significant challenge[348]. At present, the most commonly used surrogates include LC3B and p62. Ongoing autophagic flux is suggested by punctate LC3B and low p62 staining, whereas reduced or absent autophagic flux is suggested by diffuse LC3B and elevated p62 staining[348]. Both LC3B and p62 staining must be interpreted carefully; although punctate LC3B staining is highly suggestive of ongoing autophagy, lack of staining could indicate either absent autophagic flux or poor staining conditions. P62 staining, while more reproducible, does not exhibit a direct correlation with autophagic flux, and given its ability to interact with multiple partners and signal transducers, it is unlikely to be a readout of only autophagy[74]. Nonetheless, p62 and, in particular, LC3B staining remain the best tools to assess autophagy in tissue samples.

We used LC3B staining to look at the level of autophagic flux in 4NQO-treated mouse lesions. In normal epithelium, punctate LC3B staining was limited to the basal cell layer (Figure A3.5A). This finding is consistent with suggestions that autophagy may be required for the maintenance of normal stem cells[217,349,350]. Punctate LC3B staining was also observed in hyperkeratotic lesions; indeed, the overall level of LC3B staining appeared to be higher (Figure A3.5B). However, in SCCs and, to a lesser degree, in dysplasias, staining for LC3B was largely

absent, suggesting that 4NQO-induced carcinomas and dysplasias exhibit low or no autophagic flux (Figure A3.5D, C). It is important to note that the lack of LC3B staining observed in these samples was not due to poor staining procedures, as other less histologically advanced areas of the tongue did exhibit punctate LC3B staining. The lack of ongoing autophagy in SCCs and dysplasias in the model may suggest that autophagy is tumor-suppressive within 4NQO-induced dysplasias and carcinomas. Interestingly, we did observe some areas of highly enriched LC3B staining in a subset of normal or hyperkeratotic lesions (Figure 3.5E, F). It is possible that these areas represent cells in which autophagy has been induced to inhibit further progression to dysplasia or carcinomas. However, given the limitations of LC3B staining and the lack of more quantifiable markers, these observations remain speculative.

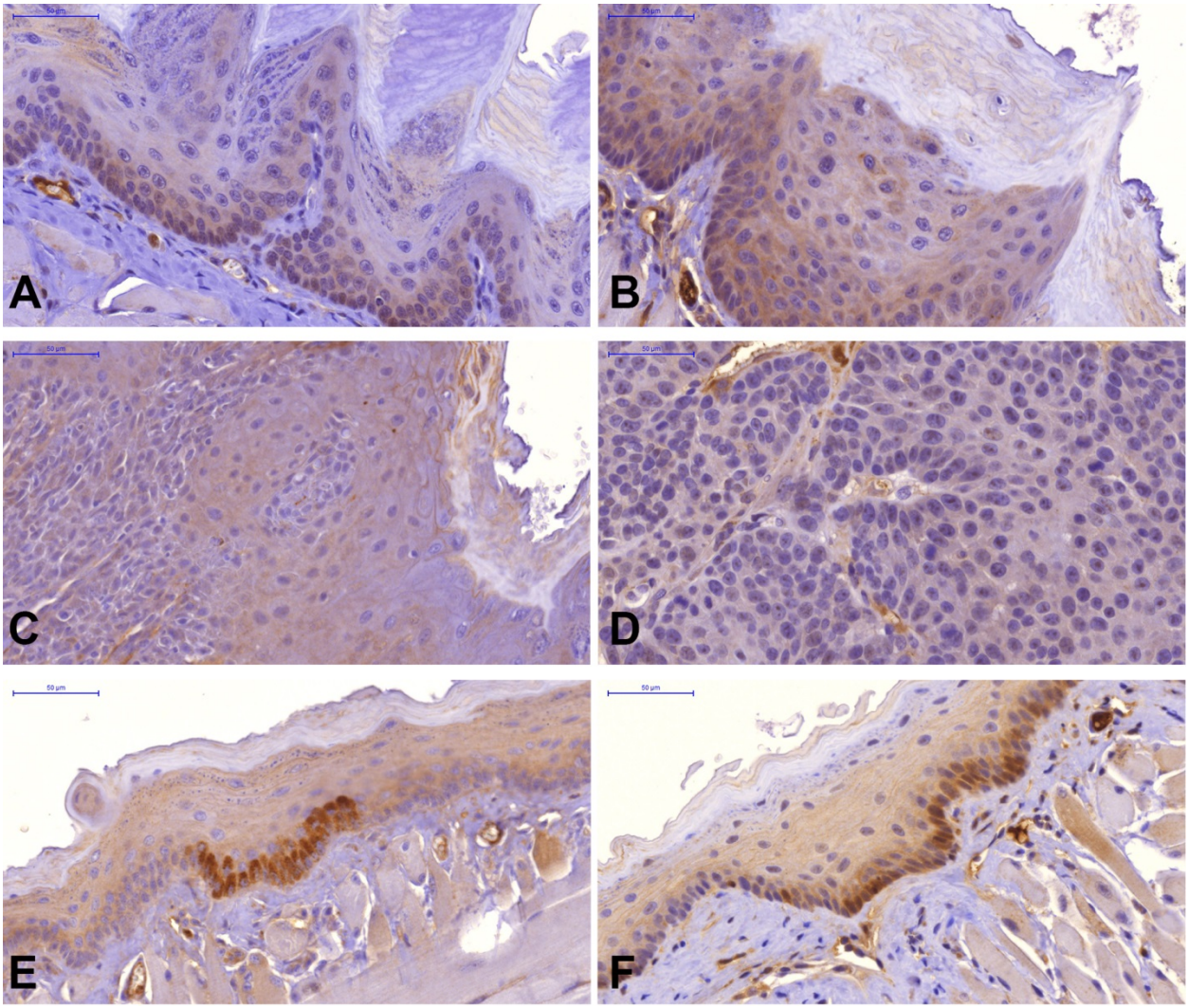

Figure A3.5 Immunohistochemical staining of LC3B in the 4NQO mouse model of HNSCC. (A-E) Tissue sections from 4NQO-treated mice containing areas of normal (A), hyperkeratosis (B), dysplasia (C), and squamous cell carcinoma (D) were immunohistochemically stained for LC3B. In some areas, regions of highly intense staining were observed (E, F). Scale bar indicates 50 µM.

Conclusions

In this chapter, we have validated the 4NQO model for carcinogen-induced HNSCC and characterized the resultant lesions with respect to basal cell markers and autophagic flux. As anticipated, 4NQO-treated mice developed progressive lesions ranging from hyperkeratosis to SCC, with earlier lesions predominating up until 16 weeks post-treatment and SCCs arising in the majority of mice by the 24-week timepoint. When we examined the expression of the K14 and p63 basal cell markers, we observed that the basal cell population increased in response to 4NQO treatment and led to the appearance of hyperkeratosis, dysplasias, and SCCs, with increased staining observed at each stage. This observation demonstrates that the lesions arising in these mice develop from basal epithelial cells and that they continue to exhibit markers of basal/stem cells. Furthermore, the findings suggest that an epithelial-specific basal stem cell gene, like K14, could be used to drive gene expression specifically in the tissue of origin of HNSCC in this model. Importantly, subpopulations of cancer stem-like cells (CSCs) expressing basal/stem cell markers have been reported in HNSCC[212,351–353] and may contribute to the therapeutic resistance of HNSCC[354]. CSCs have also been linked to EMT in HNSCC, which progresses largely through local invasion[212,355–358]. Our finding that 4NQO-induced lesions exhibit these basal/stem cell markers suggests that the model may be well suited to exploring this particular aspect of human pathophysiology.

In the normal epithelial, autophagy is confined to the basal cell layer, suggesting that autophagy may be important to tumorigenesis in these lesions. We assessed levels of autophagy using punctate LC3B as a marker of autophagic flux. Punctate LC3B staining was observed in normal and hyperkeratotic epithelium but was significantly suppressed in dysplasias and carcinomas. This may reflect the current consensus on the role of autophagy in cancer

progression; it is possible that autophagic flux in early lesions reflects a cellular attempt to combat cellular stress and thereby suppress malignant transformation, whereas the down-regulation of autophagy in advanced lesions reflects their successful suppression of autophagy in order to achieve malignancy. Although these options are correlative, they are consistent with some observations of transcriptional repression of Atg7, and thus autophagy down-regulation, in HNSCC patient samples[125]. One limitation of the 4NQO model is that lesions rarely metastasize; therefore, we were unable to examine levels of autophagic flux in lymph node metastases. However, our observations do provide correlative evidence of a role for autophagy in HNSCC progression.

CHAPTER A4

AUTOPHAGY IS REQUIRED FOR PROGRESSION IN THE 4-NITROQUINOLINE 1-OXIDE MODEL OF HEAD AND NECK SQUAMOUS CELL CARCINOMA

Introduction

Autophagy is a conserved catabolic process by which damaged organelles or proteins are engulfed by a double-membrane phagophore that elongates and closes around the cargo to form an autophagosome, which subsequently fuses with a lysosome to promote degradation of the intracellular content and release amino acids, fatty acids, sugars, and nucleotides for biosynthetic intermediates or to generate ATP. Phagophore elongation and closure requires to conjugation reactions that culminate in phosphatidylethanolamine (PE) conjugation to Atg8/LC3 to link Atg8/LC3 to the forming autophagosome. Two key proteins involved in these conjugation reactions include Atg7, which acts as an E1-like ubiquitin ligates, and Atg5, which functions within the Atg5-Atg12~Atg16L complex and acts in the final step of conjugation. The majority of the *in vivo* GEMMs of autophagy rely on targeted deletion of the genes encoding these proteins to cause autophagy deficiency.

Early *in vivo* studies of autophagy demonstrated that *Atg5*- and *Atg7*-null embryos die shortly after birth[283,284]. Thus, currently available GEMMs of autophagy rely on homozygous expression of a floxed *Atg* allele in combination with Cre recombinase, which may be controlled by a tissue-specific promoter[137,156–158] or delivered directly to the target tissues[135,136,141]. All of these models rely on additional genetic alterations to induce tumor formation, including oncogene activation or tumor suppressor deletion. We were interested in creating a carcinogen-

induced model of HNSCC to study the role of autophagy in tumor progression that more faithfully replicated human pathology than tissue-wide expression or deletion of cancer-associated genes. To drive *Atg5-flox* or *Atg7-flox* deletion specifically in keratinized epithelial tissues like those lining the mouse oral cavity, we made use of a *K14*-driven *Cre*. *K14*-driven expression was particularly attractive due to its known expression pattern[337,340,359] as well as its correlations with SCCs[342–344]. These mice were subjected to carcinogen-induced lesion formation following the 4NQO protocol described and validated in Chapter A3. Compared with previous models of autophagy in cancer, our model exhibits the following advantages: (1) As a carcinogen-induced model, it does not rely on the use of strong oncogene drivers or *p53* loss, allowing us to examine the effects of *Atg* deficiency in a more physiological context. (2) This will be the first *in vivo* model examining a role for autophagy in HNSCC. (3) These mice can be used as a preclinical model to test the effects of novel anti-autophagy therapies in HNSCC or to determine the differential effects of current therapies in the presence or absence of functional autophagy.

K14-Cre-mediated epithelial-specific deletion of key autophagy genes is mosaic in our model

We attempted to inhibit autophagy through the tissue-specific deletion of *Atg5-flox* or *Atg7-flox*, which encode two proteins of the same name that are required for autophagic processing of LC3 and subsequent phagophore maturation (Figure 1.1). C57BL/6 mice homozygous for *Atg5-flox* or *Atg7-flox* were crossed with C57BL/6 mice expressing *K14*-driven Cre recombinase (*K14-Cre*) to generate mice homozygous for the *Atg5* or *Atg7* floxed allele and heterozygous for *K14-Cre*. In these mice, Cre recombinase should be expressed in K14-positive

cells, including the basal epithelial layer of the tongue, and was anticipated to be sufficient to drive site-specific recombination and deletion of the floxed alleles, thus resulting in the generation of mice deficient for autophagy in the epithelium of the oral cavity.

PCR of tail DNA isolated from *Atg7-flox;K14-Cre+* mice confirmed that the wildtype *Atg7* band was not detected in mice homozygous for *Atg7-flox*. Furthermore, the reactions confirmed successful amplification of the deletion-specific *Atg7-flox* band specifically in *Cre+* but not *Cre-* mice (Figure A4.1A). Interestingly, the floxed-in band was also detected in samples from *Cre+* mice. Similar results were also observed in PCR reactions on *Atg5-flox;Cre* mice (Figure A4.1B). The wildtype *Atg5* band was observed only in *Atg5-flox* heterozygous mice, and the deletion-specific *Atg5-flox* band was observed only in *Cre+* mice. However, as in *Atg7-flox;Cre+* mice, the floxed-in band was observed both in *Cre-* and *Cre+* mice, albeit at a lower relative intensity in the *Cre+* samples. The presence of this floxed-in band in all *Cre+* mice may be indicative of either failure of Cre recombinase activity of the floxed locus in K14-positive epithelial cells; alternatively this band may reflect amplification of contaminating non-K14-positive stromal cells harboring the floxed-in locus.

To assess whether the detection of the floxed-in band in PCR analysis represented true Cre recombinase failure or merely the presence of contaminating DNA, we sought to perform IHC analysis on *Cre+* mice. This analysis was significantly hampered by the lack of robust commercially available autophagy antibodies for IHC on mouse tissues, a well-known fact within the field of autophagy research (personal communication). Although to date we have been able to find no appropriate Atg5 mouse IHC antibody, we were able to stain for Atg7. Samples from *Atg7-flox* mice lacking *Cre* exhibited Atg7 staining throughout the keratinized epithelium, consistent with our previous observations of positive LC3B staining in this tissue (Figure

A3.5A). In *Atg7-flox;Cre+* mice, we observed fields of epithelial cells that were negative for Atg7 staining, consistent with successful Cre-specific deletion of *Atg7-flox*. However, these cells represented a subset of cells in the epithelial layer; staining for Atg7 was mosaic throughout the tongue epithelium (Figure A4.2). The clear delineation of clusters of Atg7-positive and Atg7-negative cells supports the model that stem cells within the basal epithelial cell give rise to clonal cell populations and suggests that lesions arising in 4NQO-treated mice are clonal derivatives of transformed basal epithelial cells. However, the fact that deletion of *Atg7-flox* is mosaic complicates the use of these mice to model autophagy-deficiency, as only a subset of the epithelial cells are incapable of undergoing autophagy. Although we have been unable to stain for Atg5 in *Atg5-flox;Cre+* samples, we suspect that deletion of the *Atg5-flox* allele is similarly inefficient due to our PCR analysis and personal communications with other users of these mice.

Inefficient Cre-mediated deletion of autophagy-related genes has been reported by other researchers[133,137,162]. This inefficient deletion could be the result of lack of Cre expression, lack of Cre activity, inherent properties of the *Atg5* and/or *Atg7* loci, or strong selective pressure against autophagy inhibition. Mice mosaic for Atg7 continued to exhibit strong and uniform K14 expression, suggesting that K14-driven Cre expression should be intact. To determine whether Cre recombinase activity was affected, we crossed *K14-Cre* mice to mice harboring *Rosa26-LSL-tdTomato*. In *Rosa26-LSL-TdTomato* mice, successful expression of active Cre results in the deletion of a stop codon in the *Rosa26-LSL-tdTomato* locus, resulting in the expression of the red fluorescing tdTomato protein. We observed uniform red fluorescence in samples from *K14-Cre;Rosa26-LSL-tdTomato* mice specifically in the keratinized epithelial layer (Figure A4.3). Lesions of varying degrees of severity arising in 4NQO-treated *K14-Cre;Rosa26-LSL-tdTomato* mice all exhibited positive red fluorescence, with no observations of any fluorescence-negative

nests of cells. Thus, failure to delete *Atg7-flox* and, presumably, *Atg5-flox* is not due to a lack of Cre recombinase activity. The reason for the mosaicism is likely either inherent to the floxed allele or reflective of selective pressures.

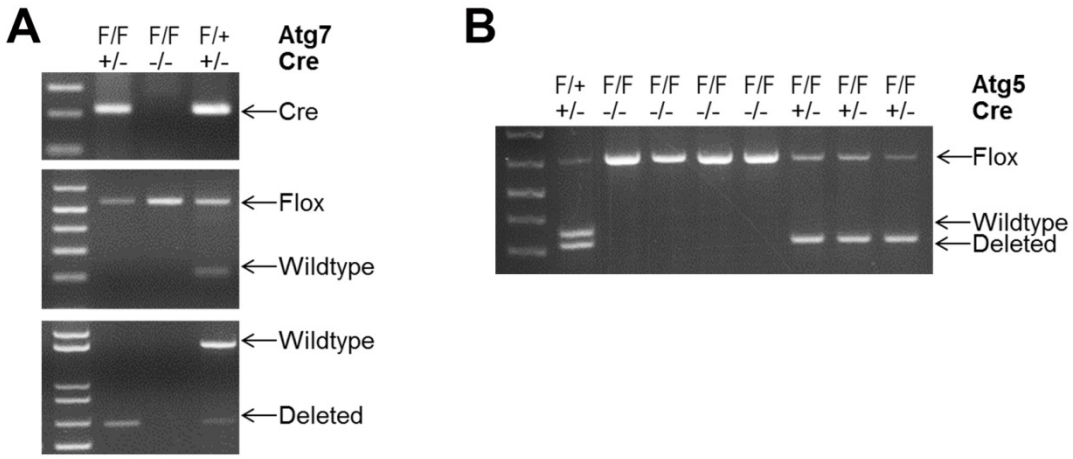

Figure A4.1 Cre-mediated deletion of *Ag5-flox* and *Atg7-flox* is mosaic at the genetic level. (A, B) Tail DNA samples from mice of the indicated genotypes were collected and subject to PCR for *Atg7* (A) or *Atg5* (B) using the primers indicated in Table A2.1. F indicates the floxed allele.

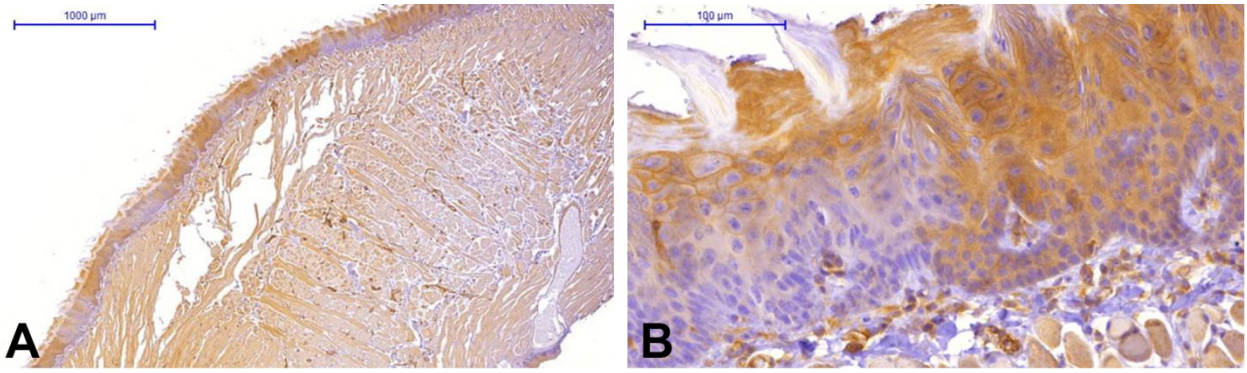

Figure A4.2. Cre-mediated deletion of *Atg7-flox* is mosaic at the protein level. (A) Immunohistochemical staining of a tongue tissue section from an *Atg7-flox;Cre+* mouse for Atg7; negative areas of staining in the epithelium indicated successful Cre-mediated deletion of *Atg7-flox*. (B) Close-up of the image in (A).

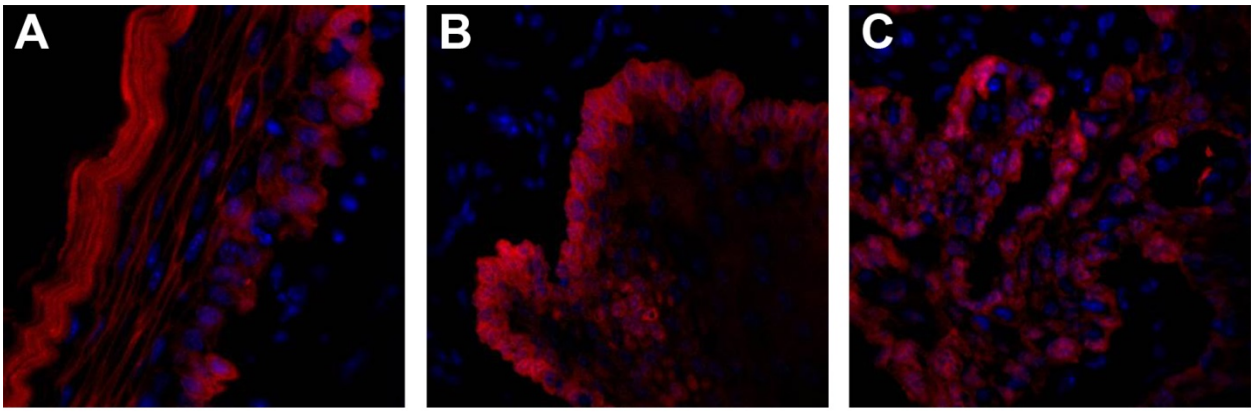

Figure A4.3 Cre recombinase is activity in K14-expressing cells and their progeny in 4NQO-treated mice. Imaging of tdTomato fluorescence on frozen sections from 4NQO-treated *Rosa26-LSL-tdTomato;Cre+* mice. tdTomato is actively expressed downstream of Cre in normal epithelium (A), dysplasias (B), and squamous cell carcinomas (C), indicating that Cre activity is not affected in any of these lesions.

Autophagy may be required for progression in HNSCC

Autophagy-competent control mice and mosaic autophagy-deficient *Atg5-flox;K14-Cre* and *Atg7-flox;K14-Cre* mice were treated with 4NQO in their drinking water for eight weeks, and tongues harvested from mice sacrificed 4-24 weeks post-treatment were histologically diagnosed, as described in Chapter A2. For the majority of the time course, the lesion incidence in mosaic autophagy-deficient mice did not differ from the lesion incidence in control autophagy-competent mice; less progressed lesions predominated at earlier time points, and carcinomas and dysplasias began to represent the majority of the lesions by 16 weeks post-treatment (Figure A4.4). However, although all control mice exhibited dysplasias or carcinomas at 24 weeks post-treatment, a subset of mosaic autophagy-deficient mice exhibited only hyperkeratosis or histologically normal oral epithelium (Figure A4.4). This difference was statistically significant ($p<0.05$), potentially suggesting that autophagy was required for progression from normal and hyperkeratotic lesions to dysplasia and carcinoma in this 4NQO mouse model.

Given that the *Atg5-flox;K14-Cre* and *Atg7-flox;K14-Cre* mice are only mosaically autophagy-deficient in the oral epithelium, we wondered whether the dysplasias and SCCs arising in these mice were truly deficient in autophagy or whether they arose from cells in which Cre had failed to delete the floxed allele (i.e., autophagy-competent "control" cells). We attempted PCR on lesions isolated from fixed slides using laser-capture microdissection (LCM), but we were unsuccessful in amplification of any *Atg5* or*Atg7* allele (data not shown). Although we were unable to stain for Atg5 in *Atg5-flox;K14-Cre* mice, as discussed previously, we were able to stain a subset of the 24-week carcinomas arising in *Atg7-flox;K14-Cre* mice (Figure A4.5A, C). All of the 24-week SCCs in *Atg7-flox;K14-Cre* mice positively expressed Atg7,

demonstrating the failure of Cre-mediated deletion in these cells. The observance of Atg7-negative epithelium in other areas on these SCC-harboring tongues suggests a selective pressure for tumor progression in only the autophagy-competent Atg7-positive subset of cells. Interestingly, although these tumors were positive for Atg7 and thus able to undergo autophagy, the tumors exhibited high levels of p62 staining (Figure A4.5B, D), suggesting that they were not undergoing autophagic flux. Although this observation is consistent with the lack of autophagic flux observed in tumors from control autophagy-competent mice (Figure A3.5), it is particularly perplexing given the apparent necessity for autophagy for progression from hyperkeratosis to dysplasia in this model (as discussed above; Figure A4.4). Nonetheless, it appears that although autophagy prevents the progression from normal and hyperkeratotic lesions to dysplasias and SCCs, autophagic flux is down-regulated once a lesion achieves malignancy.

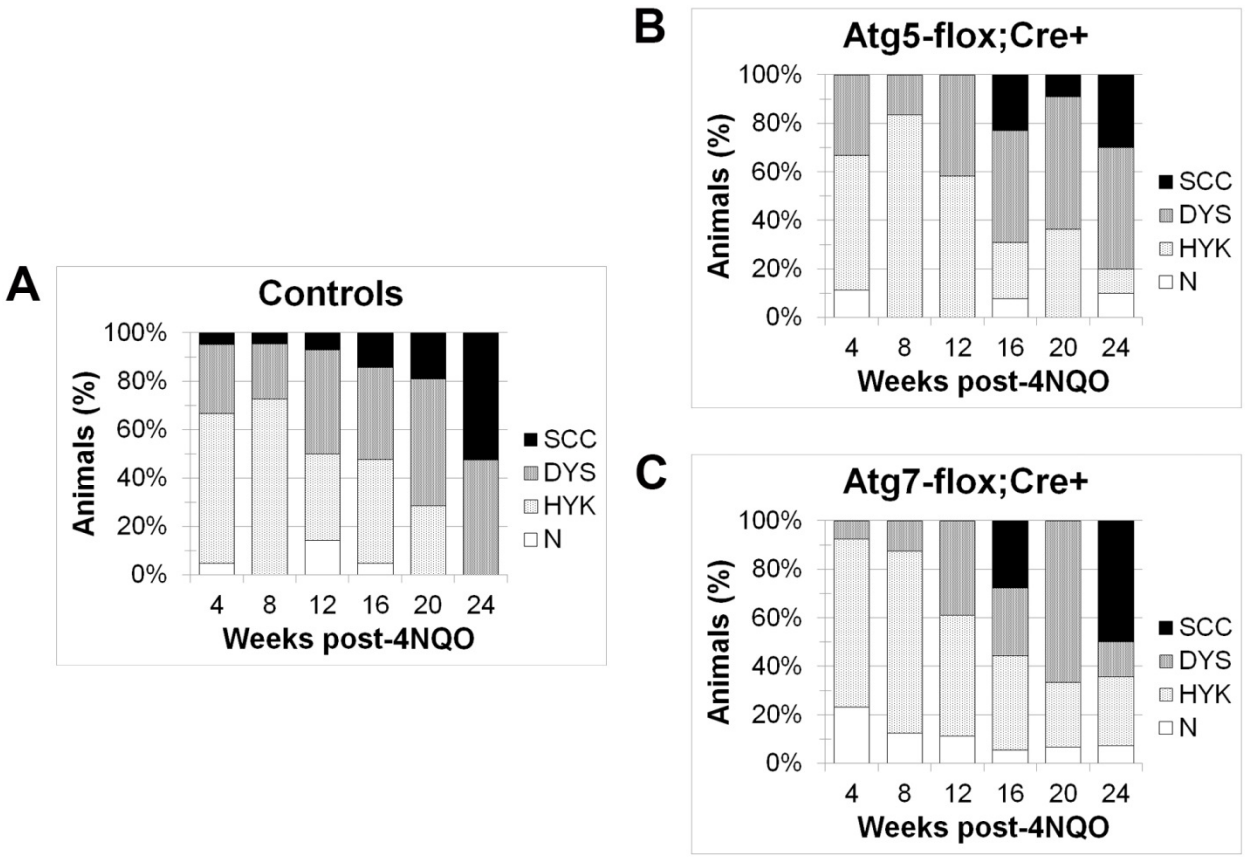

Figure A4.4 Incidence of each histologic diagnosis of 4NQO-treated mice. (A-C) Control autophagy-competent (A) and mosaic autophagy-deficient *Atg5-flox;Cre+* (B) and *Atg7-flox;Cre+* (C) mice were treated for 8 weeks with 100 µg/ml 4NQO before resuming normal water. The incidence of each lesion type at the indicated timepoints post-4NQO treatment is presented. The mosaic autophagy-deficient mice exhibited a statistically significant reduction in the number of dysplasias and carcinomas at the 24-week timepoint ($p<0.01$)

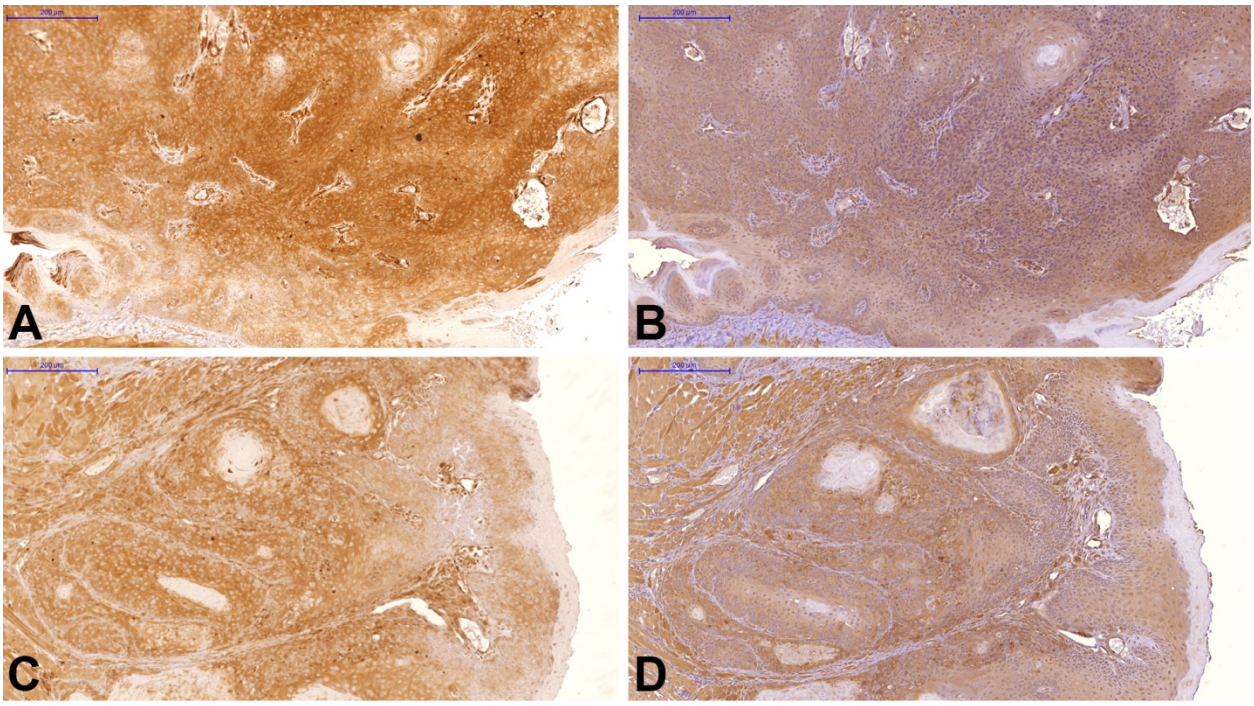

Figure A4.5 Carcinomas arising in *Atg7-flox;Cre+* mice express Atg7 but do not exhibit autophagic flux. (A, B) Immunohistochemical staining for Atg7 in SCCs from two *Atg7-flox;Cre+* mice demonstrating positive Atg7 staining. (C, D) Immunohistochemical staining for p62 in serial sections of the tissues in (A, B, respectively) demonstrating elevated p62 and thus low autophagic flux.

Conclusions

In this chapter, we combined the 4NQO model of HNSCC with *K14-Cre*-mediated deletion of key autophagy genes to study the role of autophagy in carcinogen-induced HNSCC. Based on our observations that the 4NQO-induced SCCs exhibit little/no autophagic flux (Chapter A3), we anticipated that loss of autophagy in the basal epithelium would accelerate tumor formation. Instead, we observed that nearly 30% of the autophagy-deficient mice exhibited histologically normal tongues or hyperkeratosis at 24 weeks, whereas 100% of the control autophagy-competent mice exhibited dysplasias or SCCs. This may suggest that autophagy is required for malignant progression in this model, in contrast to the majority of the autophagy GEMMs, in which autophagy deficiency tends to accelerate the onset of benign or low-grade lesions.

When we sought to validate autophagy deficiency in the *Cre+* mice using IHC for Atg7, we observed that deletion of *Atg7* (and presumably *Atg5*, based on PCR evidence) was mosaic. The inability of Cre to uniformly delete autophagy-related genes has been reported by other researchers[133,137,162], and many of the other published studies using Cre-mediated deletion of *Atg5* or *Atg7* do not publish IHC images confirming deletion. The inefficient deletion of these key autophagy genes is not due to lack of *K14* expression in 4NQO-induced lesions or lack of Cre activity, as *K14-Cre;Rosa26-LSL-tdTomato* mice exhibited tdTomato expression throughout the oral epithelial. Thus, failure to effectively delete *Atg* genes may reflect inherent properties of the alleles or strong selective pressure against autophagy. This later explanation seems more likely, particularly given reports that autophagy is important in the maintenance of stem cells like *K14*-expressing basal cells[217].

Regardless of the cause, the mosaicism of deletion makes the interpretation of our model significantly more challenging. Conclusively determining whether autophagy inhibition prevents progression to dysplasias or SCCs in this model requires being able to definitively establish the Atg7 or Atg5 status in these lesions. The best method currently available to us is Atg7 IHC, but the antibody is not sufficiently robust for broad-scale screening. Nonetheless, we have been able to determine that the SCCs arising in mosaic autophagy-deficient mice all continued to express Atg7, suggesting that these lesions arose from autophagy-competent lesions. These data imply that if we were able to generate mice that were uniformly deficient in Atg7 or Atg5 in *K14*-expressing tissues, none of the mice would progress beyond hyperplastic lesions. Therefore, our preliminary analysis indicates that in our 4NQO model of HNSCC, autophagy is required for progression to dysplasia (Chapter A4), although autophagic flux is subsequently repressed in cells that successfully undergo malignant transformation (Chapter A3).

CHAPTER A5

DISCUSSION

Summary and significance

In this appendix, we have explored the role of autophagy in tumor progression using the 4NQO mouse model of carcinogen-induced HNSCC combined with *K14*-driven Cre deletion of *Atg5-flox* or *Atg7-flox*. This new model represents the first autophagy GEMM that relies not on genetic alteration of oncogenes or tumor suppressors but on carcinogen exposure, thereby more closely representing true tumor initiation, which is rarely caused by uniform expression of an oncogene or deletion of a tumor suppressor in all cells within a tissue. Additionally, this is the first autophagy mouse model of HNSCC, a tumor type in which the role of autophagy is increasingly recognized (Chapter A1).

Our work demonstrates that lesions arising in 4NQO-treated mice derive from the basal cell layer and continue to express basal cell markers. Furthermore, autophagy is initially expressed in the basal epithelial cells and early lesions but is ultimately suppressed by the time SCCs develop. Whether autophagy becomes reactivated at a later time in SCCs remains to be determined. When autophagy was mosaically deleted in the basal epithelial cells, we observed a significant reduction in the number of mice developing dysplasias or SCCs, but only at the latest time point (24 weeks). It is possible that another method of quantifying lesion incidence (e.g., average number of lesions per mouse tongue) might better have revealed differences among the control and mosaically autophagy-deficient mice. Strikingly, all of the SCCs arising in mice mosaically deleted for *Atg7* continued to express Atg7, suggesting that autophagy was required

for transition from either hyperkeratotic lesions to dysplasia or from dysplasia to SCC. Thus, our initial interpretation of our findings is that in this model, autophagy promotes progression to dysplasia/carcinoma (thus causing a reduction in the number of mosaic autophagy-deficient mice developing these advanced lesions) but that autophagy becomes somehow maladaptive once malignant transformation occurs (thus leading to down-regulation of autophagic flux in advanced lesions). It should be noted that this model is contrary to the canonical model of autophagy in tumor progression, wherein autophagy is initially tumor suppressive but subsequently becomes tumor-promoting.

Remaining questions

As discussed in the previous section, our initial interpretation of the 4NQO-induced HNSCC autophagy model seems to contradict the canonical tumor view. However, there are many unanswered questions with respect to our model. The greatest challenge in the interpretation of our model lies with its mosaicism. Because deletion is mosaic, it is somewhat misleading to simply compare *Cre-* with *Cre+* mice. It may be more accurate to compare individual lesions with one another. However, our attempts to definitively conclude which lesions represent true deletions and which represent deletion failure has ultimately been unsuccessful despite testing all available commercial Atg5 and Atg7 antibodies, assessing Cre function, and attempting PCR on LCM tissue. The fact that in control mice, SCCs stain negative for LC3B also demonstrates that measuring autophagic flux in the mosaic deleted mice will not be useful in determining which lesions *can* (but perhaps do not) undergo autophagy. Until better IHC antibodies for mouse tissue are developed for AtgG5 and Atg7, it is likely that a complete analysis of our mice will be impossible.

However, if it were possible to determine which cells in *Cre+* mice successfully deleted *Atg5* or *Atg7*, the mosaicism of this model mice prove to be an intriguing benefit. As discussed earlier (Chapter A4), the mosaicism of *Atg* deletion is likely to reflect selective pressures. It would be interesting to determine whether the percent of autophagy-deficient basal epithelial cells changed over time under basal conditions or upon 4NQO treatment. Indeed, we have observed that mice sacrificed at later time points do seem to exhibit fewer Atg7-negative regions than do mice sacrificed at earlier time points, potentially suggesting that autophagy is required for the cells to survive the genotoxic stress of 4NQO administration and that autophagy-deficient basal epithelial cells eventually die out. Furthermore, the fact that the entire tongue with both autophagy-competent and autophagy-deficient cells is subjected to the same conditions (e.g., carcinogen exposure) allows for a built-in control group to study the effects of autophagy deficiency on tumor progression.

Our initial model, as discussed above, contradicts the traditional model of autophagy in tumor progression. It is true that our ability to interpret our findings in light of the mosaicism and technical challenges makes our initial conclusions somewhat premature; perhaps new analysis with better tools with reveal a pattern more consistent with previously published work. However, it is also important to note that our model differs from other autophagy-related GEMMs of cancer in one critical way – our model is the only carcinogen-induced model, whereas the other models rely on *Kras* activation or tumor suppressor deletion. Thus, our findings may highlight the fact that the tumor-specific effects of autophagy depend strongly on the context, including the tumor-inducing event. Indeed, Rosenfeldt *et al* have demonstrated that *p53* status is sufficient to determine the pro- versus anti-tumorigenic effect of autophagy in *Kras*-driven pancreatic cancer[137]. The development of more carcinogen-induced cancer autophagy models would be

interesting to clarify this point. Alternatively, the combination of the 4NQO model with autophagy deficiency at a different level (e.g., FIP200) could reveal whether the mosaicism observed here is common to any genetic autophagy inhibition as well as whether inhibiting autophagy at different levels in the autophagy pathway (phagophore initiation vs. elongation vs. closure) has the same tumor effects. This last point is particularly important in light of the fact that different pharmacologic autophagy therapies target the pathway at different points (Chapter 6).

Should we be able to unambiguously determine which lesions in our mouse model are successfully deleted for autophagy genes, this model is ideally suited as a preclinical therapeutic model. One could envision treating the 4NQO-exposed mice concurrent with the carcinogen exposure, after exposure but before the development of carcinomas, or after the successful establishment of primary tumors with autophagy inhibitors or inducers combined with other common HNSCC chemotherapies (e.g., mTOR inhibitors, EGFR-blocking antibodies) to determine the clinical utility of prophylactically or retroactively treating smokers or chronic alcohol abusers with autophagy combination therapy. Additionally, we could make use of the autophagy-mosaic mice following a similar protocol to determine whether autophagy inhibition/induction therapies might have unanticipated effects on cells with lower levels of autophagic flux.

Our initial findings using an autophagy-mosaic carcinogen-induced mouse model of HNSCC are intriguing but leave many unanswered questions. Given the number of groups working with *Atg5-flox* and *Atg7-flox* mouse models, the development of robust, reliable antibodies is of critical importance. Once the tools are in place to better interpret our model, its initial disadvantages may prove to be a boon, as mosaic autophagy deficiency may better model

tissue-wide autophagic flux and allows for direct comparison of autophagy-deficient and autophagy-proficient cells exposed to the same conditions.

What is the future of autophagy mouse models?

The mosaic autophagy deficiency and unreliable tools to measure autophagy *in vivo* remain research topics that are much-discussed among autophagy investigators but that are infrequently addressed in the published literature. Indeed, although some groups have commented on the mosaic nature of *Atg* gene deletion in their mouse models[133,137,162], other groups have made no mention of this finding. Of course, it is possible that deletion of *Atg* genes is only mosaic in certain tissues due to different selective pressures for autophagy or, less likely, different activity levels of tissue-specific Cre. However, until the field as a whole comes together to address this issue in a unified manner, it becomes difficult to know whether the effects observed in these models are cell-autonomous (i.e., autophagy deficiency within a cell alters its tumorigenic potential), cell non-autonomous (i.e., autophagy deficiency within a cell alters the tumorigenic potential of its neighbors), or both or whether they happen to reflect differences in the degree of deletion between different mice or in different tissues.

A further issue with the currently available autophagy mouse models is the overreliance on *Atg5* and *Atg7* deletion. Of the available models (including the one presented in this appendix)[135–137,141,156–158], all but one[158] relies on *Atg5* or *Atg7* deletion. Setting aside questions concerning the utility of approaching the question of autophagy deficiency in cancer by creating models that differ almost exclusively in tissue origin, this emphasis on *Atg5/Atg7* deletion is short-sighted for several reasons. First, as was discussed in Chapter 6, most of the clinically available therapies do not affect autophagy at the level of Atg5 or Atg7 but instead act far

upstream or downstream. Thus, cancer models relying on *Atg5* or *Atg7* deletion may poorly model the affects our potential therapeutic interventions may have on the natural progression of cancers. Second, and perhaps more importantly for basic science researchers, it is well-established that *Atg* genes frequently have non-autophagy functions[164]. Therefore, by limiting our models to only Atg5 and Atg7 deficiency, we may be generalizing *Atg5*- or *Atg7*-specific effects to autophagy as a whole or missing non-autophagy effects that may be observed clinically when other autophagy proteins are targeted. Once recent example of this problem was reported by Chen *et al*. By creating a knock-in mouse model expressing a FIP200 mutant that was unable to interact with its autophagy partner, Atg13, the authors were able to separate the autophagic functions of FIP200 from its non-autophagic functions and link these functions to different biological processes *in vivo*[165].

Thus, future autophagy mouse models must carefully determine whether the deletion of *Atg* genes is mosaic and should include the use of new *Atg* gene deletions or *Atg* gene mutants that separate autophagic and non-autophagic functions. Researchers may also want to consider the generation of inducible deletion models in the future. Give the amount of focus on the temporal dependence of the role of autophagy in tumor progression, it is somewhat surprising that there is no available model to inhibit autophagy at different stages of tumorigenesis to observe the regression or promotion of tumor growth. This type of inducible model would represent a large step forward from our current models that require researchers to interpret the pro- versus anti-tumor effects at different stages based on the incidence of benign and malignant lesions over time.

Future autophagy mouse models will need to break away from the current habit of "reinventing the wheel" to create models that can offer us new insights. There are clearly many

questions left unanswered with respect to the initial oncogenic event, the level at which autophagy is inhibited, the extent of *Atg* gene deletion across a tissue, the time-dependent outcomes of autophagy inhibition, and the non-canonical effects of autophagy deficiency. Perhaps most importantly, however, the field will need to establish reliable tools to measure the expression and patterns of autophagy proteins like Atg7 and to measure autophagic flux in a more unbiased way. Only then will we truly be able to interpret the results of cancer models of autophagy like the one described in this appendix.

REFERENCES

1. Kornfeld, S. & Mellman, I. The Biogenesis of Lysosomes. *Annu. Rev. Cell Biol.* **5,** 483–525 (1989).

2. Saftig, P. & Klumperman, J. Lysosome biogenesis and lysosomal membrane proteins: trafficking meets function. *Nat. Rev. Mol. Cell Biol.* **10,** 623–635 (2009).

3. Mizushima, N., Yoshimori, T. & Ohsumi, Y. in *Annual Review of Cell and Developmental Biology, Vol 27* (eds. Schekman, R., Goldstein, L. & Lehmann, R.) **27,** 107–132 (Annual Reviews, 2011).

4. Yorimitsu, T. & Klionsky, D. J. Autophagy: molecular machinery for self-eating. *Cell Death Differ.* **12,** 1542–1552 (2005).

5. Mizushima, N. & Komatsu, M. Autophagy: Renovation of Cells and Tissues. *Cell* **147,** 728–741 (2011).

6. Mizushima, N., Levine, B., Cuervo, A. M. & Klionsky, D. J. Autophagy fights disease through cellular self-digestion. *Nature* **451,** 1069–1075 (2008).

7. Kroemer, G., Mariño, G. & Levine, B. Autophagy and the Integrated Stress Response. *Mol. Cell* **40,** 280–293 (2010).

8. He, C. & Klionsky, D. J. Regulation Mechanisms and Signaling Pathways of Autophagy. *Annu. Rev. Genet.* **43,** 67–93 (2009).

9. Settembre, C. *et al.* TFEB Links Autophagy to Lysosomal Biogenesis. *Science* **332,** 1429–1433 (2011).

10. Novikoff, A. B. The proximal tubule cell in experimental hydronephrosis. *J. Biophys. Biochem. Cytol.* **6,** 136–138 (1959).

11. Ashford, T. P. & Porter, K. R. Cytoplasmic Components in Hepatic Cell Lysosomes. *J. Cell Biol.* **12,** 198–202 (1962).

12. Clark, S. L. Cellular differentiation in the kidneys of newborn mice studies with the electron microscope. *J. Biophys. Biochem. Cytol.* **3,** 349–362 (1957).

13. Duve, C. de & Wattiaux, R. Functions of Lysosomes. *Annu. Rev. Physiol.* **28,** 435–492 (1966).

14. Klionsky, D. J. Autophagy: from phenomenology to molecular understanding in less than a decade. *Nat. Rev. Mol. Cell Biol.* **8,** 931–937 (2007).

15. Takeshige, K., Baba, M., Tsuboi, S., Noda, T. & Ohsumi, Y. Autophagy in yeast demonstrated with proteinase-deficient mutants and conditions for its induction. *J. Cell Biol.* **119,** 301–311 (1992).

16. Suzuki, K. *et al.* The pre-autophagosomal structure organized by concerted functions of APG genes is essential for autophagosome formation. *EMBO J.* **20,** 5971–5981 (2001).

17. Kim, J., Huang, W.-P., Stromhaug, P. E. & Klionsky, D. J. Convergence of multiple autophagy and cytoplasm to vacuole targeting components to a perivacuolar membrane compartment prior to de novo vesicle formation. *J. Biol. Chem.* **277,** 763–773 (2002).

18. Matsuura, A., Tsukada, M., Wada, Y. & Ohsumi, Y. Apg1p, a novel protein kinase required for the autophagic process in Saccharomyces cerevisiae. *Gene* **192,** 245–250 (1997).

19. Nakatogawa, H., Suzuki, K., Kamada, Y. & Ohsumi, Y. Dynamics and diversity in autophagy mechanisms: lessons from yeast. *Nat. Rev. Mol. Cell Biol.* **10,** 458–467 (2009).

20. Mizushima, N., Sugita, H., Yoshimori, T. & Ohsumi, Y. A new protein conjugation system in human. The counterpart of the yeast Apg12p conjugation system essential for autophagy. *J. Biol. Chem.* **273,** 33889–33892 (1998).

21. Wirth, M., Joachim, J. & Tooze, S. A. Autophagosome formation—The role of ULK1 and Beclin1–PI3KC3 complexes in setting the stage. *Semin. Cancer Biol.* **23,** 301–309 (2013).

22. Hosokawa, N. *et al.* Nutrient-dependent mTORC1 Association with the ULK1–Atg13–FIP200 Complex Required for Autophagy. *Mol. Biol. Cell* **20,** 1981–1991 (2009).

23. Ganley, I. G. *et al.* ULK1·ATG13·FIP200 Complex Mediates mTOR Signaling and Is Essential for Autophagy. *J. Biol. Chem.* **284,** 12297–12305 (2009).

24. Egan, D. F. *et al.* Phosphorylation of ULK1 (hATG1) by AMP-Activated Protein Kinase Connects Energy Sensing to Mitophagy. *Science* **331,** 456–461 (2011).

25. Kim, J., Kundu, M., Viollet, B. & Guan, K.-L. AMPK and mTOR regulate autophagy through direct phosphorylation of Ulk1. *Nat. Cell Biol.* **13,** 132–141 (2011).

26. Bach, M., Larance, M., James, D. E. & Ramm, G. The serine/threonine kinase ULK1 is a target of multiple phosphorylation events. *Biochem. J.* **440,** 283–291 (2011).

27. Shang, L. *et al.* Nutrient starvation elicits an acute autophagic response mediated by Ulk1 dephosphorylation and its subsequent dissociation from AMPK. *Proc. Natl. Acad. Sci.* **108,** 4788–4793 (2011).

28. Mack, H. I. D., Zheng, B., Asara, J. M. & Thomas, S. M. AMPK-dependent phosphorylation of ULK1 regulates ATG9 localization. *Autophagy* **8,** 1197–1214 (2012).

29. Tooze, S. A. & Yoshimori, T. The origin of the autophagosomal membrane. *Nat. Cell Biol.* **12,** 831–835 (2010).

30. Jung, C. H. *et al.* ULK-Atg13-FIP200 Complexes Mediate mTOR Signaling to the Autophagy Machinery. *Mol. Biol. Cell* **20,** 1992–2003 (2009).

31. Jung, C. H., Seo, M., Otto, N. M. & Kim, D.-H. ULK1 inhibits the kinase activity of mTORC1 and cell proliferation. *Autophagy* **7,** 1212–1221 (2011).

32. Dunlop, E. A., Hunt, D. K., Acosta-Jaquez, H. A., Fingar, D. C. & Tee, A. R. ULK1 inhibits mTORC1 signaling, promotes multisite Raptor phosphorylation and hinders substrate binding. *Autophagy* **7,** 737–747 (2011).

33. Löffler, A. S. *et al.* Ulk1-mediated phosphorylation of AMPK constitutes a negative regulatory feedback loop. *Autophagy* **7,** 696–706 (2011).

34. Chen, G.-C. *et al.* Genetic interactions between Drosophila melanogaster Atg1 and paxillin reveal a role for paxillin in autophagosome formation. *Autophagy* **4,** 37–45 (2008).

35. Itakura, E. & Mizushima, N. Characterization of autophagosome formation site by a hierarchical analysis of mammalian Atg proteins. *Autophagy* **6,** 764–776 (2010).

36. Di Bartolomeo, S. *et al.* The dynamic interaction of AMBRA1 with the dynein motor complex regulates mammalian autophagy. *J. Cell Biol.* **191,** 155–168 (2010).

37. McKnight, N. C. *et al.* Genome-wide siRNA screen reveals amino acid starvation-induced autophagy requires SCOC and WAC: SCOC, FEZ1 and WAC regulate autophagy. *EMBO J.* **31,** 1931–1946 (2012).

38. Funderburk, S. F., Wang, Q. J. & Yue, Z. The Beclin 1–VPS34 complex – at the crossroads of autophagy and beyond. *Trends Cell Biol.* **20,** 355–362 (2010).

39. Itakura, E., Kishi, C., Inoue, K. & Mizushima, N. Beclin 1 Forms Two Distinct Phosphatidylinositol 3-Kinase Complexes with Mammalian Atg14 and UVRAG. *Mol. Biol. Cell* **19,** 5360–5372 (2008).

40. Sun, Q. *et al.* Identification of Barkor as a mammalian autophagy-specific factor for Beclin 1 and class III phosphatidylinositol 3-kinase. *Proc. Natl. Acad. Sci.* **105,** 19211–19216 (2008).

41. Matsunaga, K. *et al.* Two Beclin 1-binding proteins, Atg14L and Rubicon, reciprocally regulate autophagy at different stages. *Nat. Cell Biol.* **11,** 385–396 (2009).

42. Zhong, Y. *et al.* Distinct regulation of autophagic activity by Atg14L and Rubicon associated with Beclin 1–phosphatidylinositol-3-kinase complex. *Nat. Cell Biol.* **11,** 468–476 (2009).

43. Fan, W., Nassiri, A. & Zhong, Q. Autophagosome targeting and membrane curvature sensing by Barkor/Atg14(L). *Proc. Natl. Acad. Sci.* **108,** 7769–7774 (2011).

44. Lipinski, M. M. *et al.* A Genome-Wide siRNA Screen Reveals Multiple mTORC1 Independent Signaling Pathways Regulating Autophagy under Normal Nutritional Conditions. *Dev. Cell* **18,** 1041–1052 (2010).

45. Pattingre, S. *et al.* Bcl-2 Antiapoptotic Proteins Inhibit Beclin 1-Dependent Autophagy. *Cell* **122,** 927–939 (2005).

46. Maiuri, M. C. *et al.* Functional and physical interaction between Bcl-XL and a BH3-like domain in Beclin-1. *EMBO J.* **26,** 2527–2539 (2007).

47. Luo, S. *et al.* Bim Inhibits Autophagy by Recruiting Beclin 1 to Microtubules. *Mol. Cell* **47,** 359–370 (2012).

48. Mizushima, N. *et al.* A protein conjugation system essential for autophagy. *Nature* **395,** 395–398 (1998).

49. Fujioka, Y., Noda, N. N., Nakatogawa, H., Ohsumi, Y. & Inagaki, F. Dimeric Coiled-coil Structure of Saccharomyces cerevisiae Atg16 and Its Functional Significance in Autophagy. *J. Biol. Chem.* **285,** 1508–1515 (2010).

50. Matsushita, M. *et al.* Structure of Atg5·Atg16, a Complex Essential for Autophagy. *J. Biol. Chem.* **282,** 6763–6772 (2007).

51. Mizushima, N. *et al.* Dissection of autophagosome formation using Apg5-deficient mouse embryonic stem cells. *J. Cell Biol.* **152,** 657–667 (2001).

52. Kabeya, Y. *et al.* LC3, a mammalian homologue of yeast Apg8p, is localized in autophagosome membranes after processing. *EMBO J.* **19,** 5720–5728 (2000).

53. Kirisako, T. *et al.* Formation Process of Autophagosome Is Traced with Apg8/Aut7p in Yeast. *J. Cell Biol.* **147,** 435–446 (1999).

54. Hanada, T. *et al.* The Atg12-Atg5 Conjugate Has a Novel E3-like Activity for Protein Lipidation in Autophagy. *J. Biol. Chem.* **282,** 37298–37302 (2007).

55. Fujita, N. *et al.* The Atg16L Complex Specifies the Site of LC3 Lipidation for Membrane Biogenesis in Autophagy. *Mol. Biol. Cell* **19,** 2092–2100 (2008).

56. Weidberg, H. *et al.* LC3 and GATE-16/GABARAP subfamilies are both essential yet act differently in autophagosome biogenesis. *EMBO J.* **29,** 1792–1802 (2010).

57. He, H. *et al.* Post-translational Modifications of Three Members of the Human MAP1LC3 Family and Detection of a Novel Type of Modification for MAP1LC3B. *J. Biol. Chem.* **278,** 29278–29287 (2003).

58. Bai, H., Inoue, J., Kawano, T. & Inazawa, J. A transcriptional variant of the LC3A gene is involved in autophagy and frequently inactivated in human cancers. *Oncogene* **31,** 4397–4408 (2012).

59. Kirisako, T. *et al.* The Reversible Modification Regulates the Membrane-Binding State of Apg8/Aut7 Essential for Autophagy and the Cytoplasm to Vacuole Targeting Pathway. *J. Cell Biol.* **151,** 263–275 (2000).

60. Fujita, N. *et al.* An Atg4B Mutant Hampers the Lipidation of LC3 Paralogues and Causes Defects in Autophagosome Closure. *Mol. Biol. Cell* **19,** 4651–4659 (2008).

61. Ichimura, Y. *et al.* A ubiquitin-like system mediates protein lipidation. *Nature* **408,** 488–492 (2000).

62. Tanida, I. *et al.* HsAtg4B/HsApg4B/Autophagin-1 Cleaves the Carboxyl Termini of Three Human Atg8 Homologues and Delipidates Microtubule-associated Protein Light Chain 3- and GABAA Receptor-associated Protein-Phospholipid Conjugates. *J. Biol. Chem.* **279,** 36268–36276 (2004).

63. Klionsky, D. J. *et al.* Guidelines for the use and interpretation of assays for monitoring autophagy. *Autophagy* **8,** 445–544 (2012).

64. Lamb, C. A., Dooley, H. C. & Tooze, S. A. Endocytosis and autophagy: Shared machinery for degradation. *Bioessays* **35,** 34–45 (2013).

65. Liang, C. *et al.* Beclin1-binding UVRAG targets the class C Vps complex to coordinate autophagosome maturation and endocytic trafficking. *Nat. Cell Biol.* **10,** 776–787 (2008).

66. Hyttinen, J. M. T., Niittykoski, M., Salminen, A. & Kaarniranta, K. Maturation of autophagosomes and endosomes: A key role for Rab7. *Biochim. Biophys. Acta BBA - Mol. Cell Res.* **1833,** 503–510 (2013).

67. Peng, J. *et al.* Atg5 regulates late endosome and lysosome biogenesis. *Sci. China Life Sci.* **57,** 59–68 (2014).

68. Werner, G., Hagenmaier, H., Drautz, H., Baumgartner, A. & Zahner, H. Metabolic products of microorganisms. 224. Bafilomycins, a new group of macrolide antibiotics production, isolation, chemical-structure and biological-activity. *J. Antibiot. (Tokyo)* **37,** 110–117 (1984).

69. Bowman, E. J., Siebers, A. & Altendorf, K. Bafilomycins: a class of inhibitors of membrane ATPases from microorganisms, animal cells, and plant cells. *Proc. Natl. Acad. Sci.* **85,** 7972–7976 (1988).

70. Hanada, H., Moriyama, Y., Maeda, M. & Futai, M. Kinetic studies of chromaffin granule H+-ATPase and effects of bafilomycin A1. *Biochem. Biophys. Res. Commun.* **170,** 873–878 (1990).

71. Yamamoto, A. *et al.* Bafilomycin A1 prevents maturation of autophagic vacuoles by inhibiting fusion between autophagosomes and lysosomes in rat hepatoma cell line, H-4-II-E cells. *Cell Struct. Funct.* **23,** 33–42 (1998).

72. Birgisdottir, A. B., Lamark, T. & Johansen, T. The LIR motif - crucial for selective autophagy. *J. Cell Sci.* **126,** 3237–3247 (2013).

73. Komatsu, M., Kageyama, S. & Ichimura, Y. p62/SQSTM1/A170: Physiology and pathology. *Pharmacol. Res.* **66,** 457–462 (2012).

74. Moscat, J. & Diaz-Meco, M. T. p62 at the Crossroads of Autophagy, Apoptosis, and Cancer. *Cell* **137,** 1001–1004 (2009).

75. Pankiv, S. *et al.* p62/SQSTM1 Binds Directly to Atg8/LC3 to Facilitate Degradation of Ubiquitinated Protein Aggregates by Autophagy. *J. Biol. Chem.* **282,** 24131–24145 (2007).

76. Komatsu, M. *et al.* Homeostatic Levels of p62 Control Cytoplasmic Inclusion Body Formation in Autophagy-Deficient Mice. *Cell* **131,** 1149–1163 (2007).

77. Kirkin, V., McEwan, D. G., Novak, I. & Dikic, I. A Role for Ubiquitin in Selective Autophagy. *Mol. Cell* **34,** 259–269 (2009).

78. Novak, I. *et al.* Nix is a selective autophagy receptor for mitochondrial clearance. *EMBO Rep.* **11,** 45–51 (2010).

79. Komatsu, M. *et al.* The selective autophagy substrate p62 activates the stress responsive transcription factor Nrf2 through inactivation of Keap1. *Nat. Cell Biol.* **12,** 213–223 (2010).

80. Sanz, L., Diaz-Meco, M. T., Nakano, H. & Moscat, J. The atypical PKC-interacting protein p62 channels NF-kappa B activation by the IL-1-TRAF6 pathway. *Embo J.* **19,** 1576–1586 (2000).

81. Moscat, J., Diaz-Meco, M. T., Albert, A. & Campuzano, S. Cell signaling and function organized by PB1 domain interactions. *Mol. Cell* **23,** 631–640 (2006).

82. Jin, Z. *et al.* Cullin3-Based Polyubiquitination and p62-Dependent Aggregation of Caspase-8 Mediate Extrinsic Apoptosis Signaling. *Cell* **137,** 721–735 (2009).

83. Kirkin, V. *et al.* A role for NBR1 in autophagosomal degradation of ubiquitinated substrates. *Mol. Cell* **33,** 505–516 (2009).

84. Lamark, T., Kirkin, V., Dikic, I. & Johansen, T. NBR1 and p62 as cargo receptors for selective autophagy of ubiquitinated targets. *Cell Cycle* **8,** 1986–1990 (2009).

85. Rozenknop, A. *et al.* Characterization of the Interaction of GABARAPL-1 with the LIR Motif of NBR1. *J. Mol. Biol.* **410,** 477–487 (2011).

86. Hanna, R. A. *et al.* Microtubule-associated Protein 1 Light Chain 3 (LC3) Interacts with Bnip3 Protein to Selectively Remove Endoplasmic Reticulum and Mitochondria via Autophagy. *J. Biol. Chem.* **287,** 19094–19104 (2012).

87. Liu, L. *et al.* Mitochondrial outer-membrane protein FUNDC1 mediates hypoxia-induced mitophagy in mammalian cells. *Nat. Cell Biol.* **14,** 177–185 (2012).

88. Jin, S. M. & Youle, R. J. PINK1-and Parkin-mediated mitophagy at a glance. *J. Cell Sci.* **125,** 795–799 (2012).

89. Sorbara, M. T. & Girardin, S. E. Emerging themes in bacterial autophagy. *Curr. Opin. Microbiol.* **23,** 163–170 (2015).

90. Wild, P. *et al.* Phosphorylation of the Autophagy Receptor Optineurin Restricts Salmonella Growth. *Science* **333,** 228–233 (2011).

91. Korac, J. *et al.* Ubiquitin-independent function of optineurin in autophagic clearance of protein aggregates. *J. Cell Sci.* **126,** 580–592 (2013).

92. Thurston, T. L. M., Ryzhakov, G., Bloor, S., von Muhlinen, N. & Randow, F. The TBK1 adaptor and autophagy receptor NDP52 restricts the proliferation of ubiquitin-coated bacteria. *Nat. Immunol.* **10,** 1215–1221 (2009).

93. Von Muhlinen, N. *et al.* LC3C, Bound Selectively by a Noncanonical LIR Motif in NDP52, Is Required for Antibacterial Autophagy. *Mol. Cell* **48,** 329–342 (2012).

94. Mancias, J. D., Wang, X., Gygi, S. P., Harper, J. W. & Kimmelman, A. C. Quantitative proteomics identifies NCOA4 as the cargo receptor mediating ferritinophagy. *Nature* **509,** 105–109 (2014).

95. Jiang, S., Wells, C. D. & Roach, P. J. Starch-binding domain-containing protein 1 (Stbd1) and glycogen metabolism: Identification of the Atg8 family interacting motif (AIM) in Stbd1 required for interaction with GABARAPL1. *Biochem. Biophys. Res. Commun.* **413,** 420–425 (2011).

96. Cecconi, F. c-Cbl targets active Src for autophagy. *Nat. Cell Biol.* **14,** 48–49 (2012).

97. Haigis, M. C. & Sinclair, D. A. Mammalian Sirtuins: Biological Insights and Disease Relevance. *Annu. Rev. Pathol. Mech. Dis.* **5,** 253–295 (2010).

98. Lee, I. H. *et al.* A role for the NAD-dependent deacetylase Sirt1 in the regulation of autophagy. *Proc. Natl. Acad. Sci.* **105,** 3374–3379 (2008).

99. Morselli, E. *et al.* Caloric restriction and resveratrol promote longevity through the Sirtuin-1-dependent induction of autophagy. *Cell Death Dis.* **1,** e10 (2010).

100. Morselli, E. *et al.* The life span-prolonging effect of Sirtuin-1 is mediated by autophagy. *Autophagy* **6,** 186–188 (2010).

101. Ruderman, N. B. *et al.* AMPK and SIRT1: a long-standing partnership? *Am. J. Physiol. - Endocrinol. Metab.* **298,** E751–E760 (2010).

102. Yorimitsu, T., Nair, U., Yang, Z. & Klionsky, D. J. Endoplasmic Reticulum Stress Triggers Autophagy. *J. Biol. Chem.* **281,** 30299–30304 (2006).

103. Ogata, M. *et al.* Autophagy Is Activated for Cell Survival after Endoplasmic Reticulum Stress. *Mol. Cell. Biol.* **26,** 9220–9231 (2006).

104. Rouschop, K. M. A. *et al.* The unfolded protein response protects human tumor cells during hypoxia through regulation of the autophagy genes MAP1LC3B and ATG5. *J. Clin. Invest.* **120,** 127–141 (2010).

105. Bernales, S., Schuck, S. & Walter, P. ER-Phagy: Selective Autophagy of the Endoplasmic Reticulum. *Autophagy* **3,** 285–287 (2007).

106. Yorimitsu, T. & Klionsky, D. J. Eating the endoplasmic reticulum: quality control by autophagy. *Trends Cell Biol.* **17,** 279–285 (2007).

107. Bellot, G. *et al.* Hypoxia-Induced Autophagy Is Mediated through Hypoxia-Inducible Factor Induction of BNIP3 and BNIP3L via Their BH3 Domains. *Mol. Cell. Biol.* **29,** 2570–2581 (2009).

108. Papandreou, I., Lim, A. L., Laderoute, K. & Denko, N. C. Hypoxia signals autophagy in tumor cells via AMPK activity, independent of HIF-1, BNIP3, and BNIP3L. *Cell Death Differ.* **15,** 1572–1581 (2008).

109. Martina, J. A., Diab, H. I., Li, H. & Puertollano, R. Novel roles for the MiTF/TFE family of transcription factors in organelle biogenesis, nutrient sensing, and energy homeostasis. *Cell. Mol. Life Sci.* **71,** 2483–2497 (2014).

110. Sardiello, M. *et al.* A Gene Network Regulating Lysosomal Biogenesis and Function. *Science* **325,** 473–477 (2009).

111. Palmieri, M. *et al.* Characterization of the CLEAR network reveals an integrated control of cellular clearance pathways. *Hum. Mol. Genet.* **20,** 3852–3866 (2011).

112. Martina, J. A., Chen, Y., Gucek, M. & Puertollano, R. MTORC1 functions as a transcriptional regulator of autophagy by preventing nuclear transport of TFEB. *Autophagy* **8,** 903–914 (2012).

113. Roczniak-Ferguson, A. *et al.* The Transcription Factor TFEB Links mTORC1 Signaling to Transcriptional Control of Lysosome Homeostasis. *Sci Signal* **5,** ra42–ra42 (2012).

114. Settembre, C. *et al.* A lysosome-to-nucleus signalling mechanism senses and regulates the lysosome via mTOR and TFEB. *Embo J.* **31,** 1095–1108 (2012).

115. Vousden, K. H. & Lane, D. P. p53 in health and disease. *Nat. Rev. Mol. Cell Biol.* **8,** 275–283 (2007).

116. Balaburski, G. M., Hontz, R. D. & Murphy, M. E. p53 and ARF: unexpected players in autophagy. *Trends Cell Biol.* **20,** 363–369 (2010).

117. Green, D. R. & Kroemer, G. Cytoplasmic functions of the tumour suppressor p53. *Nature* **458,** 1127–1130 (2009).

118. Morselli, E. *et al.* p53 inhibits autophagy by interacting with the human ortholog of yeast Atg17, RB1CC1/FIP200. *Cell Cycle* **10,** 2763–2769 (2011).

119. Lee, I. H. *et al.* Atg7 modulates p53 activity to regulate cell cycle and survival during metabolic stress. *Science* **336,** 225–228 (2012).

120. Liang, X. H. *et al.* Induction of autophagy and inhibition of tumorigenesis by beclin 1. *Nature* **402,** 672–676 (1999).

121. Rubinsztein, D. C., Codogno, P. & Levine, B. Autophagy modulation as a potential therapeutic target for diverse diseases. *Nat. Rev. Drug Discov.* **11,** 709–730 (2012).

122. Cianfanelli, V. *et al.* AMBRA1 links autophagy to cell proliferation and tumorigenesis by promoting c-Myc dephosphorylation and degradation. *Nat. Cell Biol.* **17,** 20–30 (2015).

123. Kim, M. S. *et al.* Frameshift mutation of UVRAG, an autophagy-related gene, in gastric carcinomas with microsatellite instability. *Hum. Pathol.* **39,** 1059–1063 (2008).

124. Liang, C. *et al.* Autophagic and tumour suppressor activity of a novel Beclin1-binding protein UVRAG. *Nat. Cell Biol.* **8,** 688–698 (2006).

125. Kuo, W.-L. *et al.* p62/SQSTM1 Accumulation in Squamous Cell Carcinoma of Head and Neck Predicts Sensitivity to Phosphatidylinositol 3-Kinase Pathway Inhibitors. *PLoS ONE* **9,** 1–11 (2014).

126. Guertin, D. A. & Sabatini, D. M. Defining the Role of mTOR in Cancer. *Cancer Cell* **12,** 9–22 (2007).

127. Wei, Y. *et al.* EGFR-Mediated Beclin 1 Phosphorylation in Autophagy Suppression, Tumor Progression, and Tumor Chemoresistance. *Cell* **154,** 1269–1284 (2013).

128. White, E. Deconvoluting the context-dependent role for autophagy in cancer. *Nat. Rev. Cancer* **12,** 401–410 (2012).

129. Kimmelman, A. C. The dynamic nature of autophagy in cancer. *Genes Dev.* **25,** 1999–2010 (2011).

130. Galluzzi, L. *et al.* Autophagy in malignant transformation and cancer progression. *EMBO J.* **34,** 856–880 (2015).

131. Yue, Z. Y., Jin, S. K., Yang, C. W., Levine, A. J. & Heintz, N. Beclin 1, an autophagy gene essential for early embryonic development, is a haploinsufficient tumor suppressor. *Proc. Natl. Acad. Sci. U. S. A.* **100,** 15077–15082 (2003).

132. Qu, X. P. *et al.* Promotion of tumorigenesis by heterozygous disruption of the beclin 1 autophagy gene. *J. Clin. Invest.* **112,** 1809–1820 (2003).

133. Takamura, A. *et al.* Autophagy-deficient mice develop multiple liver tumors. *Genes Dev.* **25,** 795–800 (2011).

134. Mariño, G. *et al.* Tissue-specific Autophagy Alterations and Increased Tumorigenesis in Mice Deficient in Atg4C/Autophagin-3. *J. Biol. Chem.* **282,** 18573–18583 (2007).

135. Strohecker, A. M. *et al.* Autophagy Sustains Mitochondrial Glutamine Metabolism and Growth of Braf(V600E)-Driven Lung Tumors. *Cancer Discov.* **3,** 1272–1285 (2013).

136. Rao, S. *et al.* A dual role for autophagy in a murine model of lung cancer. *Nat. Commun.* **5,** (2014).

137. Rosenfeldt, M. T. *et al.* p53 status determines the role of autophagy in pancreatic tumour development. *Nature* **504,** 296–+ (2013).

138. Yang, A. *et al.* Autophagy Is Critical for Pancreatic Tumor Growth and Progression in Tumors with p53 Alterations. *Cancer Discov.* **4,** 905–913 (2014).

139. Green, D. R., Galluzzi, L. & Kroemer, G. Mitochondria and the Autophagy–Inflammation–Cell Death Axis in Organismal Aging. *Science* **333,** 1109–1112 (2011).

140. Takahashi, Y. *et al.* Bif-1 haploinsufficiency promotes chromosomal instability and accelerates Myc-driven lymphomagenesis via suppression of mitophagy. *Blood* **121,** 1622–1632 (2013).

141. Guo, J. Y. *et al.* Autophagy suppresses progression of K-ras-induced lung tumors to oncocytomas and maintains lipid homeostasis. *Genes Dev.* **27,** 1447–1461 (2013).

142. Mathew, R. *et al.* Autophagy Suppresses Tumorigenesis through Elimination of p62. *Cell* **137,** 1062–1075 (2009).

143. Duran, A. *et al.* The signaling adaptor p62 is an important NF-kappa B mediator in tumorigenesis. *Cancer Cell* **13,** 343–354 (2008).

144. Wei, H., Wang, C., Croce, C. M. & Guan, J.-L. p62/SQSTM1 synergizes with autophagy for tumor growth in vivo. *Genes Dev.* **28,** 1204–1216 (2014).

145. Deretic, V., Saitoh, T. & Akira, S. Autophagy in infection, inflammation and immunity. *Nat. Rev. Immunol.* **13,** 722–737 (2013).

146. Elgendy, M., Sheridan, C., Brumatti, G. & Martin, S. J. Oncogenic Ras-Induced Expression of Noxa and Beclin-1 Promotes Autophagic Cell Death and Limits Clonogenic Survival. *Mol. Cell* **42,** 23–35 (2011).

147. Young, A. R. J. *et al.* Autophagy mediates the mitotic senescence transition. *Genes Dev.* **23,** 798–803 (2009).

148. Liu, H. *et al.* Down-Regulation of Autophagy-Related Protein 5 (ATG5) Contributes to the Pathogenesis of Early-Stage Cutaneous Melanoma. *Sci. Transl. Med.* **5,** 202ra123–202ra123 (2013).

149. Horikawa, I. *et al.* Autophagic degradation of the inhibitory p53 isoform Δ133p53α as a regulatory mechanism for p53-mediated senescence. *Nat. Commun.* **5,** 4706 (2014).

150. Lazova, R. *et al.* Punctate LC3B Expression Is a Common Feature of Solid Tumors and Associated with Proliferation, Metastasis, and Poor Outcome. *Clin. Cancer Res.* **18,** 370–379 (2012).

151. Kim, M.-J. *et al.* Involvement of Autophagy in Oncogenic K-Ras-induced Malignant Cell Transformation. *J. Biol. Chem.* **286,** 12924–12932 (2011).

152. Guo, J. Y. *et al.* Activated Ras requires autophagy to maintain oxidative metabolism and tumorigenesis. *Genes Dev.* **25,** 460–470 (2011).

153. Lock, R. *et al.* Autophagy facilitates glycolysis during Ras-mediated oncogenic transformation. *Mol. Biol. Cell* **22,** 165–178 (2011).

154. Yang, S. *et al.* Pancreatic cancers require autophagy for tumor growth. *Genes Dev.* **25,** 717–729 (2011).

155. Parkhitko, A. *et al.* Tumorigenesis in tuberous sclerosis complex is autophagy and p62/sequestosome 1 (SQSTM1)-dependent. *Proc. Natl. Acad. Sci.* **108,** 12455–12460 (2011).

156. Xie, X., Koh, J. Y., Price, S., White, E. & Mehnert, J. M. Atg7 Overcomes Senescence and Promotes Growth of BrafV600E-Driven Melanoma. *Cancer Discov.* **5,** 410–423 (2015).

157. Santanam, U. *et al.* Atg7 cooperates with Pten loss to drive prostate cancer tumor growth. *Genes Dev.* **30,** 399–407 (2016).

158. Wei, H. *et al.* Suppression of autophagy by FIP200 deletion inhibits mammary tumorigenesis. *Genes Dev.* **25,** 1510–1527 (2011).

159. Futreal, P. A. *et al.* BRCA1 Mutations in Primary Breast and Ovarian Carcinomas. *Science* **266,** 120–122 (1994).

160. Laddha, S. V., Ganesan, S., Chan, C. S. & White, E. Mutational Landscape of the Essential Autophagy Gene BECN1 in Human Cancers. *Mol. Cancer Res.* **12,** 485–490 (2014).

161. Tang, H. *et al.* Decreased BECN1 mRNA Expression in Human Breast Cancer is Associated With Estrogen Receptor-Negative Subtypes and Poor Prognosis. *Ebiomedicine* **2,** 255–263 (2015).

162. Hara, T. *et al.* Suppression of basal autophagy in neural cells causes neurodegenerative disease in mice. *Nature* **441,** 885–889 (2006).

163. Nishida, Y. *et al.* Discovery of Atg5/Atg7-independent alternative macroautophagy. *Nature* **461,** 654–658 (2009).

164. Subramani, S. & Malhotra, V. Non-autophagic roles of autophagy-related proteins. *EMBO Rep.* **14,** 143–151 (2013).

165. Chen, S. *et al.* Distinct roles of autophagy-dependent and -independent functions of FIP200 revealed by generation and analysis of a mutant knock-in mouse model. *Genes Dev.* **30,** 856–869 (2016).

166. Gupta, G. P. & Massagué, J. Cancer Metastasis: Building a Framework. *Cell* **127,** 679–695 (2006).

167. Valastyan, S. & Weinberg, R. A. Tumor Metastasis: Molecular Insights and Evolving Paradigms. *Cell* **147,** 275–292 (2011).

168. Chaffer, C. L. & Weinberg, R. A. A Perspective on Cancer Cell Metastasis. *Science* **331,** 1559–1564 (2011).

169. Chambers, A. F., Groom, A. C. & MacDonald, I. C. Dissemination and growth of cancer cells in metastatic sites. *Nat. Rev. Cancer* **2,** 563–572 (2002).

170. Minna, J. D., Kurie, J. M. & Jacks, T. A big step in the study of small cell lung cancer. *Cancer Cell* **4,** 163–166 (2003).

171. Nguyen, D. X., Bos, P. D. & Massagué, J. Metastasis: from dissemination to organ-specific colonization. *Nat. Rev. Cancer* **9,** 274–284 (2009).

172. Kalluri, R. & Weinberg, R. A. The basics of epithelial-mesenchymal transition. *J. Clin. Invest.* **119,** 1420–1428 (2009).

173. Thiery, J. P., Acloque, H., Huang, R. Y. J. & Nieto, M. A. Epithelial-Mesenchymal Transitions in Development and Disease. *Cell* **139,** 871–890 (2009).

174. Carmeliet, P. & Jain, R. K. Principles and mechanisms of vessel normalization for cancer and other angiogenic diseases. *Nat. Rev. Drug Discov.* **10,** 417–427 (2011).

175. Guo, W. & Giancotti, F. G. Integrin signalling during tumour progression. *Nat. Rev. Mol. Cell Biol.* **5,** 816–826 (2004).

176. Paget, S. The distribution of secondary growths in cancer of the breast. *Lancet* **1,** 99–101 (1889).

177. Ewing, J. in *Neoplastic Diseases. A Treatise on Tumors* 77–89 (W.B. Saunders Co., 1928).

178. Langley, R. R. & Fidler, I. J. The seed and soil hypothesis revisited—The role of tumor-stroma interactions in metastasis to different organs. *Int. J. Cancer* **128,** 2527–2535 (2011).

179. Luzzi, K. J. *et al.* Multistep Nature of Metastatic Inefficiency: Dormancy of Solitary Cells after Successful Extravasation and Limited Survival of Early Micrometastases. *Am. J. Pathol.* **153,** 865–873 (1998).

180. Cell Migration: Integrating Signals from Front to Back. *Science* **302,** 1704–1709 (2003).

181. Parsons, J. T., Horwitz, A. R. & Schwartz, M. A. Cell adhesion: integrating cytoskeletal dynamics and cellular tension. *Nat. Rev. Mol. Cell Biol.* **11,** 633–643 (2010).

182. Amano, M. *et al.* Formation of Actin Stress Fibers and Focal Adhesions Enhanced by Rho-Kinase. *Science* **275,** 1308–1311 (1997).

183. Kurokawa, K., Nakamura, T., Aoki, K. & Matsuda, M. Mechanism and role of localized activation of Rho-family GTPases in growth factor-stimulated fibroblasts and neuronal cells. *Biochem. Soc. Trans.* **33,** 631–634 (2005).

184. Coordination of Rho GTPase activities during cell protrusion. *Nature* **461,** 99–103 (2009).

185. Zaidel-Bar, R. & Geiger, B. The switchable integrin adhesome. *J Cell Sci* **123,** 1385–1388 (2010).

186. Vicente-Manzanares, M., Choi, C. K. & Horwitz, A. R. Integrins in cell migration – the actin connection. *J. Cell Sci.* **122,** 199–206 (2009).

187. Deakin, N. O. & Turner, C. E. Paxillin comes of age. *J. Cell Sci.* **121,** 2435–2444 (2008).

188. Digman, M. A., Brown, C. M., Horwitz, A. R., Mantulin, W. W. & Gratton, E. Paxillin dynamics measured during adhesion assembly and disassembly by correlation spectroscopy. *Biophys. J.* **94,** 2819–2831 (2008).

189. Turner, C. E., Glenney, J. R. & Burridge, K. Paxillin: A New Vinculin-Binding Protein Present in Focal Adhesions. *J. Cell Biol.* **111,** 1059–1068 (1990).

190. Burridge, K., Turner, C. E. & Romer, L. H. Tyrosine Phosphorylation of Paxillin and pp125 FAK Accompanies Cell Adhesion to Extracellular Matrix: A Role in Cytoskeletal Assembly. *J. Cell Biol.* **119,** 893–903 (1992).

191. Brown, M. C., Perrotta, J. A. & Turner, C. E. Identification of LIM3 as the principal determinant of paxillin focal adhesion localization and characterization of a novel motif on

paxillin directing vinculin and focal adhesion kinase binding. *J. Cell Biol.* **135,** 1109–1123 (1996).

192. Mitra, S. K. & Schlaepfer, D. D. Integrin-regulated FAK–Src signaling in normal and cancer cells. *Curr. Opin. Cell Biol.* **18,** 516–523 (2006).

193. Huveneers, S. & Danen, E. H. J. Adhesion signaling – crosstalk between integrins, Src and Rho. *J. Cell Sci.* **122,** 1059–1069 (2009).

194. Turner, C. E. Paxillin and focal adhesion signalling. *Nat. Cell Biol.* **2,** E231–E236 (2000).

195. Klinghoffer, R. A., Sachsenmaier, C., Cooper, J. A. & Soriano, P. Src family kinases are required for integrin but not PDGFR signal transduction. *EMBO J.* **18,** 2459–2471 (1999).

196. Ilić, D. *et al.* Reduced cell motility and enhanced focal adhesion contact formation in cells from FAK-deficient mice. *Nature* **377,** 539–544 (1995).

197. Ren, X. D. *et al.* Focal adhesion kinase suppresses Rho activity to promote focal adhesion turnover. *J. Cell Sci.* **113,** 3673–3678 (2000).

198. Webb, D. J. *et al.* FAK–Src signalling through paxillin, ERK and MLCK regulates adhesion disassembly. *Nat. Cell Biol.* **6,** 154–161 (2004).

199. Fincham, V. J. & Frame, M. C. The catalytic activity of Src is dispensable for translocation to focal adhesions but controls the turnover of these structures during cell motility. *EMBO J.* **17,** 81–92 (1998).

200. Irby, R. B. *et al.* Activating SRC mutation in a subset of advanced human colon cancers. *Nat. Genet.* **21,** 187–190 (1999).

201. Kim, L. C., Song, L. & Haura, E. B. Src kinases as therapeutic targets for cancer. *Nat. Rev. Clin. Oncol.* **6,** 587–595 (2009).

202. Lazova, R., Klump, V. & Pawelek, J. Autophagy in cutaneous malignant melanoma. *J. Cutan. Pathol.* **37,** 256–268 (2010).

203. Han, C. *et al.* Overexpression of Microtubule-Associated Protein-1 Light Chain 3 Is Associated with Melanoma Metastasis and Vasculogenic Mimicry. *Tohoku J. Exp. Med.* **223,** 243–251 (2011).

204. Peng, Y.-F. *et al.* Promoting Colonization in Metastatic HCC Cells by Modulation of Autophagy. *PLOS ONE* **8,** e74407 (2013).

205. Kenific, C. M., Thorburn, A. & Debnath, J. Autophagy and metastasis: another double-edged sword. *Curr. Opin. Cell Biol.* **22,** 241–245 (2010).

206. Tracy, K. *et al.* BNIP3 Is an RB/E2F Target Gene Required for Hypoxia-Induced Autophagy. *Mol. Cell. Biol.* **27,** 6229–6242 (2007).

207. Kiyono, K. *et al.* Autophagy Is Activated by TGF-beta and Potentiates TGF-beta-Mediated Growth Inhibition in Human Hepatocellular Carcinoma Cells. *Cancer Res.* **69,** 8844–8852 (2009).

208. Suzuki, H. I., Kiyono, K. & Miyazono, K. Regulation of autophagy by transforming growth factor-β (TGF-β) signaling. *Autophagy* **6,** 645–647 (2010).

209. Mani, S. A. *et al.* The Epithelial-Mesenchymal Transition Generates Cells with Properties of Stem Cells. *Cell* **133,** 704–715 (2008).

210. Pang, R. *et al.* A Subpopulation of CD26+ Cancer Stem Cells with Metastatic Capacity in Human Colorectal Cancer. *Cell Stem Cell* **6,** 603–615 (2010).

211. Charafe-Jauffret, E. *et al.* Breast Cancer Cell Lines Contain Functional Cancer Stem Cells with Metastatic Capacity and a Distinct Molecular Signature. *Cancer Res.* **69,** 1302–1313 (2009).

212. Chao Chen *et al.* Evidence for Epithelial-Mesenchymal Transition in Cancer Stem Cells of Head and Neck Squamous Cell Carcinoma. *PLoS ONE* **6,** 1–14 (2011).

213. Oliver, L., Hue, E., Priault, M. & Vallette, F. M. Basal Autophagy Decreased During the Differentiation of Human Adult Mesenchymal Stem Cells. *Stem Cells Dev.* **21,** 2779–2788 (2012).

214. Tra, T. *et al.* Autophagy in Human Embryonic Stem Cells. *Plos One* **6,** (2011).

215. Vazquez, P. *et al.* Atg5 and Ambra1 differentially modulate neurogenesis in neural stem cells. *Autophagy* **8,** 187–199 (2012).

216. Phadwal, K., Watson, A. S. & Simon, A. K. Tightrope act: autophagy in stem cell renewal, differentiation, proliferation, and aging. *Cell. Mol. Life Sci.* **70,** 89–103 (2013).

217. Warr, M. R. *et al.* FOXO3A directs a protective autophagy program in haematopoietic stem cells. *Nature* **494,** 323–327 (2013).

218. Espina, V. *et al.* Malignant Precursor Cells Pre-Exist in Human Breast DCIS and Require Autophagy for Survival. *PLOS ONE* **5,** e10240 (2010).

219. Cufí, S. *et al.* Autophagy positively regulates the CD44+CD24-/low breast cancer stem-like phenotype. *Cell Cycle* **10,** 3871–3885 (2011).

220. Wolf, J. *et al.* A mammosphere formation RNAi screen reveals that ATG4A promotes a breast cancer stem-like phenotype. *Breast Cancer Res.* **15,** R109 (2013).

221. Li, J. *et al.* Autophagy promotes hepatocellular carcinoma cell invasion through activation of epithelialmesenchymal transition. *Carcinogenesis* **34,** 1343–1351 (2013).

222. Catalano, M. *et al.* Autophagy induction impairs migration and invasion by reversing EMT in glioblastoma cells. *Mol. Oncol.* **9,** 1612–1625 (2015).

223. Macintosh, R. L. *et al.* Inhibition of autophagy impairs tumor cell invasion in an organotypic model. *Cell Cycle* **11,** 2022–2029 (2012).

224. Qiang, L. *et al.* Regulation of cell proliferation and migration by p62 through stabilization of Twist1. *Proc. Natl. Acad. Sci. U. S. A.* **111,** 9241–9246 (2014).

225. Lock, R., Kenific, C. M., Leidal, A. M., Salas, E. & Debnath, J. Autophagy-Dependent Production of Secreted Factors Facilitates Oncogenic RAS-Driven Invasion. *Cancer Discov.* **4,** 466–479 (2014).

226. Guadamillas, M. C., Cerezo, A. & Pozo, M. A. del. Overcoming anoikis – pathways to anchorage-independent growth in cancer. *J Cell Sci* **124,** 3189–3197 (2011).

227. Avivar-Valderas, A. *et al.* Regulation of autophagy during ECM detachment is linked to a selective inhibition of mTORC1 by PERK. *Oncogene* **32,** 4932–4940 (2013).

228. Fung, C., Lock, R., Gao, S., Salas, E. & Debnath, J. Induction of Autophagy during Extracellular Matrix Detachment Promotes Cell Survival. *Mol. Biol. Cell* **19,** 797–806 (2008).

229. Peng, Y.-F. *et al.* Autophagy inhibition suppresses pulmonary metastasis of HCC in mice via impairing anoikis resistance and colonization of HCC cells. *Autophagy* **9,** 2056–2068 (2013).

230. Edinger, A. L., Cinalli, R. M. & Thompson, C. B. Rab7 Prevents Growth Factor-Independent Survival by Inhibiting Cell-Autonomous Nutrient Transporter Expression. *Dev. Cell* **5,** 571–582 (2003).

231. Lum, J. J. *et al.* Growth Factor Regulation of Autophagy and Cell Survival in the Absence of Apoptosis. *Cell* **120,** 237–248 (2005).

232. Autophagy in immunity and inflammation. *Nature* **469,** 323–335 (2011).

233. Deretic, V., Jiang, S. & Dupont, N. Autophagy intersections with conventional and unconventional secretion in tissue development, remodeling and inflammation. *Trends Cell Biol.* **22,** 397–406 (2012).

234. Aslakson, C. J. & Miller, F. R. Selective events in the metastatic process defined by analysis of the sequential dissemination of subpopulations of a mouse mammary tumor. *Cancer Res.* **52,** 1399–1405 (1992).

235. Fidler, I. J. Selection of successive tumour lines for metastasis. *Nature. New Biol.* **242,** 148–149 (1973).

236. Drasin, D. J., Robin, T. P. & Ford, H. L. Breast cancer epithelial-to-mesenchymal transition: examining the functional consequences of plasticity. *Breast Cancer Res.* **13,** 226 (2011).

237. Hagel, M. *et al.* The Adaptor Protein Paxillin Is Essential for Normal Development in the Mouse and Is a Critical Transducer of Fibronectin Signaling. *Mol. Cell. Biol.* **22,** 901–915 (2002).

238. Rogov, V., Dötsch, V., Johansen, T. & Kirkin, V. Interactions between Autophagy Receptors and Ubiquitin-like Proteins Form the Molecular Basis for Selective Autophagy. *Mol. Cell* **53,** 167–178 (2014).

239. Didier, C. *et al.* RNF5, a RING Finger Protein That Regulates Cell Motility by Targeting Paxillin Ubiquitination and Altered Localization. *Mol. Cell. Biol.* **23,** 5331–5345 (2003).

240. Bjørkøy, G. *et al.* p62/SQSTM1 forms protein aggregates degraded by autophagy and has a protective effect on huntingtin-induced cell death. *J. Cell Biol.* **171,** 603–614 (2005).

241. Kenific, C. M. *et al.* NBR1 enables autophagy-dependent focal adhesion turnover. *J. Cell Biol.* **212,** 577–590 (2016).

242. Xin, Y. *et al.* Cloning, Expression Patterns, and Chromosome Localization of Three Human and Two Mouse Homologues of GABAA Receptor-Associated Protein. *Genomics* **74,** 408–413 (2001).

243. Klionsky, D. J. & Schulman, B. A. Dynamic regulation of macroautophagy by distinctive ubiquitin-like proteins. *Nat. Struct. Mol. Biol.* **21,** 336–345 (2014).

244. Kaufmann, A., Beier, V., Franquelim, H. G. & Wollert, T. Molecular mechanism of autophagic membrane-scaffold assembly and disassembly. *Cell* **156,** 469–481 (2014).

245. Weiergräber, O. H. *et al.* Ligand Binding Mode of GABAA Receptor-Associated Protein. *J. Mol. Biol.* **381,** 1320–1331 (2008).

246. Rogov, V. V. *et al.* Structural basis for phosphorylation-triggered autophagic clearance of Salmonella. *Biochem. J.* **454,** 459–466 (2013).

247. Sandilands, E. *et al.* Autophagic targeting of Src promotes cancer cell survival following reduced FAK signalling. *Nat. Cell Biol.* **14,** 51–60 (2012).

248. Fidler, I. J. Biological behavior of malignant melanoma cells correlated to their survival in vivo. *Cancer Res.* **35,** 218–224 (1975).

249. Ichimura, Y. *et al.* Structural Basis for Sorting Mechanism of p62 in Selective Autophagy. *J. Biol. Chem.* **283,** 22847–22857 (2008).

250. Martin, G. S. The hunting of the Src. *Nat. Rev. Mol. Cell Biol.* **2,** 467–475 (2001).

251. Dehm, S. M. & Bonham, K. SRC gene expression in human cancer: the role of transcriptional activation. *Biochem. Cell Biol. Biochim. Biol. Cell.* **82,** 263–274 (2004).

252. Lutz, M. P. *et al.* Overexpression and activation of the tyrosine kinase Src in human pancreatic carcinoma. *Biochem. Biophys. Res. Commun.* **243,** 503–508 (1998).

253. Staley, C. A., Parikh, N. U. & Gallick, G. E. Decreased tumorigenicity of a human colon adenocarcinoma cell line by an antisense expression vector specific for c-Src. *Cell Growth Differ. Mol. Biol. J. Am. Assoc. Cancer Res.* **8,** 269–274 (1997).

254. González, L. *et al.* Role of c-Src in human MCF7 breast cancer cell tumorigenesis. *J. Biol. Chem.* **281,** 20851–20864 (2006).

255. Roskoski Jr., R. Src protein-tyrosine kinase structure, mechanism, and small molecule inhibitors. *Pharmacol. Res.* **94,** 9–25 (2015).

256. Gubens, M. A. *et al.* A phase II study of saracatinib (AZD0530), a Src inhibitor, administered orally daily to patients with advanced thymic malignancies. *Lung Cancer* **89,** 57–60 (2015).

257. Herold, C. I. *et al.* Phase II Trial of Dasatinib in Patients with Metastatic Breast Cancer Using Real-Time Pharmacodynamic Tissue Biomarkers of Src Inhibition to Escalate Dosing. *Clin. Cancer Res.* **17,** 6061–6070 (2011).

258. Gangadhar, T. C., Clark, J. I., Karrison, T. & Gajewski, T. F. Phase II study of the Src kinase inhibitor saracatinib (AZD0530) in metastatic melanoma. *Invest. New Drugs* **31,** 769–773 (2012).

259. Puls, L. N., Eadens, M. & Messersmith, W. Current status of SRC inhibitors in solid tumor malignancies. *The Oncologist* **16,** 566–578 (2011).

260. Strickler, J. H. *et al.* Phase I study of dasatinib in combination with capecitabine, oxaliplatin and bevacizumab followed by an expanded cohort in previously untreated metastatic colorectal cancer. *Invest. New Drugs* **32,** 330–339 (2014).

261. Schaller, M. D. & Schaefer, E. M. Multiple stimuli induce tyrosine phosphorylation of the Crk-binding sites of paxillin. *Biochem. J.* **360,** 57–66 (2001).

262. Webb, D. J. *et al.* Paxillin phosphorylation sites mapped by mass spectrometry. *J. Cell Sci.* **118,** 4925–4929 (2005).

263. Zhu, Y. *et al.* Modulation of Serines 17 and 24 in the LC3-interacting Region of Bnip3 Determines Pro-survival Mitophagy versus Apoptosis. *J. Biol. Chem.* **288,** 1099–1113 (2013).

264. Hanke, J. H. *et al.* Discovery of a Novel, Potent, and Src Family-selective Tyrosine Kinase Inhibitor STUDY OF Lck- AND FynT-DEPENDENT T CELL ACTIVATION. *J. Biol. Chem.* **271,** 695–701 (1996).

265. Schaller, M. D. & Parsons, J. T. pp125FAK-dependent tyrosine phosphorylation of paxillin creates a high-affinity binding site for Crk. *Mol. Cell. Biol.* **15,** 2635–2645 (1995).

266. Bellis, S. L., Miller, J. T. & Turner, C. E. Characterization of tyrosine phosphorylation of paxillin in vitro by focal adhesion kinase. *J. Biol. Chem.* **270,** 17437–17441 (1995).

267. Ezratty, E. J., Partridge, M. A. & Gundersen, G. G. Microtubule-induced focal adhesion disassembly is mediated by dynamin and focal adhesion kinase. *Nat. Cell Biol.* **7,** 581–590 (2005).

268. Ezratty, E. J., Bertaux, C., Marcantonio, E. E. & Gundersen, G. G. Clathrin mediates integrin endocytosis for focal adhesion disassembly in migrating cells. *J. Cell Biol.* **187,** 733–747 (2009).

269. Wang, Y., Cao, H., Chen, J. & McNiven, M. A. A direct interaction between the large GTPase dynamin-2 and FAK regulates focal adhesion dynamics in response to active Src. *Mol. Biol. Cell* **22,** 1529–1538 (2011).

270. Till, A. *et al.* Evolutionary trends and functional anatomy of the human expanded autophagy network. *Autophagy* **11,** 1652–1667 (2015).

271. Abbi, S. *et al.* Regulation of Focal Adhesion Kinase by a Novel Protein Inhibitor FIP200. *Mol. Biol. Cell* **13,** 3178–3191 (2002).

272. Caino, M. C. *et al.* Metabolic stress regulates cytoskeletal dynamics and metastasis of cancer cells. *J. Clin. Invest.* **123,** 2907–2920 (2013).

273. Carroll, B. *et al.* The TBC/RabGAP Armus Coordinates Rac1 and Rab7 Functions during Autophagy. *Dev. Cell* **25,** 15–28 (2013).

274. Kadandale, P., Stender, J. D., Glass, C. K. & Kiger, A. A. Conserved role for autophagy in Rho1-mediated cortical remodeling and blood cell recruitment. *Proc. Natl. Acad. Sci.* **107,** 10502–10507 (2010).

275. Belaid, A. *et al.* Autophagy Plays a Critical Role in the Degradation of Active RHOA, the Control of Cell Cytokinesis, and Genomic Stability. *Cancer Res.* **73,** 4311–4322 (2013).

276. Chan, E. Y. W., Kir, S. & Tooze, S. A. siRNA Screening of the Kinome Identifies ULK1 as a Multidomain Modulator of Autophagy. *J. Biol. Chem.* **282,** 25464–25474 (2007).

277. Mleczak, A., Millar, S., Tooze, S. A., Olson, M. F. & Chan, E. Y. W. Regulation of autophagosome formation by Rho kinase. *Cell. Signal.* **25,** 1–11 (2013).

278. Gurkar, A. U. *et al.* Identification of ROCK1 kinase as a critical regulator of Beclin1-mediated autophagy during metabolic stress. *Nat. Commun.* **4,** 2189 (2013).

279. Kim, S. I. *et al.* Autophagy Promotes Intracellular Degradation of Type I Collagen Induced by Transforming Growth Factor (TGF)-β1. *J. Biol. Chem.* **287,** 11677–11688 (2012).

280. Tuloup-Minguez, V. *et al.* Autophagy modulates cell migration and β1 integrin membrane recycling. *Cell Cycle* **12,** 3317–3328 (2013).

281. Iioka, H., Iemura, S., Natsume, T. & Kinoshita, N. Wnt signalling regulates paxillin ubiquitination essential for mesodermal cell motility. *Nat. Cell Biol.* **9,** 813–821 (2007).

282. Turner, C. E. Paxillin is a major phosphotyrosine-containing protein during embryonic development. *J. Cell Biol.* **115,** 201–207 (1991).

283. Komatsu, M. *et al.* Impairment of starvation-induced and constitutive autophagy in Atg7-deficient mice. *J. Cell Biol.* **169,** 425–434 (2005).

284. Kuma, A. *et al.* The role of autophagy during the early neonatal starvation period. *Nature* **432,** 1032–1036 (2004).

285. Janku, F., McConkey, D. J., Hong, D. S. & Kurzrock, R. Autophagy as a target for anticancer therapy. *Nat. Rev. Clin. Oncol.* **8,** 528–539 (2011).

286. Nagelkerke, A., Bussink, J., Geurts-Moespot, A., Sweep, F. C. G. J. & Span, P. N. Therapeutic targeting of autophagy in cancer. Part II: Pharmacological modulation of treatment-induced autophagy. *Semin. Cancer Biol.* **31,** 99–105 (2015).

287. Duffy, A., Le, J., Sausville, E. & Emadi, A. Autophagy modulation: a target for cancer treatment development. *Cancer Chemother. Pharmacol.* **75,** 439–447 (2014).

288. Jones, S. A., Mills, K. H. G. & Harris, J. Autophagy and inflammatory diseases. *Immunol. Cell Biol.* **91,** 250–258 (2013).

289. Shingu, T. *et al.* Inhibition of autophagy at a late stage enhances imatinib-induced cytotoxicity in human malignant glioma cells. *Int. J. Cancer* **124,** 1060–1071 (2009).

290. Travelli, C. *et al.* Reciprocal Potentiation of the Antitumoral Activities of FK866, an Inhibitor of Nicotinamide Phosphoribosyltransferase, and Etoposide or Cisplatin in Neuroblastoma Cells. *J. Pharmacol. Exp. Ther.* **338,** 829–840 (2011).

291. Karsli-Uzunbas, G. *et al.* Autophagy is Required for Glucose Homeostasis and Lung Tumor Maintenance. *Cancer Discov.* **4,** 914–927 (2014).

292. Leemans, C. R., Braakhuis, B. J. M. & Brakenhoff, R. H. The molecular biology of head and neck cancer. *Nat. Rev. Cancer* **11,** 9–22 (2011).

293. Argiris, A., Karamouzis, M. V., Raben, D. & Ferris, R. L. Head and neck cancer. *Lancet* **371,** 1695–1709 (2008).

294. Vokes, E., Weichselbaum, R., Lippman, S. & Hong, W. Medical Progress - Head and Neck-Cancer. *N. Engl. J. Med.* **328,** 184–194 (1993).

295. Llewellyn, C. D., Linklater, K., Bell, J., Johnson, N. W. & Warnakulasuriya, K. A. A. S. Squamous cell carcinoma of the oral cavity in patients aged 45 years and under: a descriptive analysis of 116 cases diagnosed in the South East of England from 1990 to 1997. *Oral Oncol.* **39,** 106–114 (2003).

296. Hasina, R. *et al.* ABT-510 Is an Effective Chemopreventive Agent in the Mouse 4-Nitroquinoline 1-Oxide Model of Oral Carcinogenesis. *Cancer Prev. Res. (Phila. Pa.)* **2,** 385–393 (2009).

297. Slaughter, D., Southwick, H. & Smejkal, W. Field Cancerization in Oral Stratified Squamous Epithelium - Clinical Implications of Multicentric Origin. *Cancer* **6,** 963–968 (1953).

298. Braakhuis, B. J. M., Tabor, M. P., Kummer, J. A., Leemans, C. R. & Brakenhoff, R. H. A genetic explanation of Slaughter's concept of field cancerization: Evidence and clinical implications. *Cancer Res.* **63,** 1727–1730 (2003).

299. Nordsmark, M. *et al.* Prognostic value of tumor oxygenation in 397 head and neck tumors after primary radiation therapy. An international multi-center study. *Radiother. Oncol.* **77,** 18–24 (2005).

300. Ozanne, B., Richards, C., Hendler, F., Burns, D. & Gusterson, B. Over-Expression of the Egf Receptor Is a Hallmark of Squamous-Cell Carcinomas. *J. Pathol.* **149,** 9–14 (1986).

301. Lee, J. W. *et al.* Somatic Mutations of EGFR Gene in Squamous Cell Carcinoma of the Head and Neck. *Clin. Cancer Res.* **11,** 2879–2882 (2005).

302. Loeffler-Ragg, J. *et al.* Low incidence of mutations in EGFR kinase domain in Caucasian patients with head and neck squamous cell carcinoma. *Eur. J. Cancer* **42,** 109–111 (2006).

303. Temam, S. *et al.* Epidermal Growth Factor Receptor Copy Number Alterations Correlate With Poor Clinical Outcome in Patients With Head and Neck Squamous Cancer. *J. Clin. Oncol.* **25,** 2164–2170 (2007).

304. Sheu, J. J.-C. *et al.* Functional Genomic Analysis Identified Epidermal Growth Factor Receptor Activation as the Most Common Genetic Event in Oral Squamous Cell Carcinoma. *Cancer Res.* **69,** 2568–2576 (2009).

305. Amornphimoltham, P., Patel, V., Molinolo, A. & Gutkind, J. S. in *Signaling Pathways in Squamous Cancer* 407–429 (Springer Science+Business Media, LLC, 2011).

306. Molinolo, A. A. *et al.* Dissecting the Akt/Mammalian target of rapamycin signaling network: Emerging results from the head and neck cancer tissue array initiative. *Clin. Cancer Res.* **13,** 4964–4973 (2007).

307. Amornphimoltham, P. *et al.* Mammalian target of rapamycin, a molecular target in squamous cell carcinomas of the head and neck. *Cancer Res.* **65,** 9953–9961 (2005).

308. Czerninski, R., Amornphimoltham, P., Patel, V., Molinolo, A. A. & Gutkind, J. S. Targeting Mammalian Target of Rapamycin by Rapamycin Prevents Tumor Progression in an Oral-Specific Chemical Carcinogenesis Model. *Cancer Prev. Res. (Phila. Pa.)* **2,** 27–36 (2009).

309. Aissat, N. *et al.* Antiproliferative effects of rapamycin as a single agent and in combination with carboplatin and paclitaxel in head and neck cancer cell lines. *Cancer Chemother. Pharmacol.* **62,** 305–313 (2008).

310. Raimondi, A. R., Molinolo, A. & Gutkind, J. S. Rapamycin Prevents Early Onset of Tumorigenesis in an Oral-Specific K-ras and p53 Two-Hit Carcinogenesis Model. *Cancer Res.* **69,** 4159–4166 (2009).

311. Agrawal, N. *et al.* Exome Sequencing of Head and Neck Squamous Cell Carcinoma Reveals Inactivating Mutations in NOTCH1. *Science* **333,** 1154–1157 (2011).

312. Stransky, N. *et al.* The Mutational Landscape of Head and Neck Squamous Cell Carcinoma. *Science* **333,** 1157–1160 (2011).

313. Van Dyck, E. *et al.* Bronchial airway gene expression in smokers with lung or head and neck cancer. *Cancer Med.* **3,** 322–36 (2014).

314. Lu, S.-L., Herrington, H. & Wang, X.-J. Mouse models for human head and neck squamous cell carcinomas. *Head Neck* **28,** 945–954 (2006).

315. Gimenez-Conti, I. B. & Slaga, T. J. The hamster cheek pouch carcinogenesis model. *J. Cell. Biochem. Suppl.* **17F,** 83–90 (1993).

316. Kanojia, D. & Vaidya, M. M. 4-nitroquinoline-1-oxide induced experimental oral carcinogenesis. *Oral Oncol.* **42,** 655–667 (2006).

317. Vitale-Cross, L. *et al.* Chemical Carcinogenesis Models for Evaluating Molecular-Targeted Prevention and Treatment of Oral Cancer. *Cancer Prev. Res. (Phila. Pa.)* **2,** 419–422 (2009).

318. Zhou, G. *et al.* Dual Inhibition of Vascular Endothelial Growth Factor Receptor and Epidermal Growth Factor Receptor is an Effective Chemopreventive Strategy in the Mouse 4-NQO Model of Oral Carcinogenesis. *Cancer Prev. Res. (Phila. Pa.)* **3,** 1493–1502 (2010).

319. Tang, X. H., Knudsen, B., Bemis, D., Tickoo, S. & Gudas, L. J. Oral cavity and esophageal carcinogenesis modeled in carcinogen-treated mice. *Clin. Cancer Res.* **10,** 301–313 (2004).

320. Sano, D. & Myers, J. N. Xenograft models of head and neck cancers. *Head Neck Oncol.* **1,** 32 (2009).

321. Peng, S. *et al.* Tumor grafts derived from patients with head and neck squamous carcinoma authentically maintain the molecular and histologic characteristics of human cancers. *J. Transl. Med.* **11,** 198 (2013).

322. Masood, R. *et al.* A novel orthotopic mouse model of head and neck cancer and lymph node metastasis. *Oncogenesis* **2,** e68 (2013).

323. Nakagawa, H. *et al.* The targeting of the cyclin D1 oncogene by an Epstein-Barr virus promoter in transgenic mice causes dysplasia in the tongue, esophagus and forestomach. *Oncogene* **14,** 1185–1190 (1997).

324. Opitz, O. G. *et al.* A mouse model of human oral-esophageal cancer. *J. Clin. Invest.* **110,** 761–769 (2002).

325. Lu, S.-L. *et al.* Overexpression of Transforming Growth Factor β1 in Head and Neck Epithelia Results in Inflammation, Angiogenesis, and Epithelial Hyperproliferation. *Cancer Res.* **64,** 4405–4410 (2004).

326. Caulin, C. *et al.* Inducible Activation of Oncogenic K-ras Results in Tumor Formation in the Oral Cavity. *Cancer Res.* **64,** 5054–5058 (2004).

327. Vitale-Cross, L., Amornphimoltham, P., Fisher, G., Molinolo, A. A. & Gutkind, J. S. Conditional Expression of K-ras in an Epithelial Compartment that Includes the Stem Cells Is Sufficient to Promote Squamous Cell Carcinogenesis. *Cancer Res.* **64,** 8804–8807 (2004).

328. Hwang, J. *et al.* Cigarette smoke-induced autophagy is regulated by SIRT1–PARP-1-dependent mechanism: Implication in pathogenesis of COPD. *Arch. Biochem. Biophys.* **500,** 203–209 (2010).

329. Sannigrahi, M., Singh, V., Sharma, R., Panda, N. & Khullar, M. Role of autophagy in head and neck cancer and therapeutic resistance. *Oral Dis.* **21,** 283–291 (2015).

330. Griffin, L. M., Cicchini, L. & Pyeon, D. Human papillomavirus infection is inhibited by host autophagy in primary human keratinocytes. *Virology* **437,** 12–19 (2013).

331. Nomura, H. *et al.* Overexpression and altered subcellular localization of autophagy-related 16-like 1 in human oral squamous-cell carcinoma: correlation with lymphovascular invasion and lymph-node metastasis. *Hum. Pathol.* **40,** 83–91 (2009).

332. Tang, J.-Y. *et al.* High LC3 expression correlates with poor survival in patients with oral squamous cell carcinoma. *Hum. Pathol.* **44,** 2558–2562 (2013).

333. Tang, J.-Y. *et al.* Immunopositivity of Beclin-1 and ATG5 as Indicators of Survival and Disease Recurrence in Oral Squamous Cell Carcinoma. *Anticancer Res.* **33,** 5611–5616 (2013).

334. Kapoor, V., Paliwal, D., Baskar Singh, S., Mohanti, B. K. & Das, S. N. Deregulation of Beclin 1 in patients with tobacco-related oral squamous cell carcinoma. *Biochem. Biophys. Res. Commun.* **422,** 764–769 (2012).

335. Wang, Y. *et al.* Decrease of autophagy activity promotes malignant progression of tongue squamous cell carcinoma. *J. Oral Pathol. Med.* **42,** 557–564 (2013).

336. Liu, J.-L. *et al.* Prognostic significance of p62/SQSTM1 subcellular localization and LC3B in oral squamous cell carcinoma. *Br. J. Cancer* **111,** 944–954 (2014).

337. Vasioukhin, V., Degenstein, L., Wise, B. & Fuchs, E. The magical touch: genome targeting in epidermal stem cells induced by tamoxifen application to mouse skin. *Proc. Natl. Acad. Sci. U. S. A.* **96,** 8551–8556 (1999).

338. Mizushima, N., Yamamoto, A., Matsui, M., Yoshimori, T. & Ohsumi, Y. In Vivo Analysis of Autophagy in Response to Nutrient Starvation Using Transgenic Mice Expressing a Fluorescent Autophagosome Marker. *Mol. Biol. Cell* **15,** 1101–1111 (2004).

339. Osei-Sarfo, K., Tang, X.-H., Urvalek, A. M., Scognamiglio, T. & Gudas, L. J. The molecular features of tongue epithelium treated with the carcinogen 4-nitroquinoline-1-oxide and alcohol as a model for HNSCC. *Carcinogenesis* bgt223 (2013). doi:10.1093/carcin/bgt223

340. Vassar, R., Rosenberg, M., Ross, S., Tyner, A. & Fuchs, E. Tissue-Specific and Differentiation-Specific Expression of a Human K14 Keratin Gene in Transgenic Mice. *Proc. Natl. Acad. Sci. U. S. A.* **86,** 1563–1567 (1989).

341. Tyner, A. L. & Fuchs, E. Evidence for Posttranscriptional Regulation of the Keratins Expressed during Hyperproliferation and Malignant Transformation in Human Epidermis. *J. Cell Biol.* **103,** 1945–1955 (1986).

342. Kannan, S. *et al.* Differential Expression of Cytokeratin Proteins During Tumor Progression. *Epithelial Cell Biol.* **3,** 61–69 (1994).

343. Cintorino, M. *et al.* Cytokeratin expression patterns as an indicator of tumour progression in oesophageal squamous cell carcinoma. *Anticancer Res.* **21,** 4195–4201 (2001).

344. Chu, P. G., Lyda, M. H. & Weiss, L. M. Cytokeratin 14 expression in epithelial neoplasms: a survey of 435 cases with emphasis on its value in differentiating squamous cell carcinomas from other epithelial tumours. *Histopathology* **39,** 9–16 (2001).

345. Pellegrini, G. *et al.* p63 identifies keratinocyte stem cells. *Proc. Natl. Acad. Sci.* **98,** 3156–3161 (2001).

346. Gerdes, J. *et al.* Cell-Cycle Analysis of a Cell Proliferation-Associated Human Nuclear Antigen Defined by the Monoclonal-Antibody Ki-67. *J. Immunol.* **133,** 1710–1715 (1984).

347. Scholzen, T. & Gerdes, J. The Ki-67 protein: from the known and the unknown. *J. Cell. Physiol.* **182,** 311–322 (2000).

348. Sharifi, M. N., Mowers, E. E., Drake, L. E. & Macleod, K. F. Measuring autophagy in stressed cells. *Methods Mol. Biol. Clifton NJ* **1292,** 129–50 (2015).

349. Guan, J.-L. *et al.* Autophagy in stem cells. *Autophagy* **9,** 830–849 (2013).

350. Salemi, S., Yousefi, S., Constantinescu, M. A., Fey, M. F. & Simon, H.-U. Autophagy is required for self-renewal and differentiation of adult human stem cells. *Cell Res.* **22,** 432–435 (2012).

351. Prince, M. E. *et al.* Identification of a subpopulation of cells with cancer stem cell properties in head and neck squamous cell carcinoma. *Proc. Natl. Acad. Sci. U. S. A.* **104,** 973–978 (2007).

352. Bragado, P. *et al.* Analysis of Marker-Defined HNSCC Subpopulations Reveals a Dynamic Regulation of Tumor Initiating Properties. *Plos One* **7,** (2012).

353. Chen, Y.-C. *et al.* Aldehyde dehydrogenase 1 is a putative marker for cancer stem cells in head and neck squamous cancer. *Biochem. Biophys. Res. Commun.* **385,** 307–313 (2009).

354. Sinha, N., Mukhopadhyay, S., Das, D. N., Panda, P. K. & Bhutia, S. K. Relevance of cancer initiating/stem cells in carcinogenesis and therapy resistance in oral cancer. *Oral Oncol.* **49,** 854–862 (2013).

355. Yang, M.-H. *et al.* Bmi1 is essential in Twist1-induced epithelial-mesenchymal transition. *Nat. Cell Biol.* **12,** 982–992 (2010).

356. Chung, C. H. *et al.* Gene Expression Profiles Identify Epithelial-to-Mesenchymal Transition and Activation of Nuclear Factor-κB Signaling as Characteristics of a High-risk Head and Neck Squamous Cell Carcinoma. *Cancer Res.* **66,** 8210–8218 (2006).

357. Yang, M.-H. *et al.* Overexpression of NBS1 induces epithelial–mesenchymal transition and co-expression of NBS1 and Snail predicts metastasis of head and neck cancer. *Oncogene* **26,** 1459–1467 (2006).

358. Zuo, J.-H. *et al.* Activation of EGFR promotes squamous carcinoma SCC10A cell migration and invasion via inducing EMT-like phenotype change and MMP-9-mediated degradation of E-cadherin. *J. Cell. Biochem.* **112,** 2508–2517 (2011).

359. Rugg, E. *et al.* A Functional Knockout of Human Keratin-14. *Genes Dev.* **8,** 2563–2573 (1994).